HYDROGEN PEROXIDE DISPROPORTIONATION AND ORGANIC COMPOUND OXIDATION BY PEROXYCARBONATE CATALYZED BY MANGANESE(II): KINETICS AND MECHANISM

By

ANDREW P. BURKE

A DISSERTATION PRESENTED TO THE GRADUATE SCHOOL
OF THE UNIVERSITY OF FLORIDA IN PARTIAL FULFILLMENT
OF THE REQUIREMENTS FOR THE DEGREE OF
DOCTOR OF PHILOSOPHY

UNIVERSITY OF FLORIDA

2005

to my wife and parents

ACKNOWLEDGMENTS

The work presented here would not have been possible without the help and support of a number of people. I would like to acknowledge these people individually for their contributions in making the following document possible.

First, I would like to thank my advisor, Dr. David Richardson, for all of his help and support during these past five years. Dr. Richardson has helped to make me a better scientist. My presentation and writing skills have vastly improved under his advisement, and they will prove useful in all my future endeavors. I have also had the opportunity to learn from Dr. Richardson the proper method for performing chemical kinetics.

I would also like to thank the members of the Richardson group, both past and present, for all of their help during the years. Without the fun environment they created, working in the lab would have been much less enjoyable. I would like to thank my partner in crime, Dan Denevan. It was always nice having Dan to make jokes with and to have around to complain to about everything going wrong in the lab. I would also like to thank Dr. Ana Ison for all of her support during this process. Ana was always around to discuss ideas about projects. I would also like thank her for the help she provided in acquiring the GC data. I would especially like to thank Dr. Celeste Regino. Celeste taught me the intricacies of HPLC and that in order for it to do what you want you must coddle it at all times.

I would also like to thank Pat Butler for all of her hard work during my elementary education. As my SLD teacher, Mrs. Butler worked with me constantly for many years

to help me cope with a disability I never thought I would be able to overcome. Now, as I finish my dissertation to achieve my Ph.D., I appreciate even more all of the techniques she taught me to help me achieve my goals.

I could not have accomplished this goal without the support of my family, especially my parents. My parents have always supported me in all of the decisions I have made and attending graduate school was no exception. Without their support, I would never have had the courage to face new challenges and persevere in the face of opposition.

I would also like to thank my wife, Erin. I never expected to meet my wife in graduate school, nor did I expect her to be a chemistry graduate student. She has been a constant support these past 5 years, and I would have given up this dream long ago were it not for her constant vigilance in driving me toward my goal.

Most of all, I would like to thank God for all of His love and support through not only my graduate career, but my entire life. Through Him all things are possible.

TABLE OF CONTENTS

LIST OF TABLES

LIST OF FIGURES

Abstract of Dissertation Presented to the Graduate School
of the University of Florida in Partial Fulfillment of the
Requirements for the Degree of Doctor of Philosophy

HYDROGEN PEROXIDE DISPROPORTIONATION AND ORGANIC COMPOUND OXIDATION BY PEROXYCARBONATE CATALYZED BY MANGANESE(II): KINETICS AND MECHANISM

By

Andrew P. Burke

August 2005

Chair: David E. Richardson
Major Department: Chemistry

The investigation of the mechanism of hydrogen peroxide disproportionation and alkene epoxidation in aqueous solutions of bicarbonate at near neutral pH as catalyzed by manganese(II) is described. Current literature proposes that a free hydroxyl radical pathway based on Fenton chemistry is responsible for the hydrogen peroxide decay. This proposed mechanism does not adequately explain the unique requirement of bicarbonate in these reactions. Also, the proposed free hydroxyl radical mechanism does not explain why no radically coupled products in the oxidation of nucleophilic alkenes are detected. We suggest that manganese(II) is activated by peroxycarbonate, a hydrogen peroxide and bicarbonate adduct, to form a high oxidation state manganese(IV) complex. In addition, it is proposed that the carbonate radical anion is also a product of the reaction of peroxycarbonate in the presence of metal cations. Both the carbonate radical anion and the high oxidation state manganese(IV) complex are believed to be the main reactive

oxygen donors in this system responsible for the observed reactivity. Numerical simulations of the hydrogen peroxide and nucleophilic alkene epoxidation by hydrogen peroxide in solutions of bicarbonate and manganese(II) have also been conducted.

While the epoxidation of nucleophilic alkenes by hydrogen peroxide in bicarbonate solutions is catalyzed by manganese(II), the same is not true for the epoxidation of electrophilic alkenes. Investigations have been conducted using several water soluble alkenes. For these reactions, the addition of manganese(II) has been shown to inhibit the oxidation by decomposing the active oxidant, the hydroperoxide anion. Kinetic investigations of the oxidation of dibenzoylethylene in micellar media by hydroperoxide and hypochlorite will also be presented. The observed second-order rate constant for the oxidation by hydroperoxide is $660 \pm 40\ M^{-1}s^{-1}$ and that for hypochlorite is $118 \pm 2\ M^{-1}s^{-1}$.

CHAPTER 1
INTRODUCTION

General Oxidation

Oxidation-reduction (redox) reactions are some of the most important chemical reactions. These reactions are responsible for the formation of compounds from their elements, the generation of electricity, and combustion reactions, some of which produce energy at the cellular level. Redox reactions are always coupled, and the number of electrons transferred must be equal in number between the oxidation and reduction half-reactions. Redox reactions can be easily determined by identifying the oxidation states of the atoms in the ions and molecules involved in the reaction. Lewis structures provide an easy convention by which oxidation states may be assigned to atoms. Typically, all bonds must be assumed to be completely ionic, and the more electronegative atom of the bonded pair is allocated the pair of electrons. For example, consider the sulfate dianion, SO_4^{2-}.

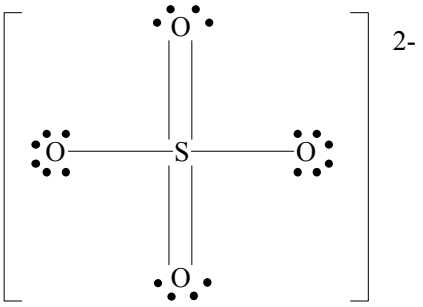

Figure 1-1. The sulfate dianion

The sulfur-oxygen bonds are polar covalent, polarized toward the oxygen atoms. Each oxygen atom is given an oxidation number of -2, eight valence electrons versus six

for the free atom. The sulfur atom is given an oxidation number of +6, zero valence electrons versus six for the free atom. The charge of the ion is given by the sum of all the formal oxidation charges, in this case 6-8 = -2.

The use of oxidation states can now be used to easily identify redox reactions. As an example, consider the reaction of sulfite and permanganate anions in acidic solution to yield the sulfate anion and manganese(II).

$$5SO_3^{2-} + 2MnO_4^- + 6H^+ \longrightarrow 5SO_4^{2-} + 2Mn^{2+} + 3H_2O \qquad (1\text{-}1)$$

In this example, the sulfur atom of sulfite begins in the +4 oxidation state and is in the +6 oxidation state on the product side, as is seen in the Equation 1-1, a loss of two electrons. By the definition of oxidation and reduction, this is an oxidation. By definition, oxidation reactions must be coupled to a reduction reaction, the permanganate must be gaining electrons. In the example above, this is seen to be true since the reactant manganese of permanganate is in the +7 oxidation state and a gain of 5 electrons yields manganese(II), as seen on the product side of the reaction.

In organic chemistry, the assignment of oxidation states is not as simple as the above example with the sulfate dianion.[1,2] It has been the traditional method, therefore, to define oxidation in organic chemistry as the "loss" of electrons by forming bonds with elements that are more electronegative than carbon, such as oxygen or nitrogen. Reduction then is the "gain" of electrons by breaking bonds with more electronegative atoms and forming bonds with hydrogen.[1,2] For example, ethanol can be transformed to form acetaldehyde. In this process, ethanol looses a bond to hydrogen and gains a bond to oxygen, an oxidation. Similarly, acetic acid can be converted to acetaldehyde. In this process, acetic acid looses a bond to oxygen and gains a bond to hydrogen, a reduction.

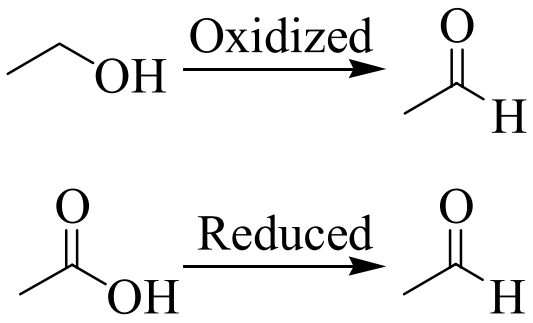

Figure 1-2. The oxidation of organic molecules is defined as formation of bonds to carbon with atoms that are more electronegative than carbon. Reduction is the loss of bonds to more electronegative atoms and bond formation with hydrogen.

Reactive Oxygen Species

Molecular oxygen and reactive oxygen species (ROS) are the main oxygen sources for oxidation processes and are highly reactive oxygen donor molecules with the ability to react with a wide variety of substrates.[3] Table 1-1 lists some of the most commonly encountered radical and non-radical reactive oxygen species.

Table 1-1. Some common reactive oxygen species

Radical	Non-radical
Superoxide, $O_2^{-}\cdot$	Hydrogen Peroxide, H_2O_2
Hydroxyl, OH·	Hypochlorous acid, HOCl
Peroxyl, ROO·	Alkyl Hydroperoxide, ROOH
Alkoxyl, RO·	
Hydroperoxyl, HOO·	

In the human body, for example, the effects of reactive oxygen species have been measured by examining the oxidative stress on cells.[4] Oxidative stress is defined as the imbalance between the cellular production of reactive oxygen species and the antioxidant mechanisms in existence to remove them.[4] The effects of these reactive oxygen species have been linked to chronic disease and aging.[5,6]

The human body has several mechanisms, including enzymes and radical scavengers, that can intervene with reactive oxygen species.[4] For example, superoxide

dismutase converts the superoxide radical anion plus two protons to hydrogen peroxide. The product hydrogen peroxide, which is yet another reactive oxygen species, can then be enzymatically decomposed by catalase to water and oxygen. The human body also uses a number of radical scavengers, such as ascorbate, urate, and tocopherol, to rid cells of high concentrations of reactive oxygen species.

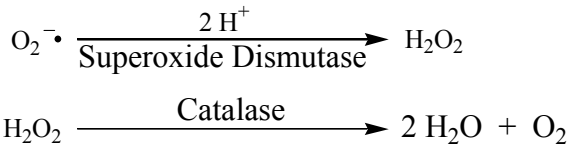

Figure 1-3. Superoxide dismutase enzymatically oxidizes the superoxide anion and two protons to hydrogen peroxide, another reactive oxygen species. Hydrogen peroxide is the disproportionated by catalase to yield water and molecular oxygen.

Hydrogen Peroxide

Hydrogen peroxide (H_2O_2) is a common reactive oxygen species which is environmentally friendly due to its decomposition to molecular oxygen and water. It is a weak, nonspecific, electrophilic oxidant with an $E^\circ = 1.77$ V vs. NHE[7] that has been used as a bleaching agent for over a century.[8] Hydrogen peroxide is only a weak oxidant under mild conditions. Recent interest in the use of H_2O_2 as a terminal oxidant has come from increasing pressure in the industrial sector to find more environmentally friendly oxidation reagents.[8] Many industries are beginning to use hydrogen peroxide in the treatment of wastewater. Recently, hydrogen peroxide was shown to remove cyanide from thermoelectric power station wastewater.[9]

Hydrogen peroxide is also an important commercial chemical in the production of epoxides. In this case, hydrogen peroxide is used to generate peracids that are then used in the epoxidation of numerous alkenes.[10] The activation of hydrogen peroxide to form peracids will be presented shortly in the introduction.

Hydrogen peroxide is produced commercially by the AO-Process,[10] which involves the hydrogenation of a 2-alkyl-9,10-anthraquinone to the corresponding hydroquinone. The hydroquinone produced is then oxidized with oxygen, or air, to regenerate the anthraquinone and produce hydrogen peroxide (Figure 1-4). The hydrogen peroxide produced is extracted with water, while the organic components can be recycled back through the hydrogenation step.

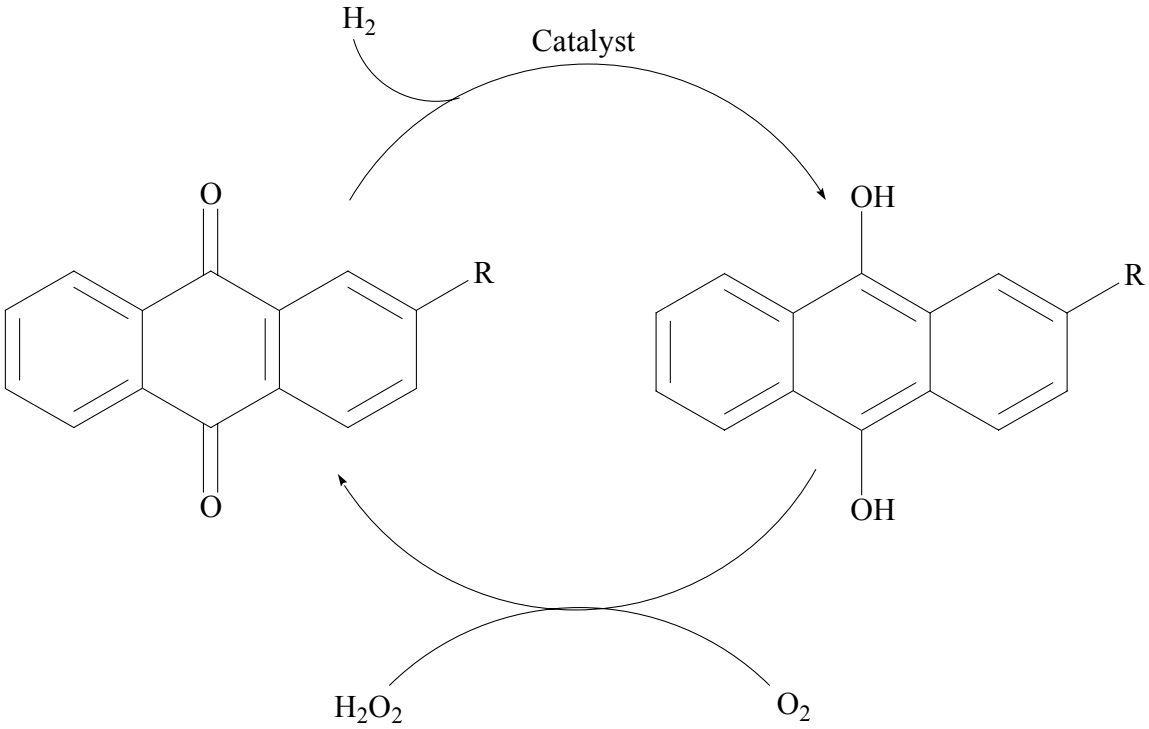

Figure 1-4. The AO-process for the industrial production of hydrogen peroxide.

Hydrogen peroxide is an excellent environmental choice for two reasons. First, the decomposition products are molecular oxygen and water. Second, due to its relative inactivity, specific methods of activation must be used which can tune the reactivity to the particular oxidative process required. Figure 1-5 illustrates the nucleophilic attack of a substrate on hydrogen peroxide. A general acid can act as a proton transfer agent to assist in the cleaving of the peroxide bond to form the oxidized nucleophile and water.

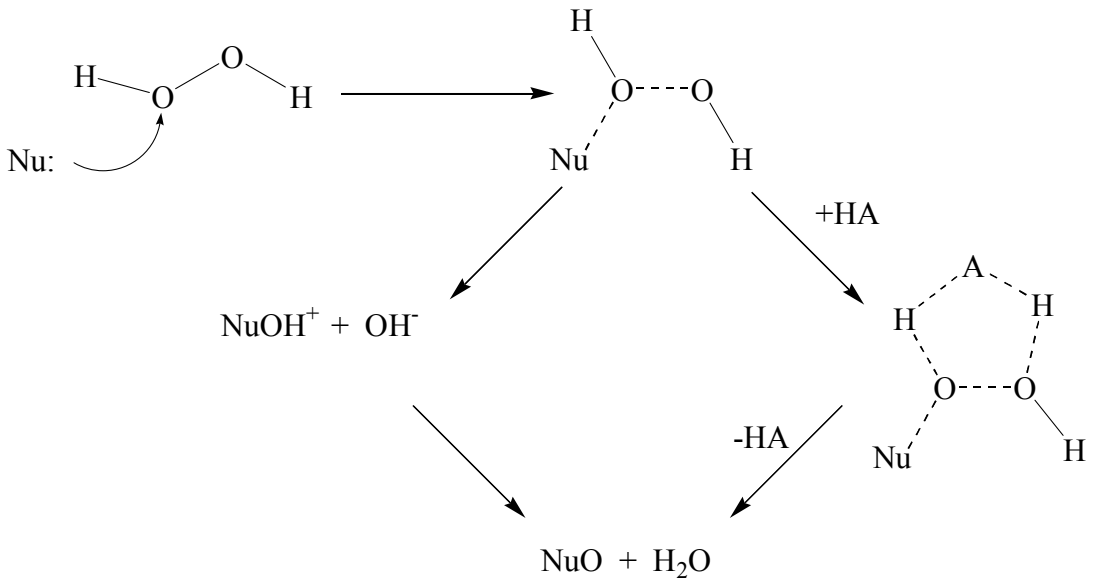

Figure 1-5. Illustration of a nucleophilic attack on hydrogen peroxide. The use of a general acid facilitates the proton transfer to yield the oxidized nucleophile and water.

Activation of Hydrogen Peroxide

UV Activation

While hydrogen peroxide may be used for some types of oxidations, activation is required for use in a wider variety of reactions. For instance, solutions of hydrogen peroxide can be irradiated using UV radiation to homolytically cleave the peroxide bond to form two hydroxyl radicals, Equation 1-2.

$$H_2O_2 \xrightleftharpoons{h\nu} 2\ HO\bullet \qquad (1\text{-}2)$$

The hydroxyl radical is a potent, nonspecific, one-electron oxidant that can readily react with alkenes (Figure 1-6) by addition to the double bond.[11] The resulting organic radical can then react with another hydroxyl radical to form the diol, or in the presence of iron(II) and acid, the alcohol. Depending on the nature of the double bond, radical polymerization can also occur, as seen in Figure 1-7.

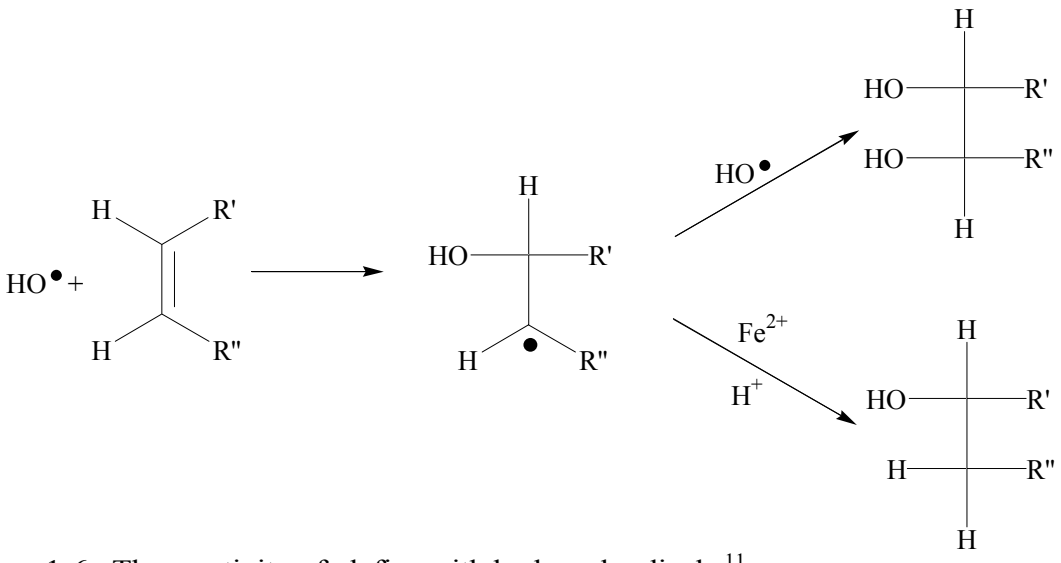

Figure 1-6. The reactivity of olefins with hydroxyl radicals.[11]

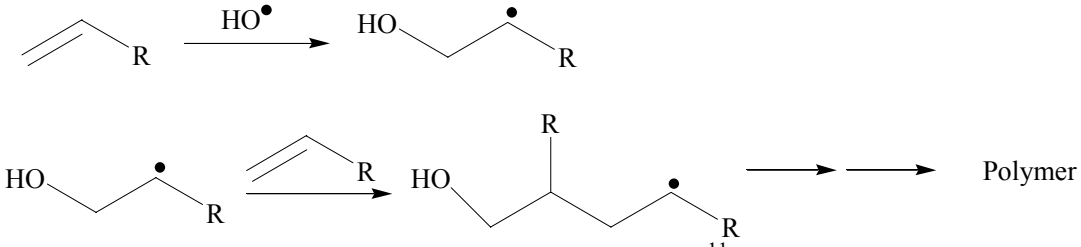

Figure 1-7. Polymerization of olefins by hydroxyl radical.[11]

Strong Base Activation

Other methods for the activation of hydrogen peroxide are known. The reaction of hydrogen peroxide with a strong base generates the hydroperoxide anion, as seen in Equation 1-3, which is an effective nucleophilic oxidant. The hydroperoxide anion can epoxidize an electrophilic alkene as seen in Figure 1-8.

$$H_2O_2 + {}^{-}OH \rightleftharpoons {}^{-}OOH + H_2O \qquad (1\text{-}3)$$

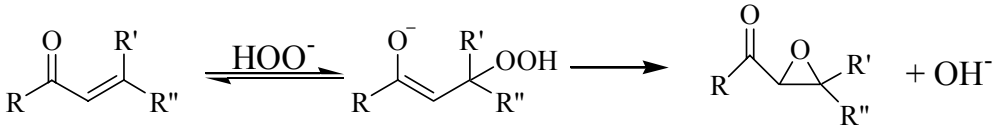

Figure 1-8. Reactivity of electrophilic olefins with nucleophilic oxidants, such as hydroperoxide, react to produce the epoxide plus the oxidants' corresponding leaving group, in this case hydroxide.

Strong Acid Activation

Hydrogen peroxide is also activated by strong acids. Protonation of one of the oxygens in hydrogen peroxide results in polarization of the O-O bond to generate OH^+, a strong electrophilic oxidant that can react with nucleophiles, such as alkenes. Water is the other product of the reaction (Equation 1-4).

$$H_2O_2 \overset{H^+}{\rightleftharpoons} HO^+ + H_2O \qquad (1\text{-}4)$$

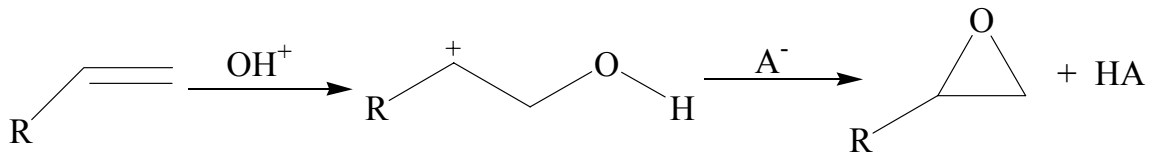

Figure 1-9. The reaction of an alkene with OH^+ generates an intermediate carbocation. A general base can then deprotonate the oxygen of the intermediate which results in ring closure to form the epoxide.

Acyl Hydroperoxides

Acyl hydroperoxides, a broad category of oxidants including the organic peracids, are electrophilic oxidants often used for the heterolytic oxidation of organic substrates. Peracids are synthesized from the acid-catalyzed equilibrium between hydrogen peroxide and the acid form of the peracid, as seen in Equation 1-5.[12] In the absence of a catalyst, the equilibrium is slow. In order to isolate the peracid from the equilibrium mixture, continuous distillation or an extraction step must be used.

$$RCO_2H + H_2O_2 \overset{H^+}{\rightleftharpoons} RCO_3H + H_2O \qquad (1\text{-}5)$$

A common example of a peracid used in organic oxidations is *m*-chloroperoxybenzoic acid (*m*-CPBA). The mechanism of the reaction of an organic nucleophile, an alkene, proceeds as shown in Figure 1-10. This example uses *m*-CPBA as the oxidant. The rate of peracid epoxidation of alkenes is influenced by three main factors. First, the reaction is dependent on the type of double bond. Second, the

substituents of the peracid affect its ability to oxidize an alkene. Third, the rate of reaction is reduced in the presence of coordinating solvents, such as ethers, which form intermolecular H-bonds.[13] The kinetic aspects of peracid oxidations are as follows: 1) the reaction is second order, 2) the reaction is stereospecific, meaning that cis-alkenes will react to give cis-epoxides and trans-alkenes will react to give trans-epoxides, and 3) the rate of reaction is increased with increasing strength of the formed acid.[13]

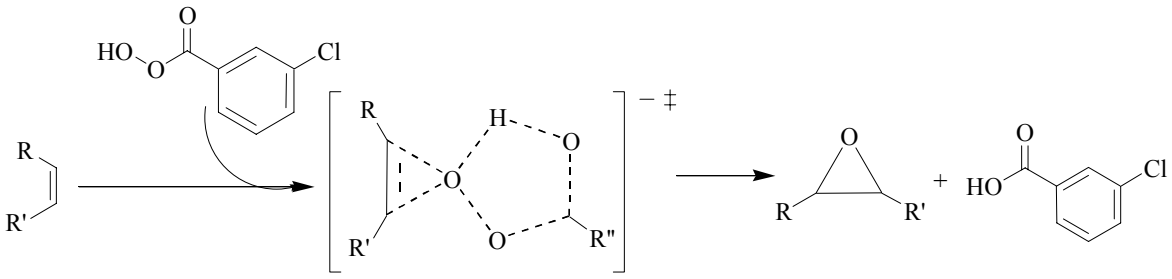

Figure 1-10. Alkene oxidation by *m*-CPBA

Iron(II) Activation

One of the best known and most studied processes for the activation of hydrogen peroxide is by iron(II) salts, the combination of which is known as Fenton's reagent. The most accepted mechanism for the activation, introduced by Haber and Weiss[14,15] and studied extensively by Barb et al.,[16-19] involves the redox cycle of iron(II). The mechanism is shown in Equations (1-6)-(1-10).

$$Fe^{2+} + H_2O_2 \rightarrow Fe^{3+} + {}^{\bullet}OH + OH^- \quad (1\text{-}6)$$

$$Fe^{2+} + {}^{\bullet}OH \rightarrow Fe^{3+} + OH^- \quad (1\text{-}7)$$

$${}^{\bullet}OH + H_2O_2 \rightarrow HOO^{\bullet} + H_2O \quad (1\text{-}8)$$

$$Fe^{2+} + HOO^{\bullet} \rightarrow Fe^{3+} + HOO^- \quad (1\text{-}9)$$

$$Fe3+ + HOO\bullet \rightarrow Fe2+ + O_2 + H+ \quad (1\text{-}10)$$

Equation 1-6 represents the initiation reaction by which hydrogen peroxide is activated to form a free hydroxyl radical. Further chain propagation reactions involving the hydroxyl radical ultimately produce peroxyl radicals, as shown in Equation 1-8 with a hydrogen abstraction. The hydroxyl and peroxyl radicals are reactive oxygen species known to be powerful oxidizing agents and have been implicated in aging and chronic disease. In the chain termination step, a peroxyl radical reacts with iron(III) to yield a proton, molecular oxygen, and regeneration of iron(II) to complete the redox cycle.

Transition-metal Organometallic Complexes

Another method for hydrogen peroxide activation is through the use of transition-metal cation complexes with organo ligands, including porphyrins. There are a wide variety of metal complexes described in the literature with any number of differing metal cations including Cu(I), Cu(II), Ni(II), Co(II), Co(III), Fe(II), Fe(III), Mn(II), and Mn(III).[8] The mechanisms by which these metal porphyrin complexes activate hydrogen peroxide vary and include production of free hydroxyl radicals as well as formation of high valent metal-oxo species.[8] In the case of free hydroxyl radical formation, mechanisms based on Fenton type chemistry are proposed, as seen in the $[Cu(phen)_2]^+$ example in Equation 1-11. In the case of high valent metal-oxo formation reactions, such

$$[Cu(phen)_2]^+ + H_2O_2 \longrightarrow [Cu(phen)_2]^{2+} + HO\bullet + HO^- \qquad (1\text{-}11)$$

as seen by Traylor et al[20] in the activation of hydrogen peroxide by iron(III) tetrakis(pentafluorophenyl) porphyrin, the mechanism of oxidation is believed to occur via an oxygen transfer from a high valent iron complex.

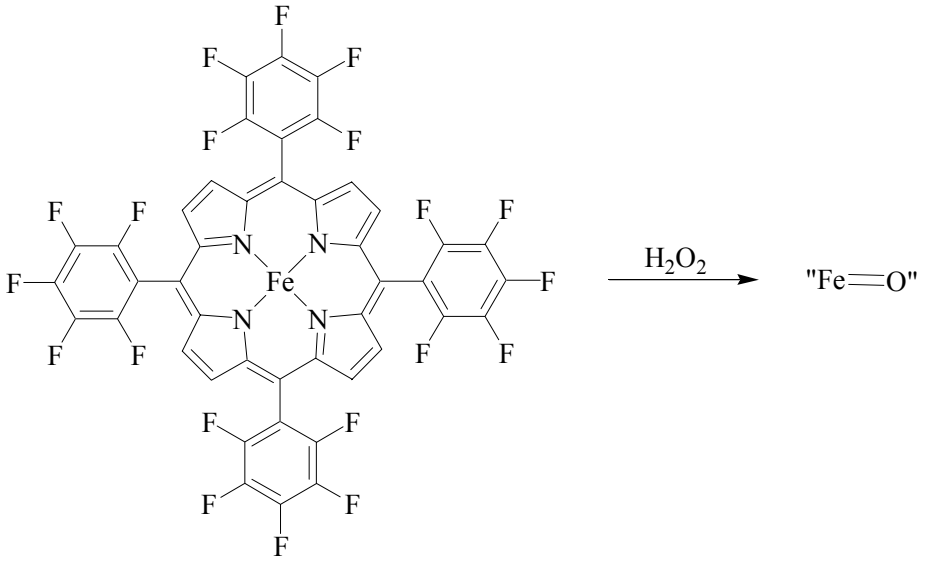

Figure 1-11. Activation of iron(III) tetrakis(pentafluorophenyl) porphyrin by hydrogen peroxide to produce a high oxidation state iron complex.[20]

Methyltrioxorhenium

Methyltrioxorhenium (MTO), first introduced by Beattie and Jones in 1979,[21] in combination with hydrogen peroxide provides a useful system for the oxidation of alkenes and other substrates such as alkynes and ketones, as reported by Herrmann.[22] Considerable research on the kinetics of the reaction of MTO with hydrogen peroxide has been studied by Espenson, who has shown that two predominant species exist in the MTO/H_2O_2 system, shown in Figure 1-12, that are more stable under acidic conditions.[23] Both are efficient oxygen donors to substrates such as phosphines and sulfides. In the reaction of alkenes with MTO/H_2O_2, both of the peroxide adducts react to form epoxide, but the monoperoxide tends to react slightly faster than the diperoxide.[24] There are three major drawbacks to the use of MTO as an alkene epoxidation catalyst: 1) MTO has a low stability in the presence of peroxide 2) MTO is both expensive and difficult to synthesize and 3) because reactions are conducted under acidic conditions, ring-opening of acid sensitive epoxides is possible.[23]

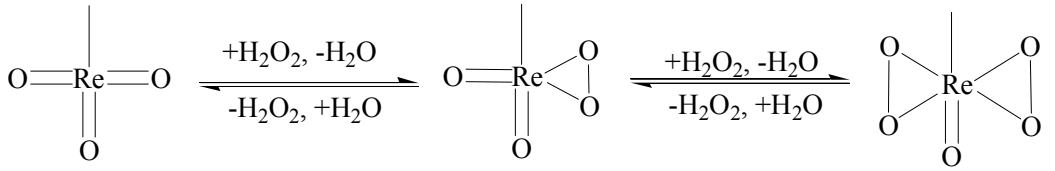

Figure 1-12. The two dominant forms in the MTO/H_2O_2 system under acid conditions. The diperoxorhenium adduct reacts slightly slower than the monoperoxorhenium complex.[23]

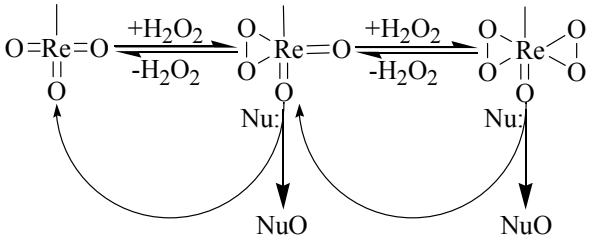

Figure 1-13. Nucleophilic attack of an olefin on the electrophilic oxygen of the hydrogen peroxide activated methyltrioxorhenium yields the oxidized nucleophile and regenerates MTO. Attack of a nucleophile on the diperoxo complex generates the oxidized nucleophile and the monoperoxorhenium complex.[24]

Asymmetric Oxidation

In addition to activating hydrogen peroxide for use as an oxidizing agent, it is also advantageous to control the addition of the oxygen atom to substrates, for instance, alkenes, to generate only one epoxide enantiomer. A number of different methods have been proposed in the literature and have used a number of different techniques to assure that the oxygen atom only adds to one face of the alkene. Three of these methods are discussed in detail below.

Sharpless Oxidation of Allylic Alcohols

A simple and relatively inexpensive method for asymmetric epoxidation of allylic alcohols using titanium(IV) tetraisopropoxide, tetrabutyl hydroperoxide (TBHP), and (+) or (-)-diethyl tartrate was introduced by Sharpless in 1980.[25] The use of the (+) or (-)-diethyl tartrate facilitates the addition of the oxygen to one face of the alkene as shown in Figure 1-14. One of the most interesting aspects of this epoxidation system is the ability

to add the oxygen to a particular face, depending on which tartrate enantiomer is used, regardless of the substitution pattern of the alkene.

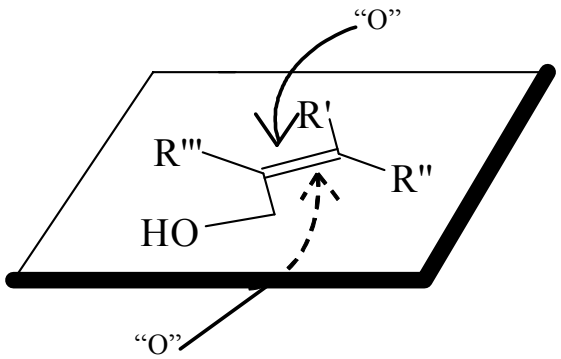

Figure 1-14. Illustration of the asymmetric epoxidation using the Sharpless method. Use of the (+) or (-)-tartrate allows for the oxygen atom to be added to only one face of the allylic alcohol.[25]

Mn(III)-salen Epoxidation Catalysts

Chiral manganese(III)-salen complexes (the salen ligand is illustrated in Figure 1-15) are another example of an asymmetric alkene epoxidation catalysts. Although the Sharpless method used tartrate as an additive for achieving asymmetric epoxidation, manganese(III)-salen catalysts rely on the chirality of the complex to provide for the asymmetric addition of the oxygen atom. The popularity of the epoxidation system comes from the ease in synthesis of the catalyst and the use of cheap, readily available oxidants, such as iodosylbenzene and hypochlorite.

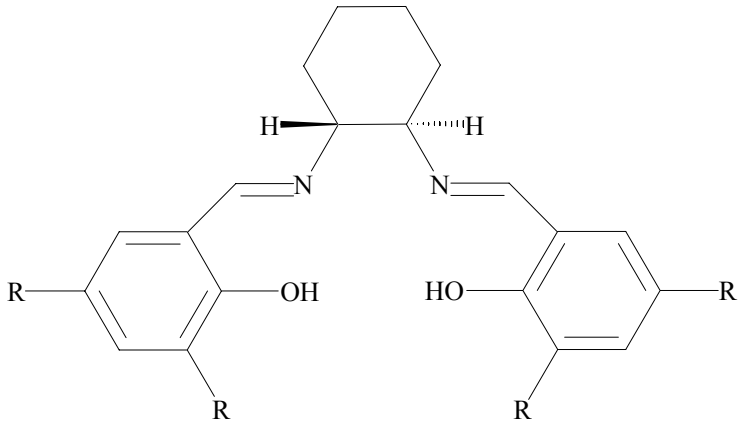

Figure 1-15. A salen ligand.

Hydrogen peroxide can also be used as the terminal oxidant, although decomposition of the oxidant by the catalyst has been observed. Katsuki[26] in 1994 reported that hydrogen peroxide could be used with Mn(III)-salen catalysts for the epoxidation of chromene. The yields were low (17-53 %), but with good ee (93-96 %). It was noted by Katsuki that in order for the reaction of Mn(III)-salen catalysts to epoxidize alkenes with hydrogen peroxide, an axial ligand was required. For the epoxidations of chromene, *N*-methylimidazole was used as the axial ligand. It has also been noted that the use of carboxylate salts as additives are useful in the epoxidation of alkenes by Mn(III)-salen catalysts.[27] In 1998, Pietikainen found that the use of manganese(III)-salen with 30 % hydrogen peroxide, along with ammonium acetate, oxidized spiro[2H-1-benzopyran-2,1'-cyclohexane] in 90 % yield and an ee of 91 %.[28]

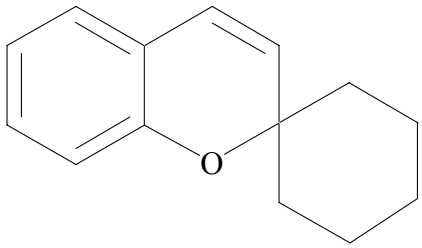

Figure 1-16. spiro[2H-1-benzopyran-2,1'-cyclohexane]

Enantiomeric excess (ee) provides a method for reporting the yield of one enantiomer in comparison to the other. In the case above for the oxidation by Pietikainen, a 91% ee was reported. This means that 9 % (100% - 91%) of the product is racemic, implying that the remaining mixture is 4.5 % of each enantiomer. The total yield of the predominant enantiomer is then 95.5 % (91 % + 4.5 %), while the other enantiomer is 4.5 %.

Chiral Ketone Epoxidation Catalysts

The use of chiral dioxiranes for the epoxidation of alkenes was first reported by Curci et al. in 1984.[29] Shi et al.[30,31] has observed that chiral ketones are effective catalysts for the asymmetric epoxidation of alkenes by the *in situ* generation of dioxiranes using potassium peroxymonosulfate (Oxone®), as seen in Figure 1-17.

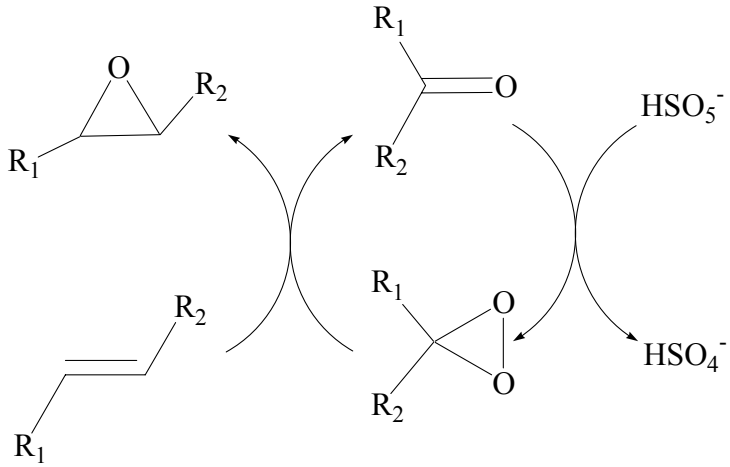

Figure 1-17. Asymmetric epoxidation of alkenes can be easily achieved using peroxymonosulfate to generate a dioxirane *in situ*.[30]

These reactions are performed in mixed solvent systems, usually 1,2-dimethoxymethane and water. The alkene is soluble in the organic solvent, while the Oxone is soluble in the aqueous layer. The ketone catalyst used is soluble in both water and the organic solvent, thus allowing the ketone to act as a phase transfer catalyst. The ketone is oxidized by peroxymonosulfate in the aqueous layer to form the dioxirane, which then transfers to the organic layer where it can oxidize the alkene and regenerate the starting ketone. The asymmetric epoxidation is facilitated by the chiral nature of the ketone. As the generated dioxirane nears the alkene, the oxygen is transferred to only one face of the alkene. The ee's that have been reported using 1,2:4,5-di-*O*-isopropylidene-D-erythro-2,3-hexodiuro-2,6-pyranose, whose structure is shown in Figure 1-18, range from 12 – 98%. The lowest ee's are for the epoxidation of cis-alkenes

(12 – 56.2%), while an ee of 76.4 – 98% has been observed for the trans-alkenes. The difference in the ee between cis and trans-alkenes has been attributed to the approach the catalyst can make to the alkene in the transition states for the two alkenes.[30]

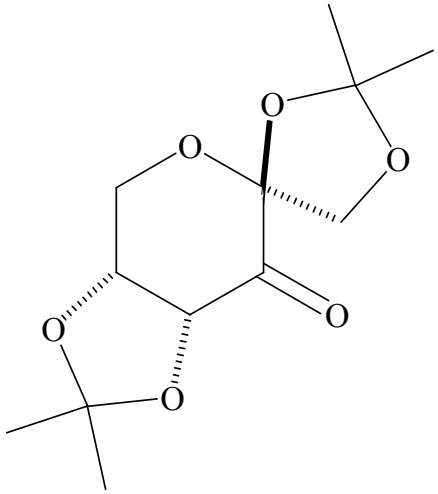

Figure 1-18. Structure of 1,2:4,5-di-*O*-isopropylidene-D-erythro-2,3-hexodiuro-2,6-pyranose used by Shi[30] for the asymmetric epoxidation of alkenes using peroxymonosulfate to generate a dioxirane *in situ*.

Peroxycarbonate

Recent work in our group has found that bicarbonate is an effective activator of H_2O_2,[32,33] known as BAP, bicarbonate activated peroxide. Equilibrium between bicarbonate and H_2O_2 produces the peroxycarbonate anion (HCO_4^-), as seen in Equation 1-12.

$$HCO_3^- + H_2O_2 \rightleftharpoons HCO_4^- + H_2O \qquad (1\text{-}12)$$

The mechanism by which this equilibrium occurs has been determined by Yao[34] and has been found to proceed through carbon dioxide as an intermediate. The presence of carbonic anhydrase or the carbonic anhydrase model complex 1,4,7,10-tetraazacyclododecanezinc(II) accelerates the equilibrium reaction through catalysis of the dehydration of bicarbonate and possible catalysis of the perhydration pathway.[34] The complete equilibrium processes is shown in Figure 1-19.

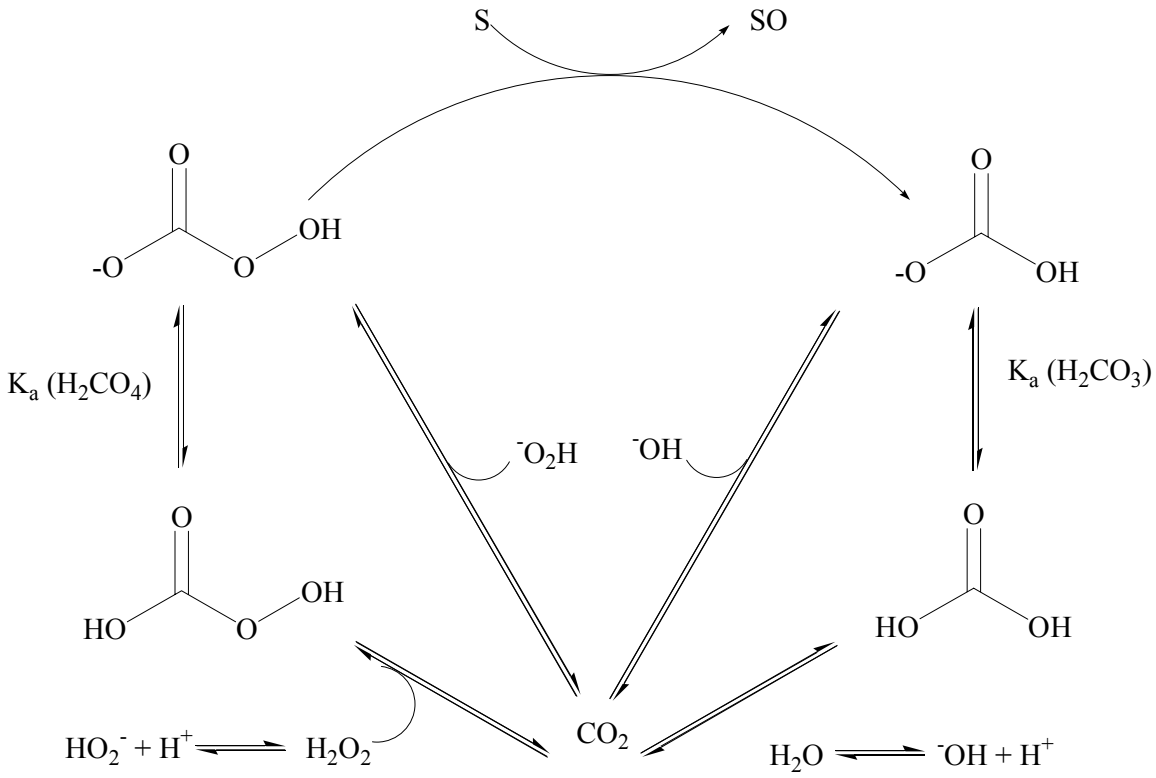

Figure 1-19. The equilibrium formation of bicarbonate and peroxycarbonate proceeds through CO_2 as an intermediate.[34]

Peroxycarbonate is a strong oxidant with an E° (HCO_4^-/HCO_3^-) of 1.8 ± 0.1 V vs. NHE.[35] Inorganic salts and metal complexes of peroxycarbonate have been isolated and analyzed by X-ray crystallography and vibrational spectroscopy.[36,37] The analysis indicates that peroxycarbonate is a true peroxide with a structure of $HOOCO_2^-$. Recently, an iron(III) complex has been isolated and characterized by X-ray crystallography, as seen in Figure 1-20.[38] Synthesis of metal complexes of peroxycarbonate will be presented in the next section of this introduction. Peroxycarbonate should not be confused with sodium percarbonate, which is simply the cocrystallite of sodium carbonate and H_2O_2 (Na_2CO_3•1.5 H_2O_2).

Peroxycarbonate is a moderately active oxidant for organic substrates, including sulfides and alkenes.[39-42] The increase in reactivity over hydrogen peroxide can be

attributed to the nature of the leaving group during a nucleophilic attack of the electrophilic oxygen of peroxide and peroxycarbonate. In the case of hydrogen peroxide, a general acid is required as a proton transfer agent, as seen in Figure 1-5. In the case of peroxycarbonate, however, an intramolecular proton transfer can release bicarbonate as the leaving group, as seen in Figure 1-21. Because bicarbonate is a weaker base than hydroxide, peroxycarbonate is a stronger electrophile over hydrogen peroxide by a factor of about 300 based on studies with sulfides.[41]

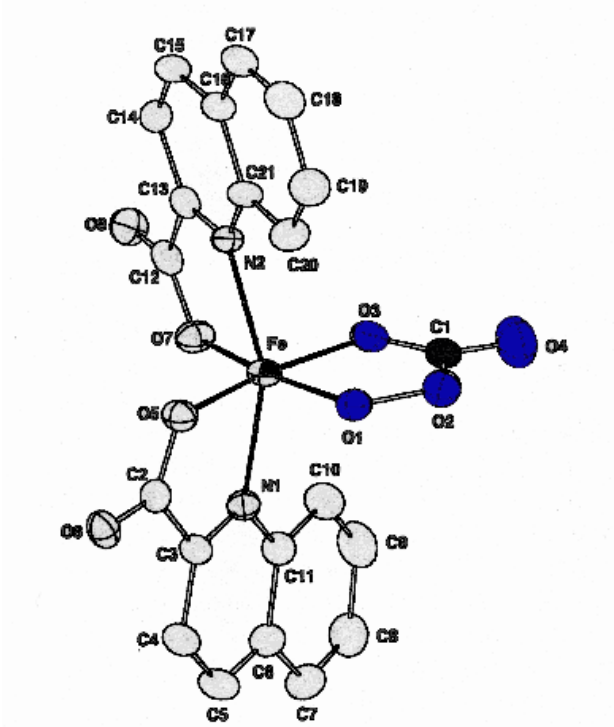

Figure 1-20. $Fe(qn)_2(O_2C(O)O]Ph_4P \cdot 1.5MeOH \cdot 0.5\ (CH_3)_2NCHO$.[38]

Typical reactions of substrates with peroxycarbonate are slow, but still much faster than background reactions with hydrogen peroxide alone. For instance, epoxidations of water soluble alkenes in the absence of bicarbonate yields negligible products in 24 hours. With the addition of bicarbonate, however, NMR analysis shows 90% conversion to the corresponding epoxide in 15 hours. A similar trend is also seen in sulfide oxidation.[43,44]

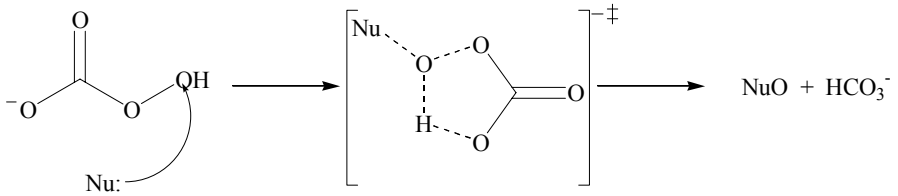

Figure 1-21. Nucleophilic attack on the peroxycarbonate anion. An intramolecular proton transfer in the transition state allows for release of bicarbonate instead of hydroxide as in the case of hydrogen peroxide.

Transition-metal Peroxycarbonate Complexes

Transition-metal complexes containing the peroxycarbonate dianion ligand, CO_4^{2-}, are known. The general formula for these peracids are $L_nM(CO_4)X_m$, where L = an ancillary ligands, n = 2 or 3, M = Pd, Pt, Rh, or Ir, X = a halogen, and m = 0 or 1.[42] The peroxycarbonate complexes are generally synthesized by passing carbon dioxide gas through a solution of the $L_nM(O_2)X_m$ parent complex dissolved in a dry solvent. Two possible mechanisms for the formation of the peroxycarbonate complexes are shown in Figure 1-22.

Oxygen label studies[43] indicate that the carbon dioxide does not insert into the M-O bond (pathway 2), but instead inserts into the O-O bond (pathway 1). These complexes are classified as heterolytic oxidants and are good electrophilic oxidants which react with nucleophiles such as alkenes and phosphines.[43]

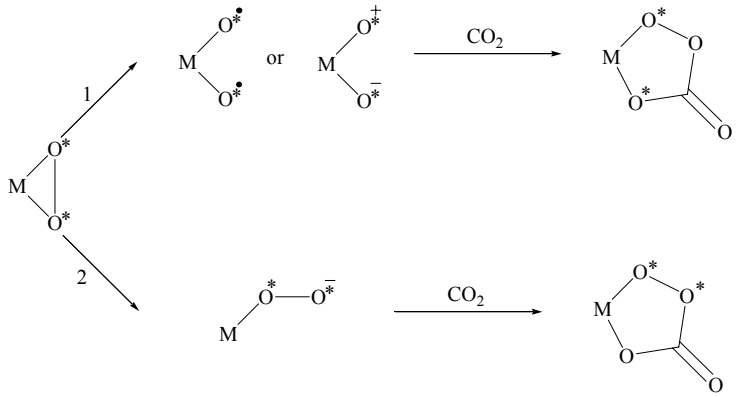

Figure 1-22. Generation of a metal peroxycarbonate ($L_nM(CO_4)X_m$) from its parent O_2 complex, $L_nM(O_2)X_m$, by passing CO_2 through a dry solution of the parent complex.[42]

For example, Nyman et al.[44,45] observed that when carbon dioxide was passed through a dry benzene solution of $(Ph_3P)_2PtO_2$, the platinum peroxycarbonate complex, whose structure is shown in Figure 1-23, was obtained. The complex was identified based on its infrared spectrum, chemical properties, and elemental analysis.

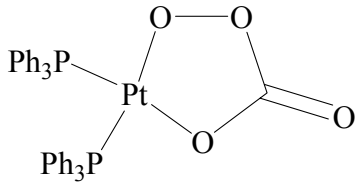

Figure 1-23. Structure of the $(Ph_3P)_2Pt(CO_4)$ complex of Nyman.[45]

Estimation of the peroxide content or oxidation power of the complex was attempted, but it was stated that no completely satisfactory method was found.[44] In general, the $(Ph_3P)_2Pt(CO_4)$ complex in the presence of acidified iodide solutions did produce an immediate color change attributed to the release of iodine, but the color faded. The loss of color was thought to occur via the oxidation of the triphenylphosphine, but no data were presented indicating that the oxidation products were identified. Unfortunately, attempts to oxidize organic species were not undertaken.

In 2001, Aresta et al.[43] examined the reactivity of $(PEt_2Ph)_3RhCl(CO_4)$ which was synthesized by passing CO_2 through the parent O_2 complex. She describes both the solution and solid state oxidation of one of the phosphine ligands. In solution, a solvent molecule displaces a phosphine ligand from the coordination sphere of the metal. The phosphine is proposed to act as a nucleophile and attack the electrophilic oxygen of the peroxycarbonate ligand. This reaction then yields the corresponding carbonato Rh complex and the oxidized phosphine (Figure 1-24, Route A).

In the solid state reaction, the presence of ethylene and the Rh complex does not yield ethylene oxide. The ethylene displaces a phosphine ligand from the coordination

sphere (Figure 1-24, Route B). The displaced phosphine then attacks the peroxycarbonate ligand and is oxidized. From these experiments it was concluded that the mechanism of oxidation does not occur by an intramolecular oxygen transfer from the peroxycarbonate ligand directly to the phosphine. For this particular complex, the phosphine must be displaced first before it can be oxidized.

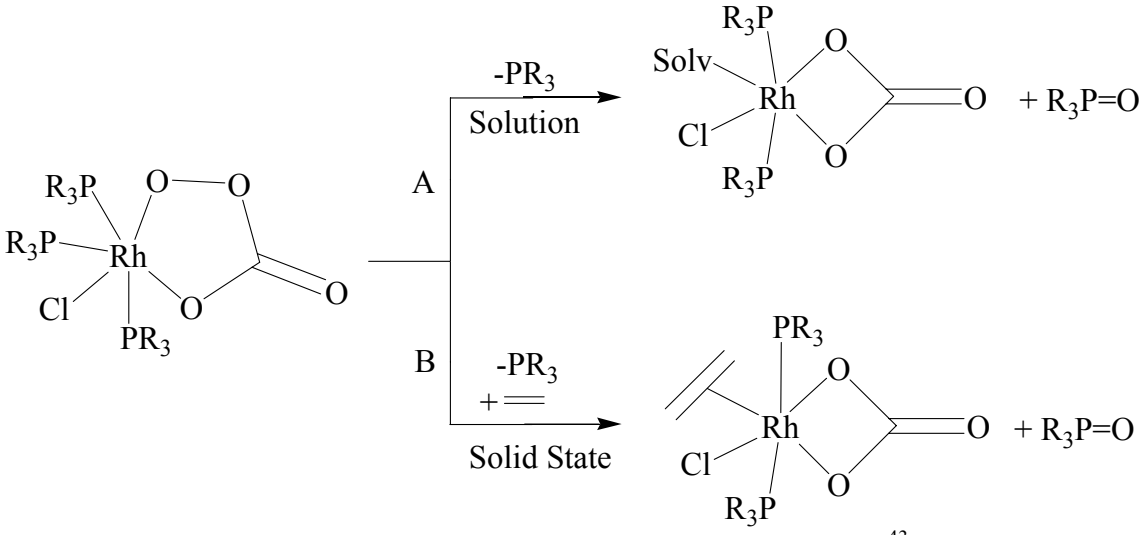

Figure 1-24. Routes for the oxidation of PR_3 by $(PEt_2Ph)_3RhCl(CO_4)$.[43] Route A shows the solution chemistry where a solvent molecule displaces a phosphine before it is oxidized. Route B shows the solid state chemistry where coordination of ethylene occurs first with the displacement of a phosphine ligand followed by oxidation of the ligand.

The $(PEt_2Ph)_3RhCl(CO_4)$ complex has also been observed to oxidize more reactive olefins, such as styrene.[43] When styrene (0.1 mL, 0.873 mmol) in 2 mL THF was allowed to react with $[(PEt_2Ph)_3RhCl(CO_4)]$ (0.100g, 0.16 mmol) under a CO_2/O_2 atmosphere (10:1 v:v), benzaldehyde, phenylacetaldehyde, phenyl methyl ketone, and styrene oxide were observed by GC/MS in a ratio of 1:3:3:5, respectively. The presence of benzaldehyde, phenylacetaldehyde, and phenyl methyl ketone suggest that the mechanism of oxidation occurs via radical chemistry as opposed to a simple oxygen transfer in which case styrene oxide would be the only product.

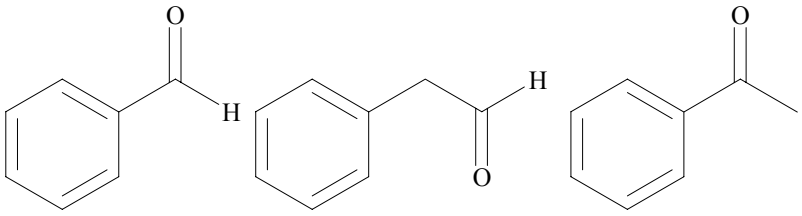

Benzaldehyde Phenylacetaldehyde Phenyl methyl ketone

Figure 1-25. Structure of products of styrene oxidation by $[(PEt_2Ph)_3RhCl(CO_4)]$ under a CO_2/O_2 atmosphere that indicate a radical mechanism.[43]

Transition-metal Activation of Peroxycarbonate in Solution

Recent work by Burgess et al.[39,40] has shown that the addition of certain transition-metal cations increases the catalytic rate of alkene epoxidation in solutions of hydrogen peroxide and bicarbonate in mixed solvent systems. Of the inorganic metal salts tested, manganese(II) sulfate produced the greatest increase in the epoxidation reaction. Along with an increase in the rate of epoxidation, the addition of Mn(II) to solutions of H_2O_2 and bicarbonate also enhances the rate of H_2O_2 disproportionation. The rate of disproportionation is enhanced to such a degree that methods must be employed to deal with the excessive amount of heat evolved. Recent studies by Bennett[46] have shown that the addition of the chelating agent diethylenetriaminepentaacetic acid (DTPA) inhibits the oxidation of alkenes, but only in some cases. This has been attributed to the removal of extraneous metal cations from the bicarbonate salts.[46]

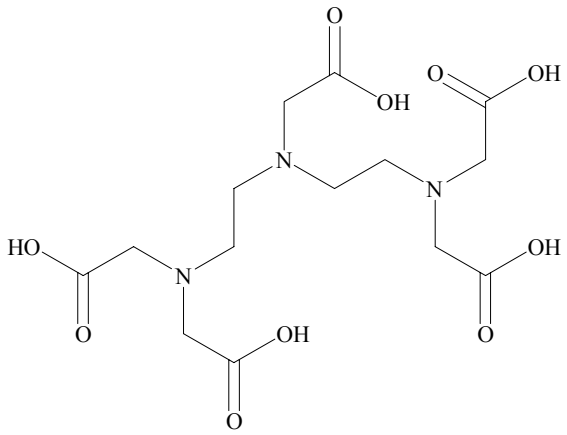

Figure 1-26. The structure of diethylenetriaminepentaacetic acid (DTPA)

In 1977, Sychev et al.[47] reported that hydrogen peroxide is rapidly disproportionated in the presence of bicarbonate and free Mn(II). In a series of papers from 1977 to 1984,[47-56] an investigation on the reaction mechanism of H_2O_2 decomposition with manganese(II) and bicarbonate was conducted. His proposed mechanism assumes that Mn(II) follows the Fenton type chemistry of Fe(II) with its reaction with H_2O_2 and therefore, proceeds via a free hydroxyl radical pathway. His work, however, does not provide adequate detail into the necessity of the bicarbonate ion in this reaction. Addition of similar anions, such as acetate, phosphate, oxalate, or borate, does not result in H_2O_2 disproportionation when Mn(II) is introduced. Also, the explanation provided by Sychev does not enlighten us in the observation that alkenes are cleanly oxidized to epoxide without detection of usual radical coupled products, as seen in the work by Aresta.[43]

Scope of the Dissertation

The goal of this current study is to further understand the reactive nature of the peroxycarbonate anion and dianion. Chapter 2 will discuss the reaction of Mn(II) and bicarbonate in the oxidation of styrene in micellar media. Both small and large scale oxidations of styrene were attempted and the results of these experiments will be presented. Questions arising from these experiments led us to investigate the hydrogen peroxide disproportionation reaction further.

The importance of peroxycarbonate in the Mn(II) catalyzed disproportionation of hydrogen peroxide will be the focus of Chapter 3. Kinetic investigations of the reaction have been conducted, and the results of these experiments will be presented. The lifetime of the catalyst was also investigated. The similarities between hydrogen peroxide disproportionation and nucleophilic alkene oxidation using Mn(II) was also of interest

during this study. A proposed mechanism for the hydrogen peroxide decomposition and alkene epoxidation will be introduced and numerical simulations of various proposed models for the disproportionation and alkene epoxidation will be presented.

Chapter 4 will discuss the use of the peroxycarbonate dianion as a nucleophilic oxidant for epoxidation of electrophilic alkenes. The results of experiments with the peroxycarbonate dianion will be compared with kinetic measurements using other nucleophilic oxidants. A summary and discussion of possible future work will comprise Chapter 5.

CHAPTER 2
OXIDATION OF NUCLEOPHILIC ALKENES IN AQUEOUS MICELLAR MEDIA

Introduction

Prior work by Bennett[46] and Yao[33] has shown that alkenes can be oxidized to the corresponding epoxides using bicarbonate-activated peroxide. Studies of hydrophobic alkenes were conducted in mixed solvent systems to all

ow for solubility of the alkene, while water-soluble alkenes were chosen for pure water studies. In general, epoxidations were found to be slow using peroxycarbonate solutions, but faster than background oxidations by hydrogen peroxide alone. It was also found that reactions proceed faster in pure water than in mixed solvent systems. The faster reaction in water has been attributed to a proton transfer, which proceeds faster in pure water than in mixed solvent systems.[32] It was also noted by Burgess et al.[40] that the addition of transition metal salts in the presence of hydrogen peroxide and bicarbonate in H_2O/DMF solutions accelerated the oxidation of alkenes. Of the transition-metals tested, manganese(II) sulfate produced the most dramatic increase in oxidation. In order to take full advantage of the use of transition-metal salts for alkene oxidation, surfactants were used to allow for the oxidation of hydrophobic alkenes in aqueous solution in the presence and absence of manganese(II) salts. The use of surfactants is also advantageous since the work by Bennett[46] indicates that the oxidation of alkenes tends to proceed faster in pure water.

Surfactants are long chain alkanes with hydrophobic tails and polar head groups, which allow for solubility in water. Three examples of common surfactants,

cetyltrimethylammonium chloride (CTACl), sodium dodecylsulfate (SDS), and Triton X-100, are found in Figure 2-1.

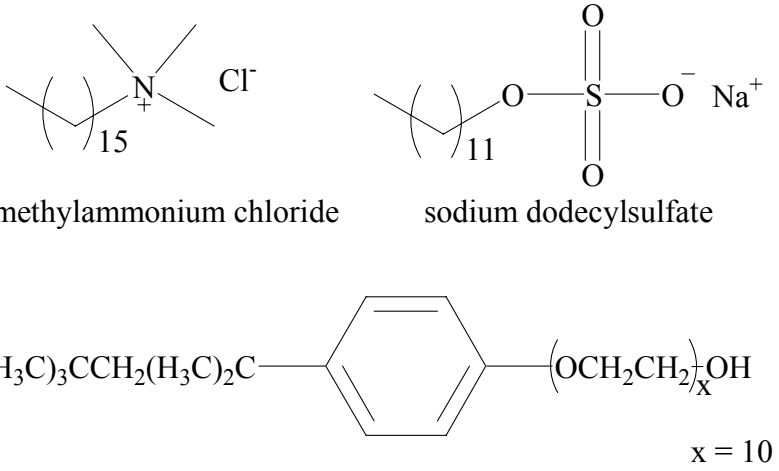

cetyltrimethylammonium chloride sodium dodecylsulfate

Triton X-100

Figure 2-1. The structures of three common surfactants. Cetyltrimethylammonium chloride is a cationic surfactant, while sodium dodecylsulfate is anionic. Triton X-100 is a non-ionic surfactant.

When dissolved in water, surfactants will begin to organize themselves into micelles after the concentration reaches a crucial level known as the critical micelle concentration (cmc),[57] which is a unique value for each surfactant and depends on the ionic strength of the solution. The detection of micellization can be accomplished by observation of the surface tension, refractive index, or conductivity (for ionic surfactants).[57]

At the cmc, the hydrophobic tails will begin to congregate, expelling water from the forming micelle's core, while the polar head groups will arrange to allow for the maximum interaction with water, as seen in Figure 2-2. The Stern layer is defined as the area around the micelle where the polar head groups are located, as are their counter ions.[57]

Normally, hydrophobic molecules are unable to dissolve is aqueous solution. However, if micelles are present, a hydrophobic molecule, such as an alkene, is able to penetrate into the hydrophobic core of the micelle and dissolve, as seen in Figure 2-3.

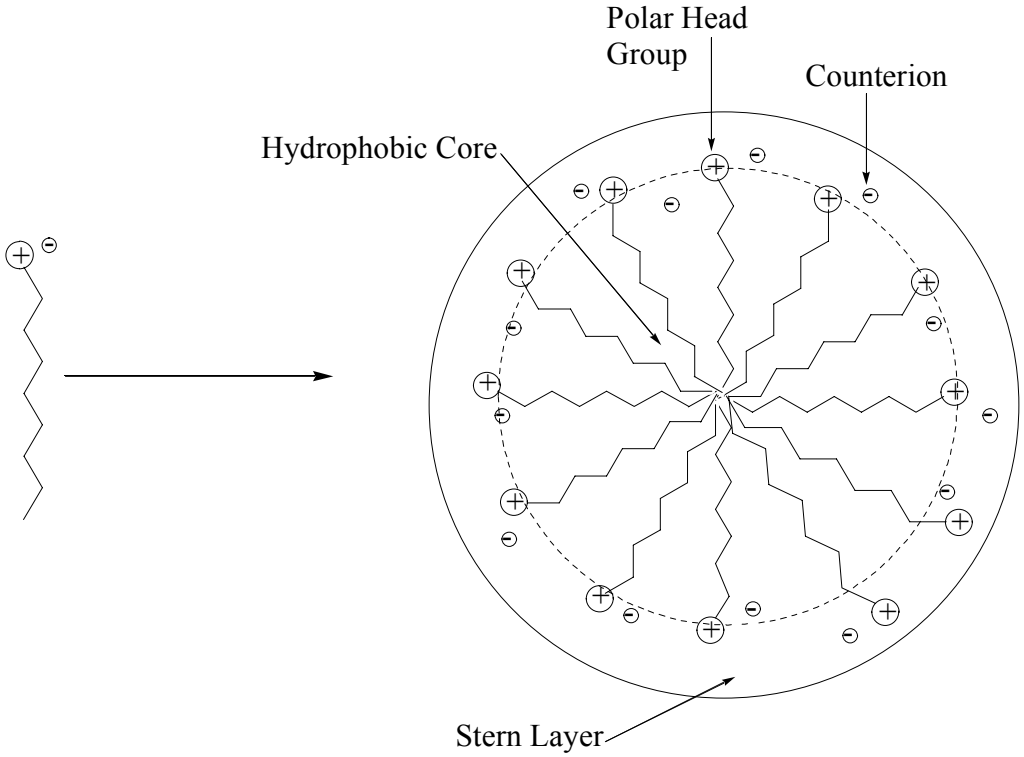

Figure 2-2. The structure of a micelle with a concentration greater then the cmc.

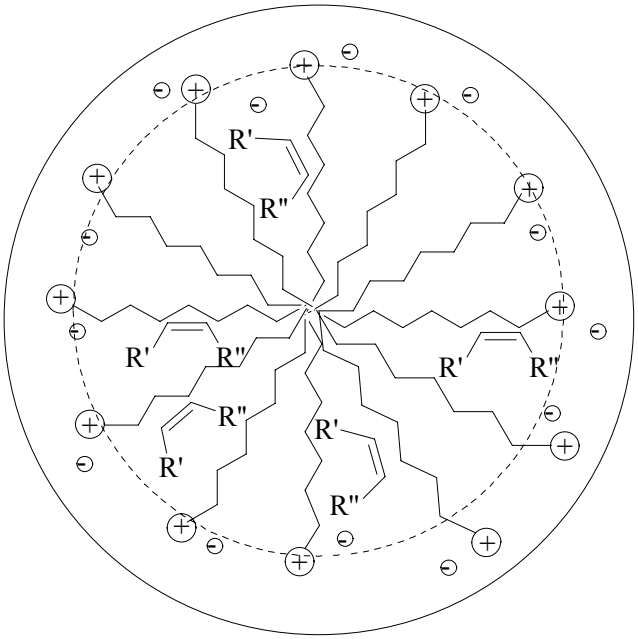

Figure 2-3. The graphical representation of an alkene dissolved in a micelle.

Results and Discussion

Styrene Oxidation in Micellar Media in the Absence of Mn(II)

Initially, styrene was oxidized in micellar media using the BAP method without the introduction of manganese(II) salts (Figure 2-4). Styrene (50 mM), CTACl (100 mM), H_2O_2 (2.00 M), and ammonium bicarbonate (1.00 M) in a volume of 250 mL were allowed to react in water for 3 days in the dark with stirring.

Analysis of the products by HPLC showed that approximately 90% of the starting styrene had reacted to yield the corresponding epoxide (~90 %), although significant hydrolysis to the corresponding diol has also been detected (~10%).

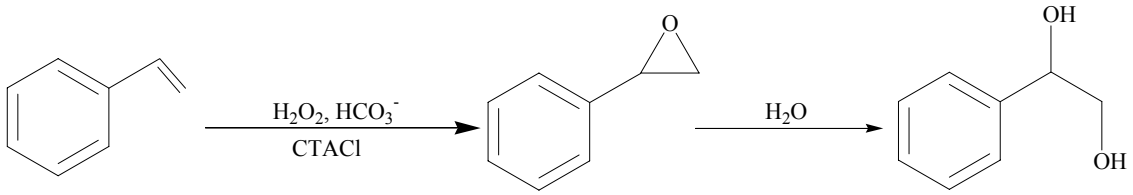

Figure 2-4. The reaction scheme for the oxidation of styrene by hydrogen peroxide in the presence of bicarbonate and cetyltrimethylammonium chloride (CTACl) without the presence of Mn(II). Hydrolysis of the product epoxide forms the corresponding diol. Reaction conditions: 0.05 M Styrene, 0.10 M CTACl, 2.00 M H_2O_2, 1.00 M NH_4HCO_3, 3 days

Large Scale Styrene Oxidation

In addition to small scale epoxidations of styrene in micellar media, large scale epoxidations were attempted. For a typical large scale epoxidation, 5 mL of styrene (175 mM), 230 mL CTACl (350 mM), 2.00 M H_2O_2, 39.6 g NH_4HCO_3 (1.00 M), and enough water (to bring the volume to 500 mL) were allowed to react in a total volume of 500 mL with stirring for 3 days in the dark at room temperature. For the small scale epoxidations, purification of the unreacted styrene and the styrene oxide product was unnecessary due to the use of HPLC for the analysis of the reaction products. For the large scale epoxidations, however, a purification method was required.

First, extraction with methylene chloride was attempted for the isolation of the styrene and styrene oxide. Since the surfactant would probably produce an emulsion, it was thought that if the reaction solution were diluted the emulsion would dissipate within a short amount of time. Unfortunately, this was not the case. The emulsion formed, even when the reaction was diluted to 2.5 L.

On occasion, allowing the emulsion to stand overnight would allow for small amounts of methylene chloride to be isolated from the extraction. Upon drying and removal of solvent, styrene oxide, the surfactant, and water were observed by ^{1}H NMR analysis. While the surfactant, CTACl in this case, is a cationic species and should not dissolve in organic solvents, the surfactant could form a reverse micelle, where the polar head groups now surround a small amount of water and the hydrophobic tails extend into the organic solvent.[57] This would explain why both surfactant and water are observed by ^{1}H NMR.

Given the unsatisfactory results from extraction, another method for purification of the organic products was required. The second method used for the purification of large scale styrene oxidations was liquid-liquid extraction. This purification method uses the same principal as extraction, but without the tendency to form emulsions. At first, for the large scale epoxidations, ether was used for the liquid-liquid extractions since only a lighter-than-water liquid-liquid extraction apparatus was immediately available. The setup of the apparatus is shown in Figure 2-5.

For the process of liquid-liquid extraction, a constant volume of organic solvent can be used to extract the organic product from the aqueous layer. This provides a convenient method for extracting slightly soluble organic products with a minimum

amount of organic solvent, as opposed to normal extraction procedures which typically require larger volumes of organic solvent.

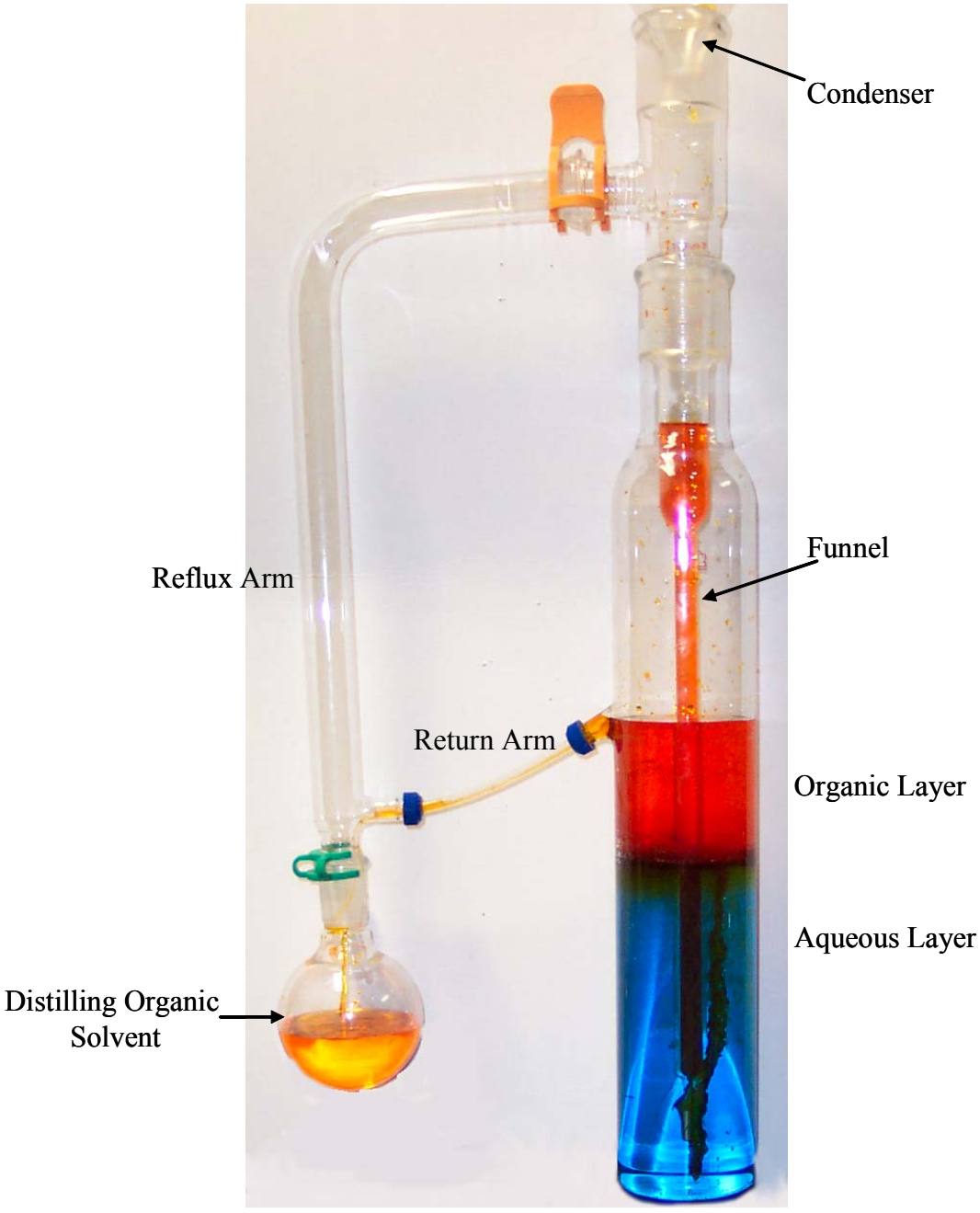

Figure 2-5. A picture of a lighter-than-water liquid-liquid extractor.

Initially, the organic solvent is layered over the aqueous solution. In addition, a small amount of organic solvent is placed in a round bottom flask connected to the reflux arm. Once the organic solvent in the round bottom has begun refluxing, it will be

liquefied in the condenser and collects in the funnel. As the organic solvent collects in the funnel, small amounts of the solvent will be pushed out the end of the funnel into the aqueous layer. As the organic solvent rises through the aqueous layer, a small amount of organic product will diffuse into the droplet. After a few minutes, enough organic solvent will have added to the solvent layered over the aqueous solution to allow the organic solvent to drip down the return arm back to the refluxing solvent. In this way, the organic product will slowly accumulate in the round bottom flask. After the extraction is complete, the solvent in the round bottom can be dried and the solvent removed to give the desired product, as would be done for a normal extraction process. The time of completion for the extraction must be determined experimentally for the unique conditions in which the extractor is being used. Heavier than water liquid-liquid extractions also exist and extract the organic product in a similar way.

For the large scale epoxidations, it was found that the highest yield of epoxide was observed after 3 days of liquid-liquid extracting. In addition to the styrene oxide, the corresponding diol was also present (~15%), when analyzed by HPLC. This is reasonable since after 3 days of reacting a 10% conversion to the diol is observed. The additional 3 days of extraction accounts for the additional 5% conversion of the epoxide to the diol product. On occasion, surfactant and water were still observed in the purified product, even when care was taken to assure that no emulsions were formed when layering the organic solvent over the aqueous layer in the extractor.

Styrene Oxidation in Micellar Media in the Presence of Mn(II)

Recent work by Burgess et al.[39,40] has shown that the introduction of transition-metal salts to oxidations of hydrophobic alkenes by H_2O_2 and bicarbonate in mixed solvent systems of dimethyl formamide (DMF) and water show a significant rate

enhancement, Figure 2-6.[39,40] Upon addition of a transition-metal salt, epoxidations with reaction times greater than 48 hours were decreased to only 16 hours. The main drawback, specifically the long reaction times, to Burgess' method has been the slow addition of the H_2O_2 and bicarbonate solutions to DMF to minimize precipitation.[40] This rate enhancement is greatest when the inorganic salt added is manganese(II) sulfate.

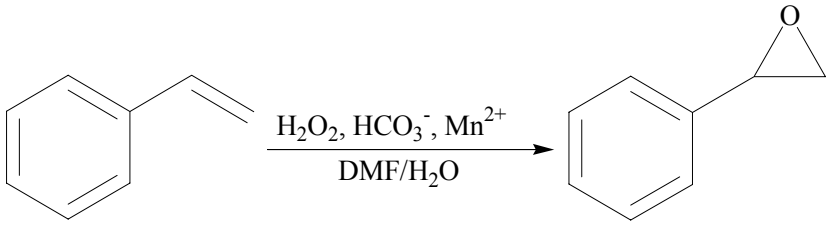

Figure 2-6. Reaction scheme used by Burgess[40] in the mixed solvent epoxidation of styrene.

Our current method of alkene epoxidation using micellar media offers a better alternative to the mixed solvent system employed by Burgess, Figure 2-7. The main drawback seen by Burgess, namely the slow addition of the H_2O_2/bicarbonate solution, is not an issue in micellar media. The organic substrate is dissolved by the micelle, and all of the remaining reactants are freely soluble in water, so precipitation is no longer of concern. When a test reaction was performed using styrene (50 mM), CTACl (100 mM), H_2O_2 (2.00 M), NH_4HCO_3 (1.00 M), and only 10 μM $MnSO_4$, the epoxidation was complete in less than 30 minutes as seen by the HPLC chromatograms in Figure 2-8, as opposed to 3 days in the absence of manganese(II).

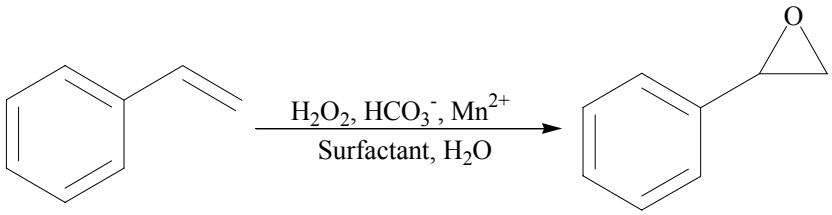

Figure 2-7. Schematic representation for the oxidation of styrene in surfactant with hydrogen peroxide and bicarbonate catalyzed by manganese(II). Reaction conditions: 50 mM styrene, 0.10 M CTACl, 2.00 M H_2O_2, and 1.00 M NH_4HCO_3, 30 minutes.

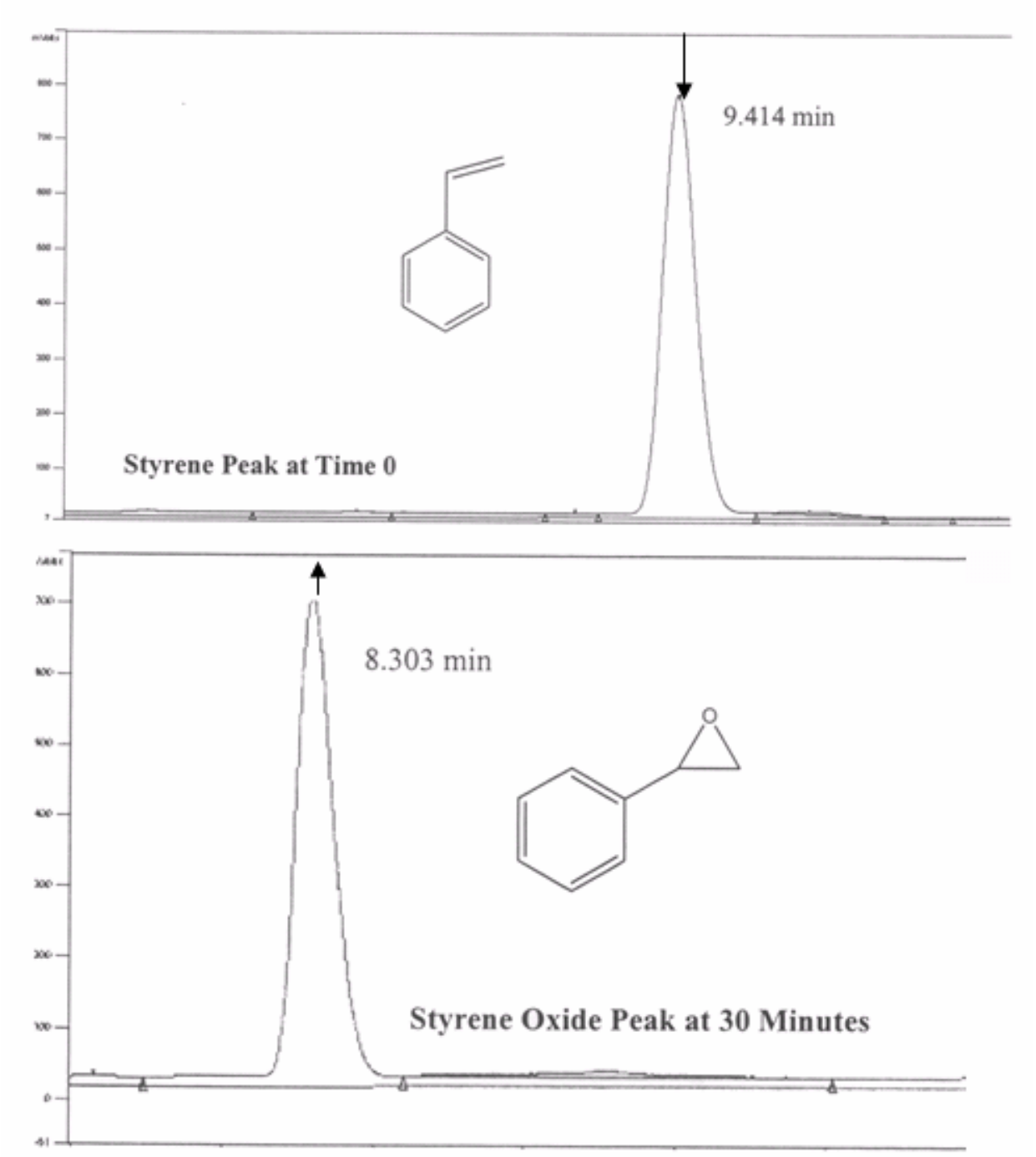

Figure 2-8. HPLC chromatograms for the initial reaction (top panel) and after 30 minutes (bottom panel) for the oxidation of styrene with H_2O_2, HCO_3^-, and Mn(II) in the presence of surfactant (CTACl). HPLC performed using a C18 reverse phase column using a non-linear gradient for 12 minutes. Mobile Phase: 25%:75% (v:v) CH_3CN:H_2O – 95%:5% CH_3CN:H_2O

Reaction Kinetics

Kinetic experiments were conducted to determine the dependence of various conditions, including the identity of the surfactant, the source of the manganese, and the bicarbonate concentration, on the manganese(II) catalyzed oxidations of styrene in micellar media. For these reactions, aliquots of reaction solutions were removed over time and added to a solution of bovine catalase to destroy any remaining H_2O_2 and therefore, quench the reaction. The aliquots were then diluted with acetonitrile and analyzed by HPLC. Figure 2-9 shows a representative graph demonstrating the disappearance of styrene versus time. From a plot of the ln(styrene area) versus time, the first-order rate constant can be determined from the slope of line, as shown in Figure 2-10.

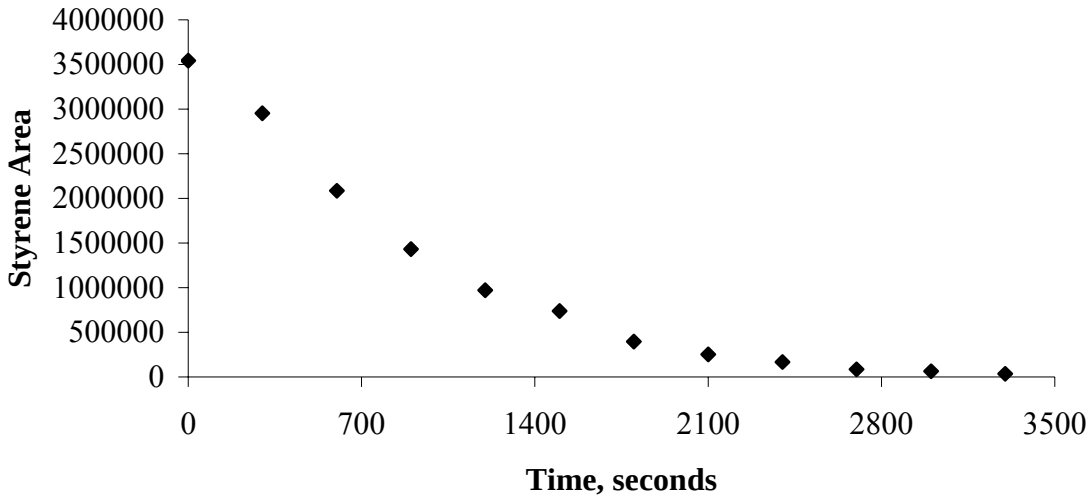

Figure 2-9. Styrene area disappearance versus time from the HPLC analysis of styrene oxidation by hydrogen peroxide in micellar media in the presence of bicarbonate and Mn(II). Reaction conditions: 0.05 M Styrene, 0.100 M CTACl, 0.25 M NH_4HCO_3, 1.00 M H_2O_2, 10 μM Mn(II).

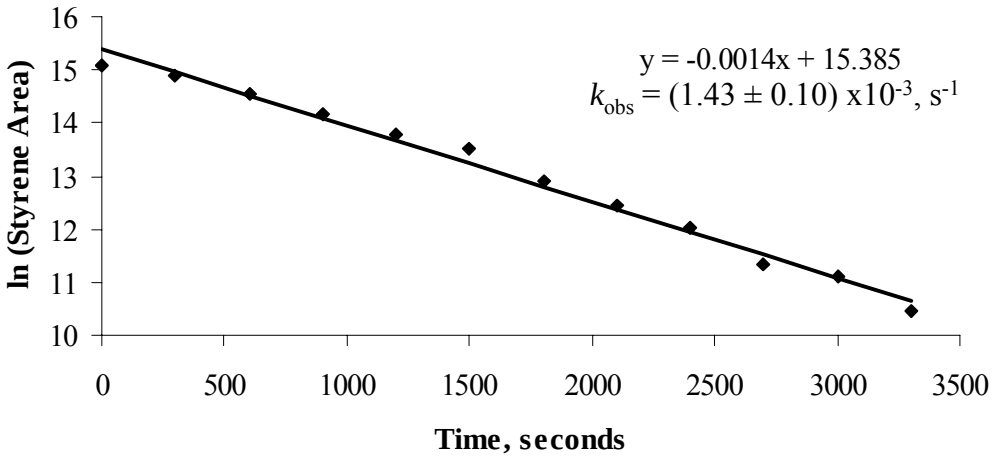

Figure 2-10. ln(styrene area) versus time to find the first-order rate constant. The line is the linear regression to the data at the 95% confidence. The k_{obs} is the negative slope of the line.

Dependence of Styrene Oxidation on Surfactant Identity

For all reactions previously described, the surfactant used was cetyltrimethylammonium chloride, a cationic surfactant. In order to determine whether the active species is charged, the oxidation of styrene was performed under the same conditions as described except for the substitution of sodium dodecylsulfate (SDS) for CTACl. If the active catalytic species is positively charged, the reaction should proceed faster in the anionic micelle due to attractive forces between the micelle and the active oxidant. If the active oxidant is negatively charged, the reaction should be slower in the anionic micelle due to the repulsive force between the micelle and the active oxidant. Conversely, if the active catalyst is uncharged, no difference in the rate of the reaction should be observed. From the data presented in Table 2-1, the observed rate constants for the oxidation of styrene in the two surfactants give the same observed first-order rate constants (within error), therefore, the conclusion must be that the active manganese oxidant is uncharged.

Table 2-1. Comparison of Styrene Oxidation in CTACl and SDS for the Mn(II) catalyzed epoxidation. Reaction conditions: 0.05 M Styrene, 0.100 M CTACl or SDS, 0.25 M NH_4HCO_3, 1.00 M H_2O_2, and 10 μM Mn(II). Errors are reported to the 95% confidence.

Surfactant	k_{obs}, s^{-1}
Cetyltrimethylammonium chloride	$(1.39 \pm 0.10) \times 10^{-3}$
Sodium dodecylsulfate	$(1.50 \pm 0.15) \times 10^{-3}$

Dependence of Styrene Oxidation on the Manganese(II) Source

In addition to testing whether the surfactant made an impact on the reaction, the addition of the metal was also examined. When bulk manganese(II) is added to the solution containing SDS, the manganese(II) ions must exchange with sodium ions at the surface of the micelle.

Manganese(II) bisdodecylsulfate ($Mn(DS)_2$) was synthesized to allow for the metal to be added already bound to the surfactant. $Mn(DS)_2$ is precipitated by the addition of saturated sodium dodecylsulfate and saturated manganese(II) chloride. Since the manganese(II) is bound to the surfactant, all of the manganese(II) should be bound to the micelle surface.

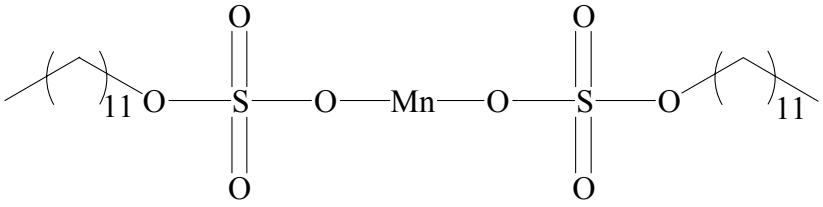

Figure 2-11. Structure of manganese(II) bisdodecylsulfate.

When the reaction was performed using 10 μM $Mn(DS)_2$, an identical observed first-order rate constant, within error, was observed in comparison with the reaction with the addition of bulk manganese(II). The results of this experiment indicate that with the addition of bulk manganese(II), the metal is in rapid equilibrium with the sodium ions at the micelle surface. So, in the case of $Mn(DS)_2$, the metal is not remaining at the micellar surface, but is rapidly being released into the bulk solution by exchange with sodium

ions. It is, therefore, unnecessary to add the metal already bound to the surfactant, since the bulk metal rapidly exchanges with sodium ions at the micellar surface.

Table 2-2. Comparison of observed rate constants for differing manganese sources for micellar styrene oxidation. Reaction conditions: 0.05 M Styrene, 0.100 M SDS, 0.25 M NH_4HCO_3, 1.00 M H_2O_2, and 10 μM Mn(II) or $Mn(DS)_2$. Errors are reported to the 95% confidence.

Manganese Source	k_{obs}, s^{-1}
Bulk Manganese (Mn^{2+})	$(1.50 \pm 0.15) \times 10^{-3}$
$Mn(DS)_2$	$(1.43 \pm 0.07) \times 10^{-3}$

Bicarbonate Dependence

The bicarbonate dependence on the styrene oxidations in micellar media was also investigated. When a plot of k_{obs} versus $[HCO_3^-]$ was made, as seen in Figure 2-12, the rate has saturated by 0.25 M bicarbonate. This finding was unexpected, since previous work on sulfide and alkene oxidations did not show saturation with bicarbonate at concentrations similar to those used here.[32,41] It is apparent, therefore, that the addition of the surfactant is concentrating the active oxidant near the micelle surface in order for the oxidation to be saturating. Since the active oxidant had not been examined at this time, it was impossible to make any conclusive remarks about how the micelle was affecting the epoxidation of styrene by manganese(II) and bicarbonate with hydrogen peroxide in the presence of surfactant. In order to further understand the use of the manganese(II) as a catalyst for the epoxidation of alkenes, the hydrogen peroxide disproportionation reaction needed to be better understood. The hydrogen peroxide disproportionation can be examined in the absence of surfactant, since all of the reactants are fully water soluble. If the active oxidant can be identified, further experiments can then be designed to probe the nature of the oxidant in micellar oxidations of alkenes. The results of experiments with the disproportionation reaction are presented in the next chapter.

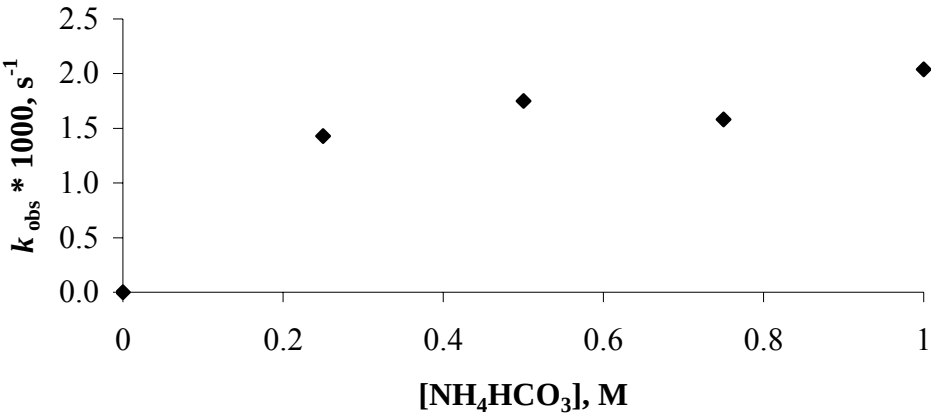

Figure 2-12. Graph of k_{obs} versus [NH_4HCO_3] for the styrene oxidation in the presence of 0.100 M CTACl. Reaction conditions: 0.05 M Styrene, 0.100 M CTACl, 1.00 M H_2O_2, and 10 μM Mn(II).

Experimental

Materials and Instrumentation

Sodium bicarbonate, sodium acetate, styrene, and manganese (II) sulfate were all analytical grades and obtained from Fisher (Atlanta, GA). Cetyltrimethylammonium chloride was obtained from Aldrich (St. Louis, MO). Hydrogen peroxide (35 and 50%) was obtained from Fisher (Atlanta, GA) and standardized often by iodometric titration. Water was purified using a Barnstead E-Pure 3-Module Deionization System. Extraneous metal ions from salt solutions were removed by passing the solutions through a Chelex 100 resin obtained from Aldrich (St. Louis, MO). Sodium bicarbonate solutions were standardized using the method below before use to assure concentration.

UV-vis kinetic experiments were obtained using a Hewlett-Packer 8453 spectrophotometer using 1.0 cm quartz cells from Starna Cells, Inc. Temperature was maintained at 25 (± 0.1) ºC using a Fisher Isotemp 1600S water bath circulator.

Styrene oxidation reactions were analyzed by High Performance Liquid Chromatography (HPLC) using a Rainin HPLX solvent delivery system with a C-18 reverse phase column. The method consisted of a non-linear gradient of mobile phase A:H_2O and mobile phase B:CH_3CN from 75:25 A:B to 5:95 over a 12 minute period. Products were detected at 221 nm.

Standardization of Sodium Bicarbonate Solutions

Solutions of sodium bicarbonate were standardized before each kinetic experiment to determine the concentration eluting from the Chelex 100 column. All solutions were delivered using volumetric pipets. A 10 mL aliquot of sodium bicarbonate solution exiting the Chelex 100 column was a placed in a clean, dry beaker. An excess amount of sodium hydroxide solution of a known concentration, by titration with potassium hydrogen phthalate, was added to the beaker. The solution was stirred to allow for complete deprotonation of the bicarbonate to form the carbonate dianion. An excess barium chloride solution is then added to precipitate all of the carbonate dianion as barium carbonate. Phenolphthalein is then added to the mixture to give a pink color due to the residual hydroxide ion. The mixture is titrated using a known concentration of hydrochloric acid until the solution just turns clear. The number of moles of hydrochloric acid added is equal to the excess moles of sodium hydroxide. The difference between the number of moles from the acid titration and the number of moles of hydroxide ion initially added equals the number of moles of bicarbonate present in the initial 10 mL aliquot (Equation 2-1). The molarity of the solution can then be determined.

$$\#\text{moles } OH_{init} - \#\text{moles } OH_{excess} = \#\text{moles bicarbonate} \quad (2\text{-}1)$$

Styrene Oxidation Reactions

Kinetic experiments of styrene oxidations were performed in micellar solutions and analyzed by the decreasing area of the styrene peak by HPLC. Reactions were performed using 0.05 M styrene, varying ammonium bicarbonate, 1.00 M H_2O_2, and 0.10 M surfactant, where the surfactant was either cetyltrimethylammonium chloride or sodium dodecylsulfate (CTACl and SDS, respectively). For reactions using manganese(II), as either manganese sulfate of $Mn(DS)_2$, 10 μM was added to the reactions. Aliquots (100 μL) of the reaction mixture were taken over time and quenched using a catalase solution, which converts any excess H_2O_2 to O_2 and H_2O, thus removing the terminal oxidant. Each of the aliquots is then diluted with CH_3CN to an appropriate concentration for HPLC analysis. The k_{obs} is calculated using pseudo-first order plots of the ln(styrene area) vs. time. First-order plots were linear for the conditions studied.

Large Scale Styrene Oxidations

Large scale styrene epoxidations were conducted in micellar solutions. Reactions were performed using 175 mM Styrene (5 mL), 350 mM CTACl, 1 M NH_4HCO_3, and 2.0 M H_2O_2 in a total volume of 500 mL, where the remaining volume is water. The reaction was allowed to stir in the dark for 3 days. The reaction mixture was then diluted to 1 L and poured into a lighter than water liquid-liquid extractor. Ether was then layered on top of the aqueous reaction solution, and the extractor was allowed to extract for 3 days. After cooling the receiving flask after 3 days, magnesium sulfate was added to dry the solvent. After filtering off the magnesium sulfate and removing the solvent under reduced pressure, the organic residue was analyzed by ^1H NMR.

Synthesis of $Mn(DS)_2$

$Mn(DS)_2$ was synthesized by mixing equal parts saturated manganese(II) chloride and saturated sodium dodecylsulfate in water to form a while solid. The solid was then filtered and washed with ice-cold water. Calculated for $C_{24}H_{50}S_2O_8Mn{\cdot}4H_2O$ Calc: C: 43.82% H:8.89% S:9.75% O:29.19%Mn:8.35% Found C: 43.65% H:9.10%

Styrene Oxidation in SDS with Mn(II) and $Mn(DS)_2$

Styrene oxidations were performed using 0.05 M styrene, 0.500 M ammonium bicarbonate, 1.00 M H_2O_2, and 0.10 M sodium dodecylsulfate. Manganese(II) was added as either 10 μM bulk manganese(II) or 10 μM $Mn(DS)_2$. Aliquots of the reaction mixture were taken over time and quenched using a catalase solution, which converts any excess H_2O_2 to O_2 and H_2O. Each aliquot is then diluted with CH_3CN to an appropriate concentration for HPLC analysis. The k_{obs} are calculated using pseudo-first order plots of the ln(styrene area) vs. time. First order plots were linear for the conditions studied.

CHAPTER 3
KINETIC INVESTIGATIONS OF THE MANGANESE(II) CATALYZED DISPROPORTIONATION OF HYDROGEN PEROXIDE IN THE PRESENCE OF BICARBONATE AND THE COMPARISON TO NUCLEOPHILIC ALKENE EPOXIDATION

Introduction

Investigations on the use of manganese(II) in the catalysis of alkene epoxidation presented in the preceding chapter raise some interesting questions about the hydrogen peroxide disproportionation under the reaction conditions. Namely, what is the active manganese species? Why is bicarbonate necessary for the reaction to proceed?

In 1977, Sychev et al.[47] reported that hydrogen peroxide disproportionates rapidly in the presence of bicarbonate and free manganese(II). In a series of papers from 1977 to 1984,[47-56] Sychev studied the mechanism of peroxide decomposition. His proposed mechanism assumes that manganese(II) follows the Fenton chemistry of iron(II) in its reaction with peroxide, and therefore, proceeds via a free hydroxyl radical pathway. His work, however, does not provide adequate detail into the unique catalytic ability of the bicarbonate ion in this reaction or the identity of the active manganese species.

In 1990, Stadtman et al.[58] also investigated the use of the manganese(II) catalysis as a method for oxidation of amino acids. The decomposition of hydrogen peroxide by manganese(II) with bicarbonate was also examined during their studies. As with the work of Sychev, Stadtman does not provide an explanation for the unique reactivity of bicarbonate or speculate about the active manganese species responsible for the catalysis.

In this chapter, kinetic investigations on the manganese(II) catalyzed decomposition of hydrogen peroxide in the presence of bicarbonate will be presented. The bicarbonate, manganese(II), and hydrogen peroxide dependencies measured during this study are similar to those reported by Sychev,[47] but differ slightly from those observed by Stadtman.[58] The observed differences in the dependence are probably due to the conditions under which the reaction was examined. For this work and for that of Sychev, the hydrogen peroxide and bicarbonate concentrations were in the 100-500 mM range, with a 0-10 μM Mn(II) concentration. For the studies performed by Stadtman, the hydrogen peroxide and bicarbonate concentrations were in the 30 mM range, with much larger Mn(II) concentrations of 0.10 mM. The dependencies measured during this study are also similar to those observed by Bennett[46] for the epoxidation of nucleophilic alkenes by hydrogen peroxide in the presence of bicarbonate catalyzed by manganese(II).

Investigations on the lifetime of the catalyst have also been conducted. While the catalyst is still active upon addition of hydrogen peroxide to spent solutions, the reactivity is about half of the original activity. These results are consistent with those reported by Stadtman. Two factors have been identified to explain the loss of activity.

Experiments have also been conducted to examine whether the manganese source has an impact on the reaction. Three different manganese sources were used in this study and include manganese(II) sulfate, potassium permanganate, and a Mn(IV)-TACN complex. The results of these experiments indicate that the source of the manganese has no effect on the observed rate of hydrogen peroxide decomposition.

Experiments were also conducted using cis-alkenes to discern information about the mechanism of oxygen transfer from the active catalyst. Results from these

experiments indicate that the oxygen atom is not being transferred in a concerted fashion, since cis/trans isomerization is observed in the epoxidation of nucleophilic alkenes.

Investigations of the radical traps used in the work by Sychev led to the interesting result that amines can react with this system to yield *N*-dealkylated products. Reports on oxidative *N*-dealkylation are not common in the literature. Current knowledge of oxidative *N*-dealkylation comes from studies with cytochrome P-450. The most accepted mechanism for the oxidative *N*-dealkylation of amines begins with a single electron transfer from the amine to a metal in a high oxidation state. A mechanism using manganese species that will be proposed in this study will be presented.

Solvent isotope effects have been measured for the nucleophilic alkene epoxidation and hydrogen peroxide decomposition. A large, inverse isotope effect was observed for the alkene oxidation, while a normal isotope effect was observed for the hydrogen peroxide decomposition. The results of the nucleophilic alkene oxidation are consistent with those observed by Bennett. An attempt to justify the difference in the observed solvent isotope effects will be presented.

Finally, a mechanism based on the work from this study will be presented in an attempt to explain both the nucleophilic alkene epoxidation and hydrogen peroxide decomposition. Numerical simulation has been employed as a tool in the attempt to understand the reaction kinetics. Several models will be presented and discussed.

Results and Discussion

Kinetics of Hydrogen Peroxide Decomposition

Hydrogen peroxide disproportionation, Figure 3-1, was followed spectrophotometrically by monitoring the decreasing peak intensity at 263 nm. The hydrogen peroxide concentration was held constant at 0.10 M, while the sodium

bicarbonate was varied in concentration from 0.0-0.60 M. The manganese(II) concentration was varied in the range from 0-30 μM.

$$2\ H_2O_2 \underset{NaHCO_3,\ buffer}{\overset{Mn(II)}{\rightleftharpoons}} 2\ H_2O\ +\ O_2$$

Figure 3-1. Hydrogen peroxide decomposition in the presence of manganese(II) and bicarbonate.

In order to maintain a constant pH of 8.4 and an ionic strength of 1.00 M, two buffering systems were tried. Initially, sodium phosphate buffer was used, but it was discovered that the phosphate anion causes the manganese to precipitate. Also, the phosphate buffer did not maintain the pH. Even with higher concentrations, the pH would continue to rise during the experiment.

Eventually, sodium acetate was employed to control ionic strength and stabilize pH. While sodium acetate is not actually a buffer at pH 8.4, the addition of the salt in the solutions allowed for the stabilization of the pH. To exclude acetate as participating in the mechanism, a set of experiments were conducted in the absence of acetate. While the pH did change slightly during these reactions, the observed rate constants were nearly identical to those in the presence of acetate.

Solutions of hydrogen peroxide, bicarbonate, and sodium acetate were allowed to equilibrate for at least 15 minutes before kinetic experiments were performed. Addition of a solution of the manganese(II) was always preformed last to initiate the reaction. To ensure that the order of reagent addition does not have an effect on the reaction, experiments were conducted which were initiated by the addition of hydrogen peroxide. These experiments gave nearly identical observed rate constants as those initiated by manganese(II), therefore, the order of reagent addition makes no significant difference to the overall reaction rates.

The disproportionation reaction was monitored for greater than two half-lives. Linear first-order plots were only obtained under certain conditions from the absorbance decay by plotting the equation $((A_t-A_\infty)/(A_0- A_\infty))$ versus time, as seen in Figure 3-2. In most cases, however, linear first-order plots were not obtained. For these instances, the first-order plots were used as an attempt to approximate an observed first-order rate constant. In all cases, the reaction accelerates near the end of the reaction. The hypothesis is that hydrogen peroxide is an inhibitor of the reaction. As the concentration of hydrogen peroxide drops, an acceleration in the peroxide decomposition will occur. Further details concerning this aspect of the reaction will be presented in the section discussing the numerical simulations.

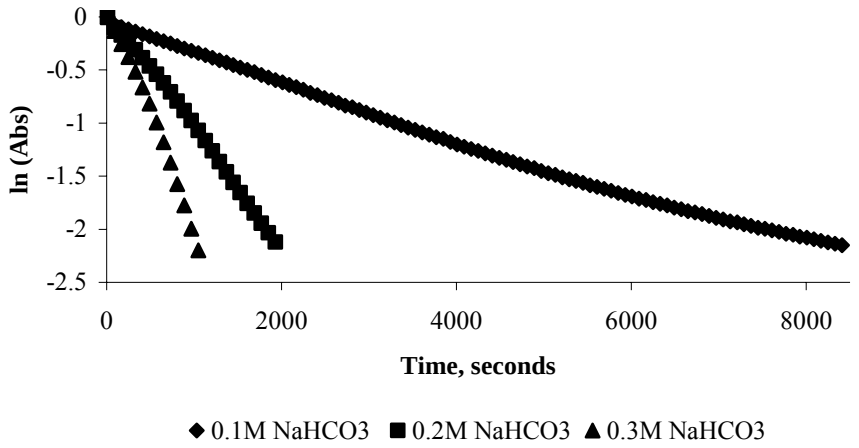

Figure 3-2. Plot of the ln($[H_2O_2]$) versus time for varying bicarbonate concentration. The 0.20 and 0.30 M bicarbonate reactions are typical of the accelerations noticed for these reactions. Reaction conditions: 0.10 M H_2O_2, 4 μM Mn(II).

The slope of the line produced by linear regression, of those plots that are linear, is the negative of k_{obs}. For reactions that were not linear, pseudo "k_{obs}" were attempted to be used to analyze the data for these reactions. Background disproportionation of peroxide in bicarbonate and acetate buffered solutions was negligible for the time scale of the catalytic disproportionations.

Manganese(II) Dependence

The plot of k_{obs} versus Mn(II) concentration gives a straight line with a y-intercept of 0 for the range of Mn(II) from 0–6.0 μM, as seen in Figure 3-3, indicating a first-order dependence of Mn(II) on the reaction in that range. Since the hypothesis is that the catalytic disproportionation of peroxide is metal dependent, a y-intercept of 0 is expected. The straight line plot indicates that only one manganese ion is found in the transition state complex. These data indicate that a multiple metal center complex is not involved in the disproportionation reaction under aqueous conditions. This is significant since much of the current literature on metal catalyzed peroxide disproportionation focuses on complexes with multiple metal centers.[59-62] Scatter in the Mn(II) data begins to appear at about 6.0 μM. The turnover in the data is attributed to precipitation of manganese(II) carbonate.

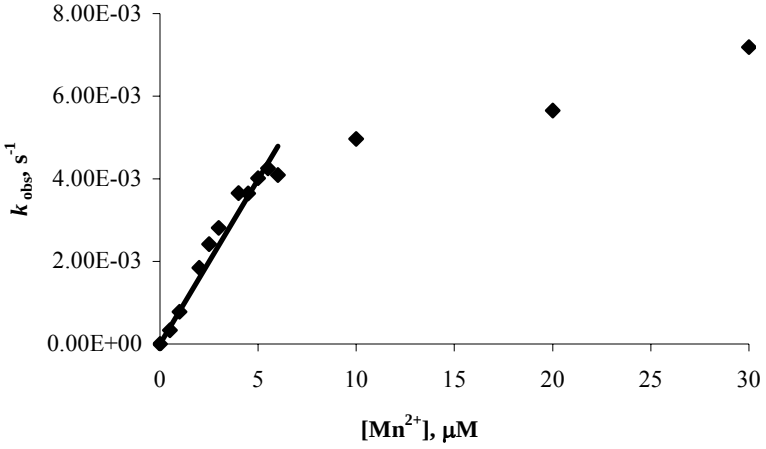

Figure 3-3. The dependence of k_{obs} on the [Mn(II)]. Reaction conditions: 0.10 M H_2O_2, 0.4 M HCO_3^-, varying [Mn(II)]. $y = ((7.98 \pm 0.62) \times 10^{-4})x$, error reported to the 95% confidence.

The solubility-product constant (K_{sp}) is defined as the equilibrium constant between the ions in solution and the precipitated solid. An example using manganese(II) carbonate is given below.

$$MnCO_3(s) \rightleftharpoons Mn^{2+}(aq) + CO_3^{2-}(aq) \quad (3\text{-}1)$$

$$K_{sp} = [Mn^{2+}]*[CO_3^{2-}] \quad (3\text{-}2)$$

The K_{sp} is reached at ~6.50 μM Mn(II), given a constant bicarbonate concentration of 0.40 M, a pH of 8.4, and a K_{sp} of 2.72 x10^{-7}, the conditions under which the Mn(II) dependence was measured. This corresponds well with the turnover in the manganese dependence, Figure 3-3. This turnover was also observed by Sychev[47] for his experiments on peroxide disproportionation in bicarbonate solutions with manganese(II), but further data as to why the turnover occurred were not presented. The explanation given in the text simply referred to possible precipitation of manganese salts.

Bicarbonate Dependence

Studies of the dependence of sodium bicarbonate on the rate law indicate a second-order dependence, as seen in Figure 3-4. The plot of k_{obs} versus $[HCO_3^-]^2$ produces a straight line with a y-intercept of 0. The data begins to scatter at higher bicarbonate concentration for two reasons. First, the reactions become very fast and getting accurate data becomes more difficult. Second, the higher bicarbonate reactions have a more pronounced curve in the ln plots (as discussed earlier), therefore the "k_{obs}" reported is not a true first-order rate constant. As with Mn(II), since the disproportionation of peroxide is dependent on the bicarbonate concentration, a y-intercept of 0 is expected. For the sodium bicarbonate, however, a second-order dependence reveals that two bicarbonate ions are present in the transition state complex of the rate determining step. Presumably, one of these bicarbonate ions is in the form of peroxycarbonate, while the other may simply be coordinated to the metal center. Similar results were found for the nucleophilic alkene epoxidations studied by Bennett[46] and the hydrogen peroxide decomposition

studies of Sychev.[47] Stadtman,[58] on the other hand, reports a third-order dependence on the bicarbonate concentration. The difference in the order of the reaction could be due to the reaction conditions that were used, since the hydrogen peroxide and bicarbonate were much lower than this study and the manganese was much higher. Currently, with the proposed mechanisms that will be presented later, a third-order dependence has not be observed in the numerical simulations.

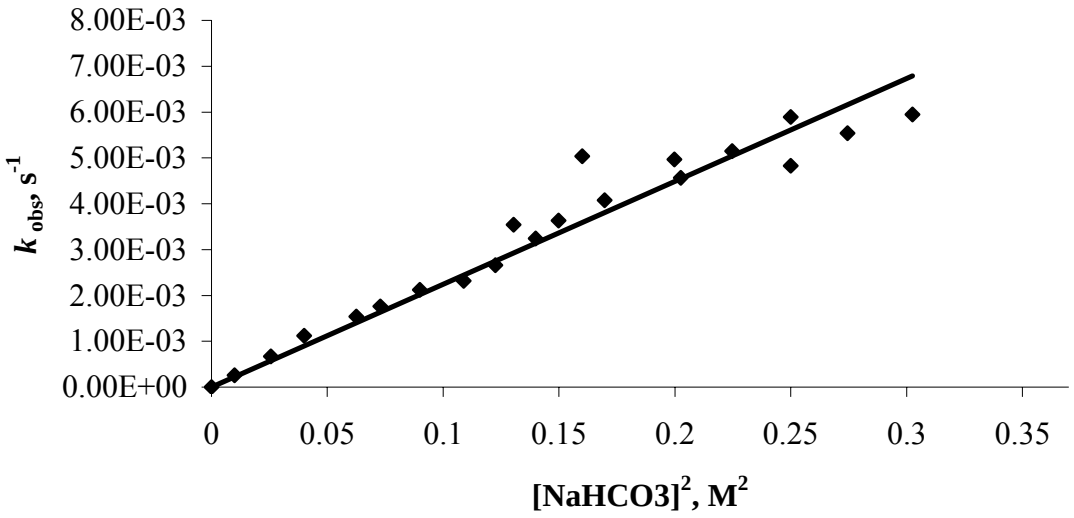

Figure 3-4. Plot of k_{obs} versus $[NaHCO_3]^2$. Reaction conditions: 0.10 M H_2O_2 and 4 μM Mn(II). $y = ((2.08 \pm 0.25)\ x10^{-3})x$, error reported to the 95% confidence.

The overall rate equation defined by the results above is given in Equation 3-3. At this time, no reliable method has been found to study the hydrogen peroxide dependence, so, its dependence for the hydrogen peroxide decomposition has yet to be observed. Numerical simulations which will be presented later indicate that there is an inverse dependence of the hydrogen peroxide concentration. It is for this reason that the ln plots curve near the end of the reactions. As the hydrogen peroxide decays, the reactions begin to accelerate.

$$v = k_{obs}[Mn(II)][HCO_3^-]^2[H_2O_2]^x \quad (3\text{-}3)$$

Comparison of Hydrogen Peroxide Reaction Kinetics to Nucleophilic Alkene Epoxidation Kinetics

In order to better understand the nature of the active catalyst in the manganese dependent hydrogen peroxide disproportionation, the results of the kinetic investigation of hydrogen peroxide decomposition need to be compared to the results observed by Bennett[46] for the manganese(II) dependent nucleophilic alkene epoxidation observed in pure water using sulfonated styrene and 4-vinylbenzoic acid. A summary of her results for the study of sulfonated styrene are presented here.

Manganese dependence on nucleophilic alkene epoxidation

Bennett[46] examined the manganese dependence on the oxidation of sulfonated styrene in bicarbonate solution (1.00 M) with 1.00 M hydrogen peroxide. The dependence on manganese was shown to be linear in the range of 0 – 5.0 μM, Figure 3-5.

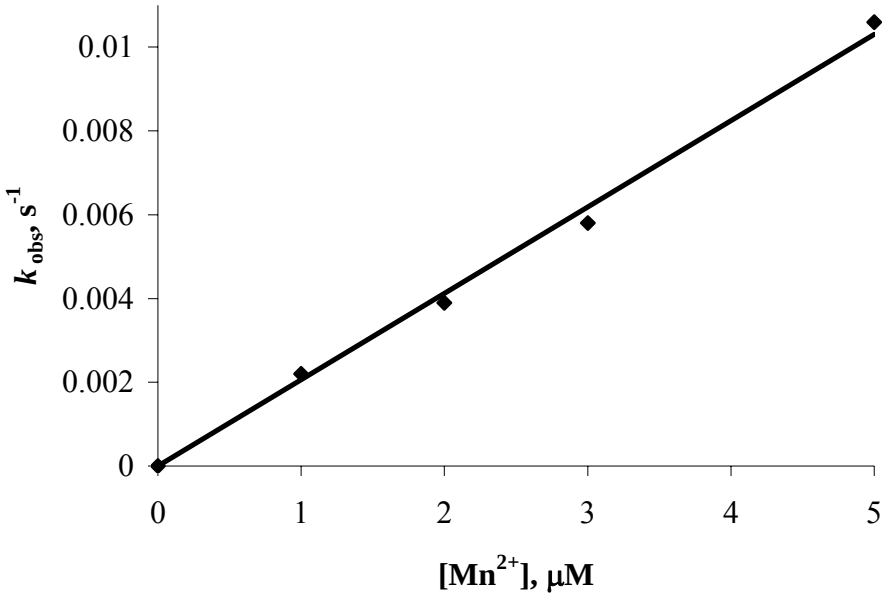

Figure 3-5. Plot of k_{obs} versus [Mn(II)] observed for nucleophilic alkene epoxidation (Bennett, 2002)[46] y = ((2.09 ± 0.25) x10^{-3})x, error reported to the 95% confidence.

These data are consistent with the manganese(II) dependence observed for the hydrogen peroxide decomposition presented earlier and support the proposal that only one manganese ion is present in the active catalyst.

Bicarbonate dependence on nucleophilic alkene epoxidation

Bennett[46] also examined the bicarbonate dependence on the oxidation of sulfonated styrene with manganese(II). The dependence of HCO_3^- on the oxidation was shown to be second-order (Figure 3-6), which is also seen in the manganese dependent hydrogen peroxide decomposition. Once again, these data indicate that two bicarbonate ions are present in the active catalyst. Presumably, one of these bicarbonate ions is present as a peroxycarbonate ion while the other bicarbonate may simply be coordinated to the metal center.

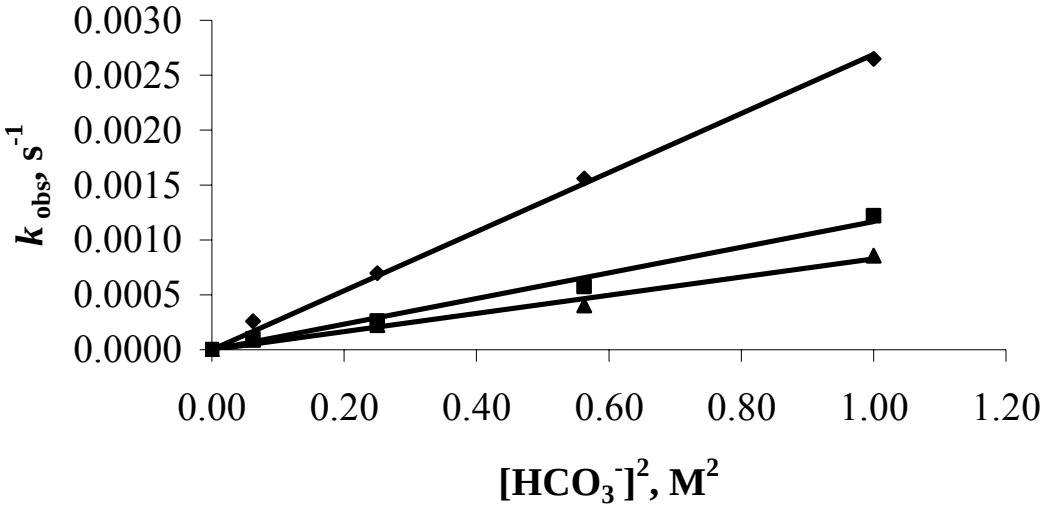

Figure 3-6. Plot of k_{obs} versus $[HCO_3^-]^2$ which shows a second-order dependence. Reaction conditions: 0.001 M *p*-vinyl benzene sulfonate, 1.00 μM Mn^{2+} (♦) 0.10 M H_2O_2 y = ((2.62 ± 0.17) x10^{-3})x (■) 0.50 M H_2O_2 y = ((1.19 ± 0.23) x10^{-3})x (▲) 0.75 M H_2O_2 y = ((8.33 ± 0.76) x10^{-4})x, errors reported to the 95% confidence. (Bennett, 2002)[46]

Hydrogen peroxide dependence on nucleophilic alkene epoxidation

Bennett[46] also observed the hydrogen peroxide dependence for the oxidation of sulfonated styrene with manganese(II). The dependence of H_2O_2 on the oxidation was shown to have an inverse relationship with increasing peroxide concentration (Figure 3-7).

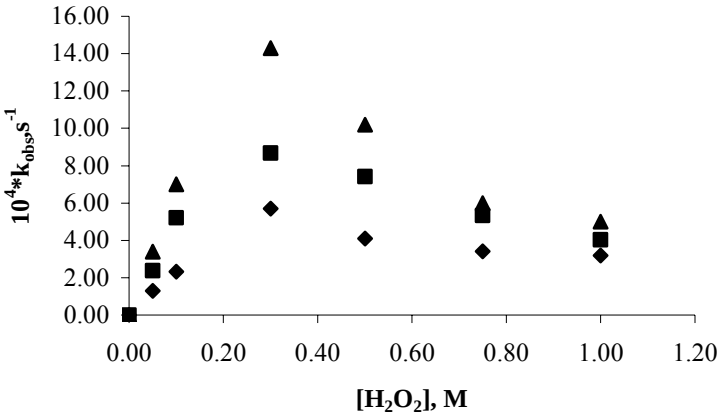

Figure 3-7. Plot of k_{obs} on the $[H_2O_2]$. Reaction conditions: 0.001 M p-vinyl benzene sulfonate (▲) 1.00 M $NaHCO_3$, 0.50 μM Mn^{2+} (■) 0.75 M $NaHCO_3$, 0.50 μM Mn^{2+} (♦) 1.00 M $NaHCO_3$, trace metal catalysis (Bennett, 2002).[46]

Two possibilities exist for the downward trend observed in the hydrogen peroxide dependence. One explanation involves the reaction of hydrogen peroxide to form a less reactive intermediate of the manganese catalyst. This explanation is plausible given the work by Espenson on the oxidation of nucleophilic alkenes by methyltrioxorhenium (MTO).[24] In the case of MTO, the addition of a second hydrogen peroxide molecule generates a diperoxo complex which has a slightly lower epoxidation rate constant than does the monoperoxide intermediate.

The other explanation for the downturn in the reaction has come from work in this study using numerical simulation to model the decomposition and epoxidation kinetics. From this work, it appears that hydrogen peroxide may actually inhibit its own

decomposition at higher concentrations. Further details about this possibility will be presented with the numerical simulations.

Catalyst Lifetime Studies

In addition to examining the kinetics of the manganese(II) catalyzed decomposition of hydrogen peroxide, the lifetime of the catalyst was also of interest. Stadtman[58] noted that the catalyst lost about half of its activity upon reintroduction of hydrogen peroxide into a spent decomposition solution. Stadtman,[58] unfortunately, gave no indication as to why the solutions were losing their catalytic ability. Figure 3-8 shows the k_{obs} versus additions of hydrogen peroxide to a solution of manganese(II) and bicarbonate.

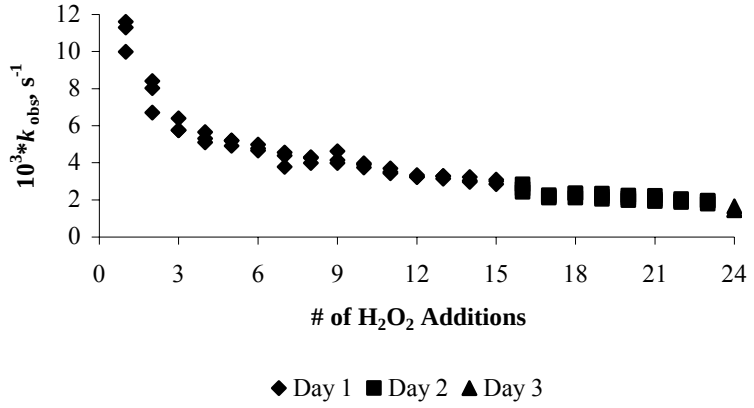

Figure 3-8. Plot of k_{obs} versus # of additions of hydrogen peroxide to a spent solution in the catalyst lifetime study over multiple days. There is a 16 hr delay before addition 16 and 24.

As noted by Stadtman,[58] the decomposition of peroxide drops by about one-third upon reintroduction of peroxide, the 2nd data points. The addition of peroxide was studied over multiple additions, and for multiple days. As can be seen in the graph, hydrogen peroxide still decomposes even after the spent solution has been sitting for 16 hrs, data points 16 and 24. These data indicate that the catalyst is able to regenerate simply by the addition of more hydrogen peroxide.

Examining the loss of activity

The first suspected reason for the decrease in activity in the catalyst lifetime studies was the loss of bicarbonate from the solutions. The bicarbonate concentration was tested by running a large scale reaction (10 mL) with 1.00 M bicarbonate, 1.00 M hydrogen peroxide and 5 μM manganese(II). The reaction was cycled a total of 10 times, each time bringing the hydrogen peroxide concentration back to 1.00 M. After the last reaction had decomposed the hydrogen peroxide, the bicarbonate concentration was analyzed by the standard barium chloride precipitation method. It was found that after 10 cycles, the bicarbonate concentration had dropped from 1.00 M to about 0.50 M.

This result indicates that one of the reasons the decomposition of hydrogen peroxide is decreasing in the catalyst lifetime study is that the concentration of bicarbonate is decreasing. Since the bicarbonate dependence has been observed to be second-order, the loss of bicarbonate will have a dramatic effect on the observed decomposition rate constant. In addition to examining the bicarbonate concentration, the hydrogen peroxide was examined as a possible source for the loss of activity.

In addition to the loss of bicarbonate, it is known that hydrogen peroxide is stabilized using tin phosphates.[10] The loss of activity may be due to manganese precipitation by the addition of phosphates to the solutions, as was observed when phosphates were used in attempting to control the pH of the decomposition solutions. The malachite green assay for phosphates was used to examine the stock 50% hydrogen peroxide solution. It was found that the stock hydrogen peroxide contained approximately 4 mM phosphate. For the cycles being run, this equates to about 25 μM of

phosphate being added to each cycle. This amount of phosphate is enough to begin manganese precipitation.

Multiple additions of distilled hydrogen peroxide and solid sodium bicarbonate

Once it was determined that bicarbonate was being lost during each cycle and phosphate being added, another catalyst lifetime study was done. For these reactions, distilled hydrogen peroxide was used. This assured that no phosphates were being added to the solutions. In addition, solid sodium bicarbonate was added before each cycle in an attempt to stabilize the bicarbonate concentration from cycle to cycle. The results of the catalyst lifetime study using these modifications are seen in Figure 3-9.

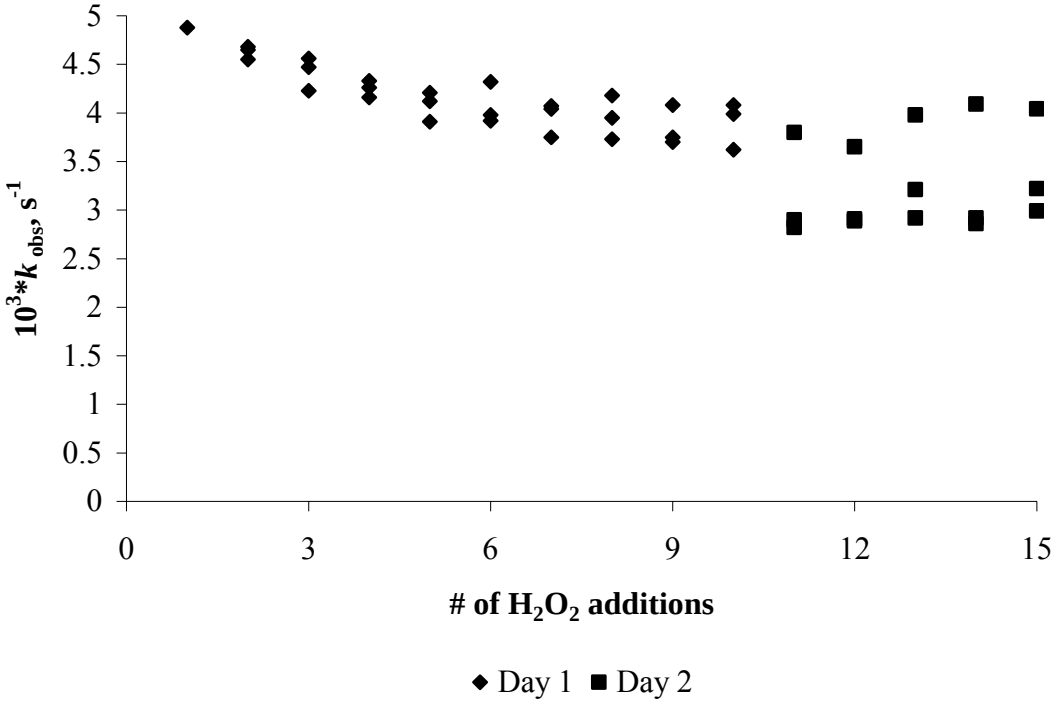

Figure 3-9. Plot of k_{obs} versus # of hydrogen peroxide additions for the catalyst lifetime study using distilled hydrogen peroxide and adding solid sodium bicarbonate. The loss of activity is now due only to dilution and the inability to maintain the bicarbonate concentration at a constant value.

The reactions are about half as fast as those not using the distilled hydrogen peroxide due to the metal contaminants that are found in the peroxide. The loss of

activity is now due to dilution and the inability to maintain a constant bicarbonate concentration. However, it must be noted that there is not as significant a loss in activity when using distilled peroxide and adding bicarbonate. This indicates that the manganese catalyst is not destroyed during the decomposition of the peroxide, but can be regenerated by the addition of more hydrogen peroxide.

Studies of the Manganese Source

In addition to examining the lifetime of the manganese catalyst, the question of whether the source of the manganese was important needed to be answered. For all kinetic experiments, the manganese source was manganese(II) sulfate. Two additional sources of manganese, permanganate and a Mn(IV)-TACN catalyst, were tested to compare their decomposition of hydrogen peroxide to the decomposition with manganese(II) sulfate.

Potassium permanganate

First, potassium permanganate was tested at a concentration of 3 and 4 μM in the presence of 0.20 M sodium bicarbonate and 0.100 M hydrogen peroxide. As seen in Table 3-1, the observed first-order rate constants for the manganese(II) sulfate and permanganate at the same concentration are well within experimental limits.

Table 3-1. Comparison of observed rate constants for the decomposition of hydrogen peroxide, 0.100 M, in 0.20 M sodium bicarbonate with 3 and 4 μM manganese(II) and permanganate. Errors reported are to the 95% confidence.

Manganese Source	Concentration	k_{obs}, s^{-1}
Mn(II)	3 μM	$(8.33 \pm 0.27) \times 10^{-4}$
MnO_4^-	3 μM	$(9.19 \pm 0.31) \times 10^{-4}$
Mn(II)	4 μM	$(1.15 \pm 0.04) \times 10^{-3}$
MnO_4^-	4 μM	$(1.18 \pm 0.04) \times 10^{-3}$

$[Mn^{IV}(Me_3TACN)(OMe)_3]PF_6$

In addition to permanganate, a Mn(IV)-TACN catalyst was synthesized for use as the manganese source in the hydrogen peroxide decomposition. In 1996, Kerschner et al.[63] synthesized $[Mn^{IV}(Me_3TACN)(OMe)_3](PF_6)$, where Me_3TACN is 1,4,7-trimethyl-1,4,7-triazacyclononane (Figure 3-10). This catalyst was capable of oxidizing water-soluble olefins, specifically 4-vinylbenzoic acid and styrylacetic acid, in the presence of bicarbonate. The stability of the catalyst was demonstrated by the repeated additions of hydrogen peroxide and alkene to produce epoxidized product.[63]

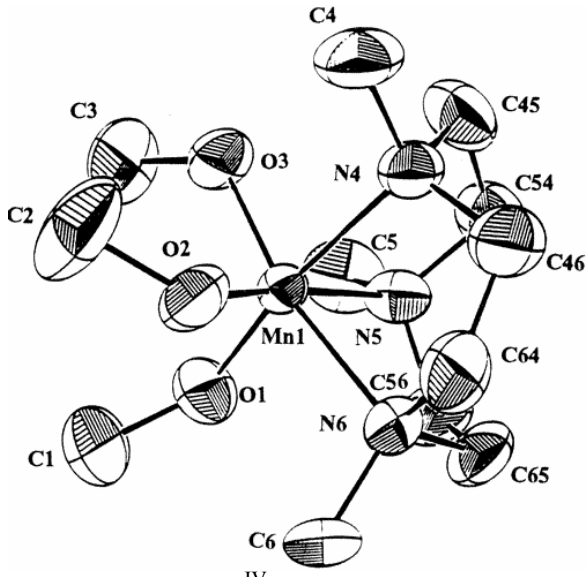

Figure 3-10. Molecular structure of $[Mn^{IV}(Me_3TACN)(OMe)_3](PF_6)$.[63]

The Mn(IV) catalyst was synthesized using the procedure reported by Kerschner.[63] The compound is obtained by the reaction of manganese(II) chloride with 1,4,7-trimethyl-1,4,7-tiazacyclononane in methanol in the presence of sodium peroxide. The complex is crystallized from methanol/water as a brown hexafluorophosphate salt.

Mn(IV) catalyst stability

Initially, the stability of the Mn(IV) catalyst was examined spectrophotometrically in both the presence of bicarbonate and hydrogen peroxide individually. A solution of

1.00 M sodium bicarbonate and 0.108 M Mn(IV) catalyst was dissolved in water, and the catalyst was monitored at 345 nm for 2 hrs, Figure 3-11. The same procedure was also done in the presence of 0.50 M hydrogen peroxide, Figure 3-12.

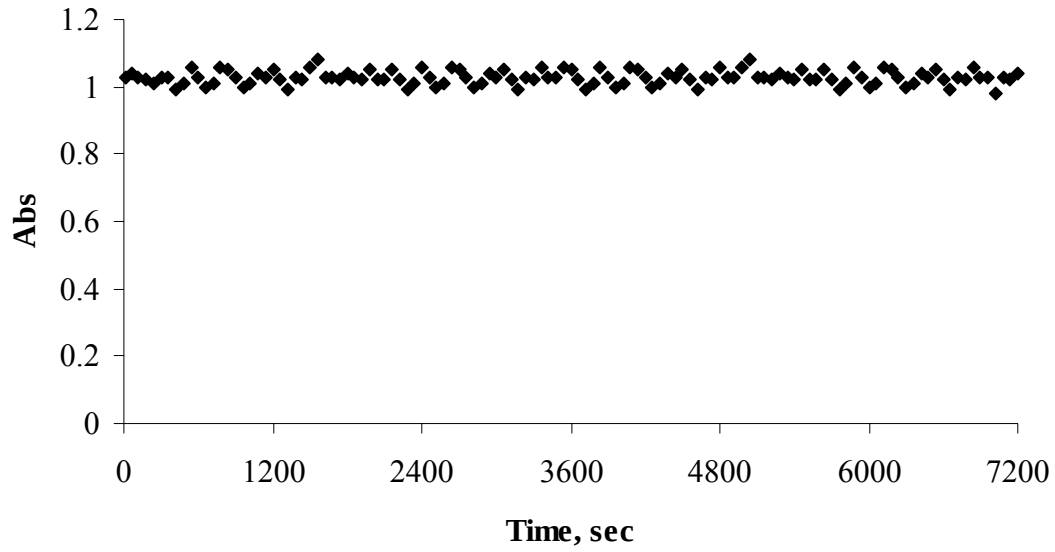

Figure 3-11. Stability of the $[Mn^{IV}(Me_3TACN)(OMe)_3](PF_6)$ at 345 nm in the presence of 1.00 sodium bicarbonate.

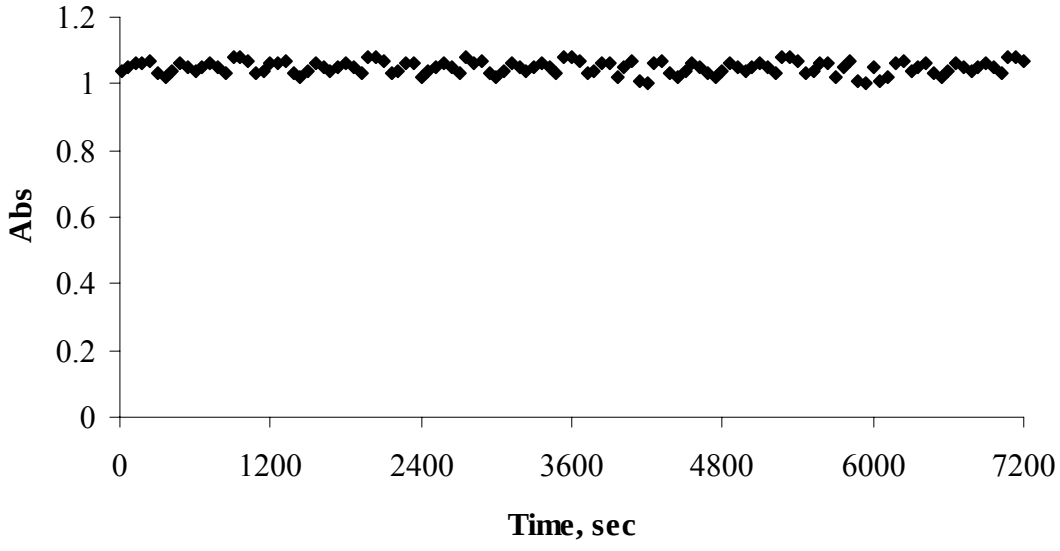

Figure 3-12. Stability of the $[Mn^{IV}(Me_3TACN)(OMe)_3](PF_6)$ at 345 nm in the presence of 0.50 M hydrogen peroxide.

After the catalyst was shown to be stable in the presence of bicarbonate and hydrogen peroxide alone, experiments were conducted to test its stability in the presence of bicarbonate and hydrogen peroxide together. A solution of 1.00 M sodium bicarbonate and 0.108 M catalyst was dissolved in water. After about 350 seconds of monitoring, 25 μL (0.100 M, final concentration) of hydrogen peroxide was added to the solution (Figure 3-13). Almost instantly, the catalyst absorbance decays to 0. Within about 3 minutes, a new absorbance is detected, and the solution is a yellow color. This new absorbance is very broad, having an absorbance of ~0.7 from ~250 nm to 500 nm, Figure 3-14. This absorbance is most likely due to the metal interaction with the *N*-dealkylated organic decay products. More about the topic of *N*-dealkylation by Mn(II) with hydrogen peroxide in the presence of bicarbonate will be presented in a later section of this chapter.

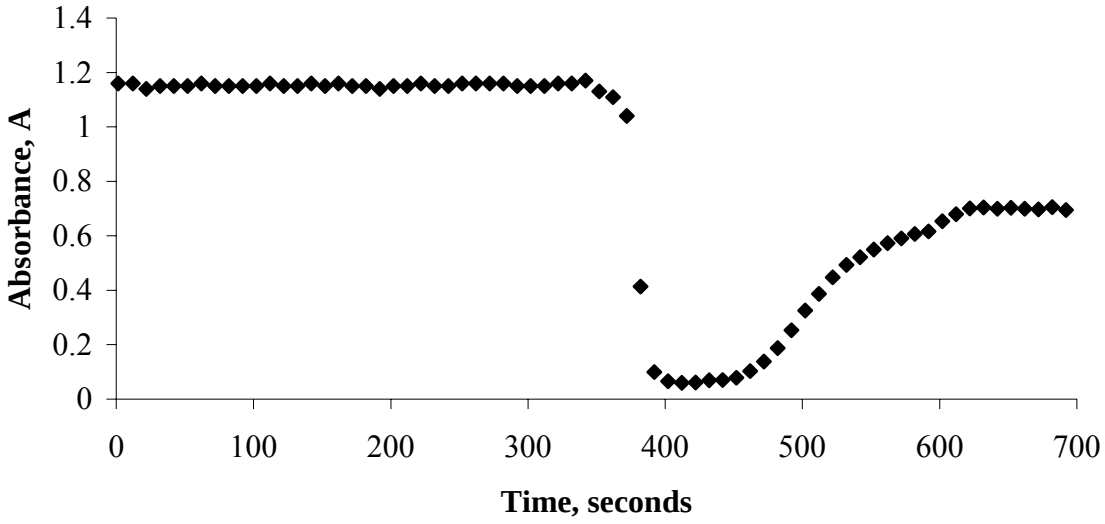

Figure 3-13. Monitoring of 0.108 M $[Mn^{IV}(Me_3TACN)(OMe)_3](PF_6)$ at 345 nm. Addition of 25 μL (0.100 M, final concentration) hydrogen peroxide was done at 350 seconds. The absorbance first decays to 0 and within a matter of minutes, the solution is bright yellow.

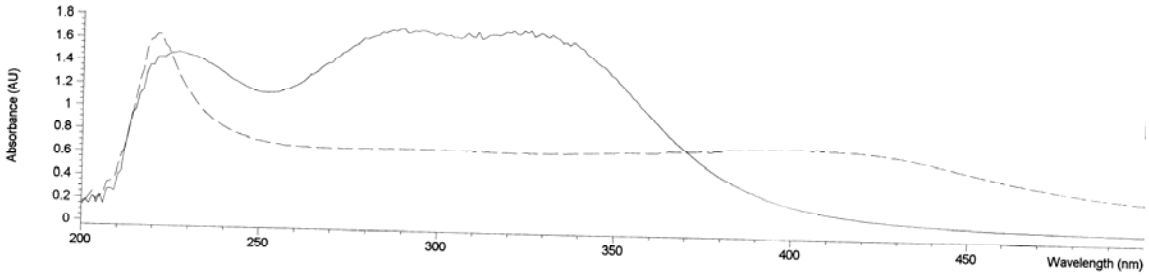

Figure 3-14. UV-vis specta of 0.108 M $[Mn^{IV}(Me_3TACN)(OMe)_3](PF_6)$. The solid line is the spectrum in the presence of 1.00 M sodium bicarbonate. The dotted line is the spectrum of the solution after 1 eq of hydrogen peroxide was added.

In a second experiment, 50 μL (0.200 M, final concentration) hydrogen peroxide was added to the catalyst to determine whether the developing yellow product(s) was the result of a limited amount of peroxide. A solution of 1.00 M sodium bicarbonate and 0.108 M catalyst was dissolved in water. The absorbance at 345 nm was monitored as before (Figure 3-15). At 312 seconds, the peroxide was added to the solution. Unlike the first experiment, the development of the yellow color did not occur. It is therefore apparent that in the presence of only 1 equivalent of hydrogen peroxide, the catalyst does not completely decay, allowing the yellow color to develop. When 2 equivalents of hydrogen peroxide are present, the catalyst is able to completely decay.

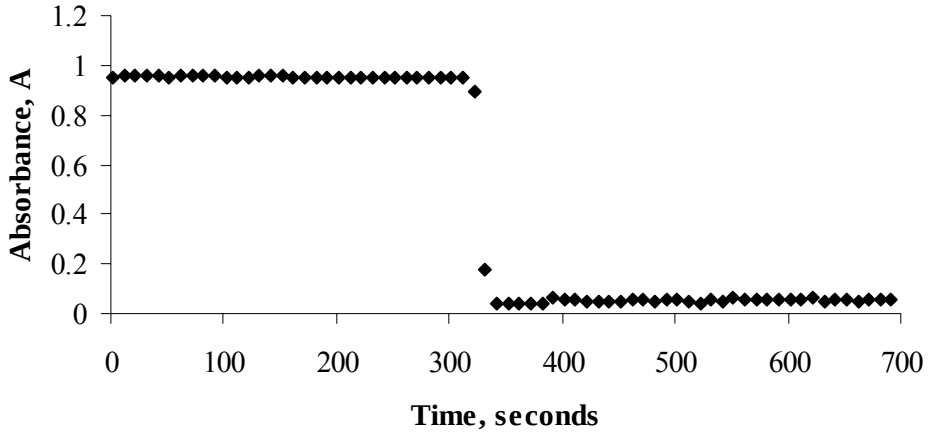

Figure 3-15. Monitoring of 0.108 M $[Mn^{IV}(Me_3TACN)(OMe)_3](PF_6)$ at 345 nm. Addition of 50 μL (0.200 M, final concentration) hydrogen peroxide was done at 312 seconds. Even after 6 minutes, the yellow color does not develop.

Finally, the $[Mn^{IV}(Me_3TACN)(OMe)_3](PF_6)$ catalyst was used with bicarbonate to decompose hydrogen peroxide. As was done with permanganate, 3 and 4 μM $[Mn^{IV}(Me_3TACN)(OMe)_3](PF_6)$ was dissolved in water with 0.200 M sodium bicarbonate and the decomposition was initiated by the addition of 25 μL (0.100 M) hydrogen peroxide. As expected, the observed rate constants for the $[Mn^{IV}(Me_3TACN)(OMe)_3](PF_6)$ catalyzed decomposition of hydrogen peroxide are similar to those for the Mn(II) ion decompositions (Table 3-2). These results indicate that the $[Mn^{IV}(Me_3TACN)(OMe)_3](PF_6)$ catalyst quickly decomposes to release the manganese ion, which then begins catalytically decomposing the hydrogen peroxide. If the catalyst did not quickly decompose, a lag in the decomposition of hydrogen peroxide might have occurred, however, this is not seen experimentally.

Table 3-2. Comparison of observed rate constants for the decomposition of hydrogen peroxide (0.100 M, final concentration) in 0.20 M sodium bicarbonate with 3 and 4 μM manganese(II) and $[Mn^{IV}(Me_3TACN)(OMe)_3](PF_6)$. Errors reported are to the 95% confidence.

Manganese Source	Concentration	k_{obs}, s^{-1}
Mn(II)	3 μM	$(8.33 \pm 0.27) \times 10^{-4}$
$[Mn^{IV}(Me_3TACN)(OMe)_3](PF_6)$	3 μM	$(8.79 \pm 0.30) \times 10^{-4}$
Mn(II)	4 μM	$(1.15 \pm 0.04) \times 10^{-3}$
$[Mn^{IV}(Me_3TACN)(OMe)_3](PF_6)$	4 μM	$(1.11 \pm 0.06) \times 10^{-3}$

Cis-trans Isomerization in the Manganese(II) Catalyzed Alkene Epoxidation

Reactions of cis-alkenes to their corresponding epoxides catalyzed by manganese(II) and hydrogen peroxide in bicarbonate solution will give some indication as to the nature of the oxygen transfer from the active oxygen species to the alkene. For example, in the case of peracid epoxidation of alkenes, cis-alkenes react to give only the cis-epoxide, as seen in Figure 3-16. The oxygen is delivered in a concerted process which retains the stereochemistry of the reactant.

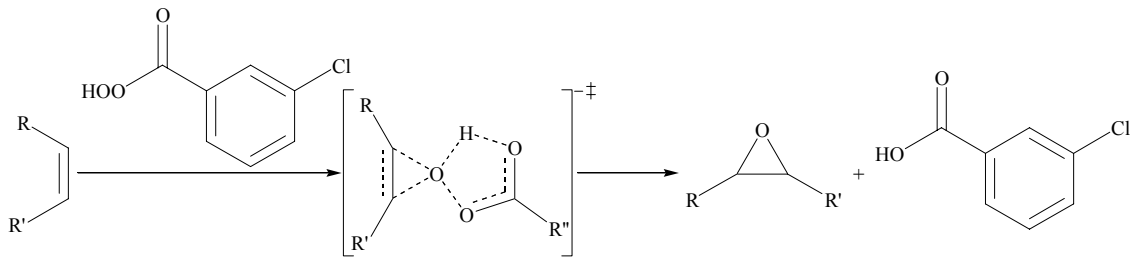

Figure 3-16. The concerted mechanism for the *m*-CPBA oxidation of nucleophilic alkenes resulting in the retention of stereochemistry.

The reaction of Mn(salen) organometallic complexes with hydrogen peroxide, on the other hand, do not produce only the cis-epoxide from the cis-alkene, but the trans-epoxide as well. For these reactions, a two step process occurs where by the C-C sigma bond remains intact, but a carbon radical is produced as an intermediate, as seen in Figure 3-17. During the lifetime of the intermediate carbon radical, before the oxygen bond of the epoxide is formed, the C-C sigma bond has the opportunity to rotate into the more stable trans conformation. In this way, the Mn(salen) catalysts will produce both the cis and trans-epoxides from the cis-alkene.

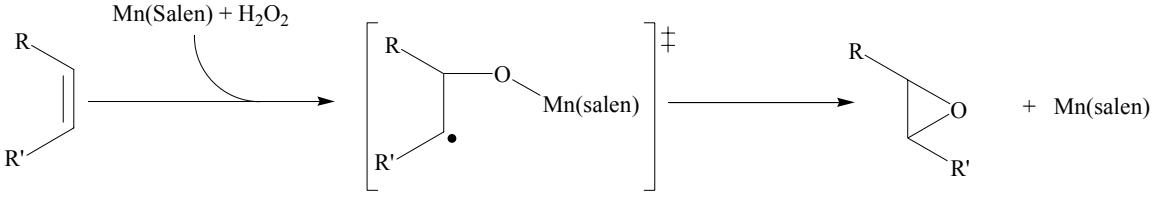

Figure 3-17. The stepwise oxidation of an alkene by Mn(salen) and hydrogen peroxide is shown. Cis/trans isomerization occurs in the transition state, where the C-C sigma bond is able to rotate into the more stable trans configuration.

Burgess et al.[40] noted that under their conditions, using water/DMF solutions, the epoxidation of cis-stilbene produced both the cis and trans-stilbene oxides, as seen in Figure 3-18. This indicates that the active oxygen species does not add the oxygen in a concerted manner, as do the peracids, for example. If the oxygen were added in a concerted manner, there would be no trans epoxide present. However, Burgess followed

these experiments in mixed solvent. The question remains as to whether the cis/trans isomerization will occur in pure aqueous solution.

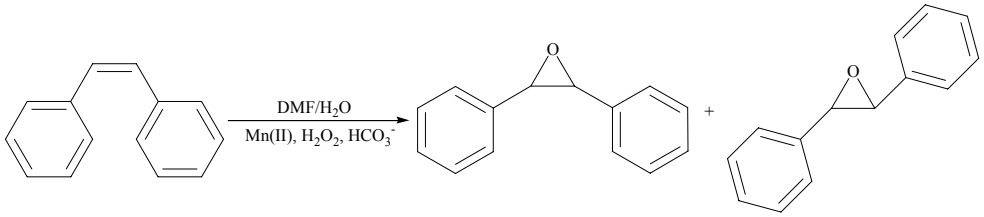

Figure 3-18. The cis/trans isomerization noted Burgess in his epoxidation of stilbene using the Mn(II), H_2O_2, bicarbonate system using a mixed solvent system of DMF/H_2O. (Burgess, 2002)[40]

To study the cis/trans isomerization in pure water, 4,4'-sulfonated stilbene was the obvious choice, based on Burgess' use of stilbene for the reactions in mixed solvent. Unfortunately, all attempts at direct synthesis by sulfonating stilbene using fuming sulfuric acid resulted in black tar. A literature search for the preparation of 4,4'-sulfonated stilbene resulted in a single paper by van Es.[64] The synthetic scheme is illustrated in Figure 3-19. All attempts at synthesizing the 4,4'-sulfonated stilbene failed.

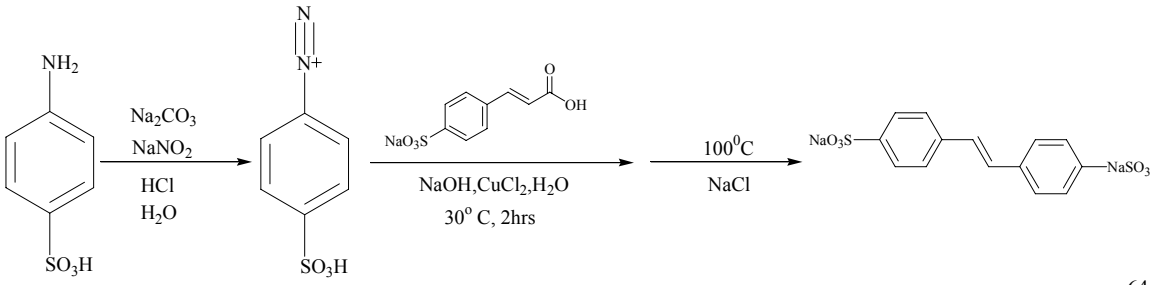

Figure 3-19. Synthetic scheme for synthesis of 4,4'-sulfonated stilbene. (van Es, 1964)[64]

Next, two water-soluble alkenes were chosen, cis and trans-2-butene-1,4 diol. These alkenes were chosen for two reasons. First, they were freely water soluble at the operating pH of 8.4. Second, the epoxides of the alkenes are easily distinguishable by ^{13}C NMR. This made analysis of the reactions relatively simple. The cis-alkene is commercially available, while the trans-alkene must be synthesized. The trans-2-butene-1,4-diol was synthesized using the method of Schloss and Hartman.[65] The synthesis

requires the reduction of 2-butyne-1,4-diol by lithium aluminum hydride in THF. The epoxidation of both the cis and trans alkenes were accomplished by the reaction with *m*-CPBA. The epoxide products' ^{1}H and ^{13}C NMR were compared to literature values for authentic samples, Figure 3-20.

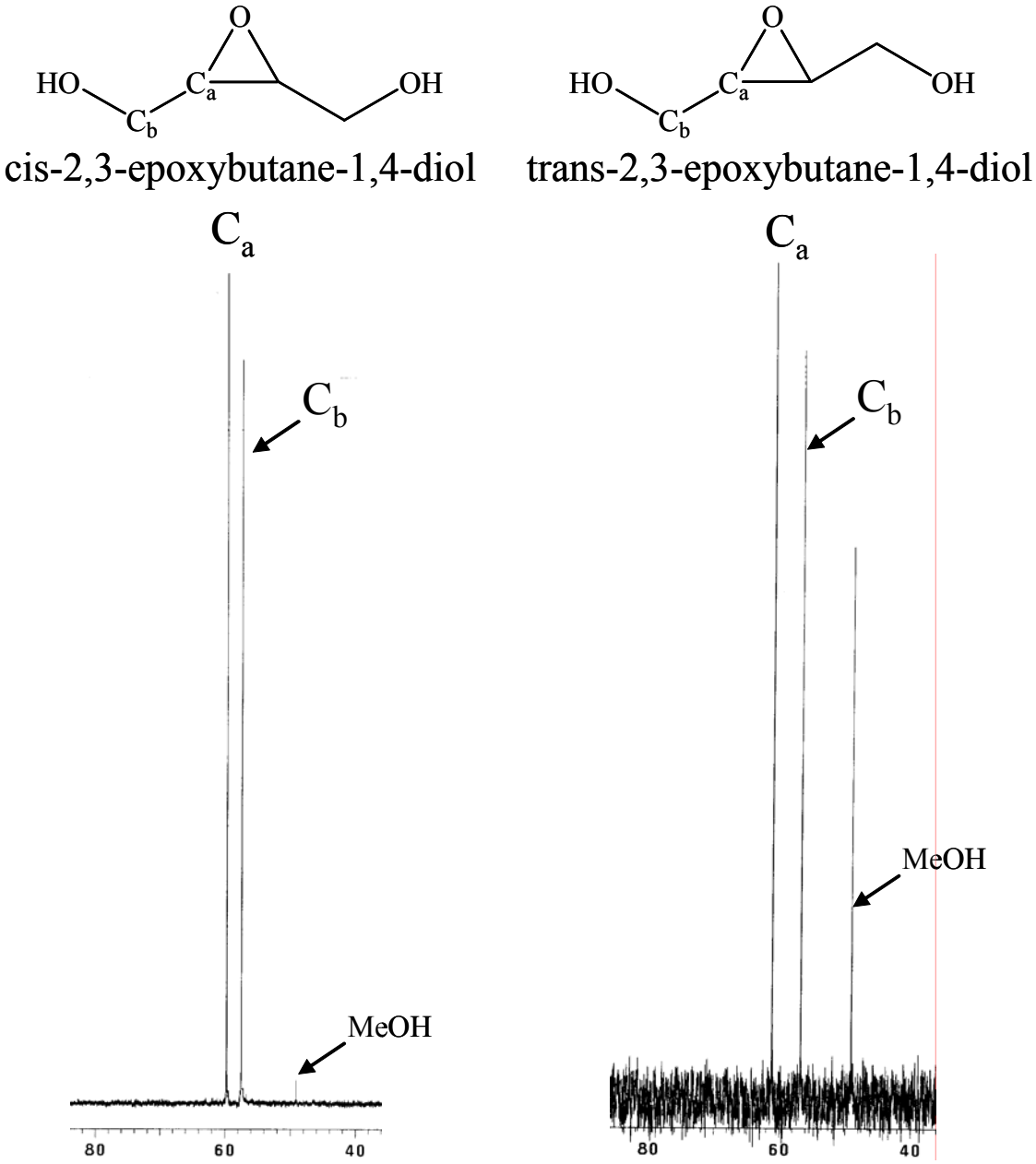

Figure 3-20. ^{13}C NMR of cis and trans-2,3-epoxybutane-1,4-diol in D_2O using methanol as an internal standard.

Cis/Trans isomerization reactions with cis-2-butene-1,4-diol

The cis-2-butene-1,4-diol (0.60 M) was dissolved in D_2O along with 1.00 M $NaHCO_3$, and 10 μM Mn(II). The reaction was initiated by the addition of hydrogen peroxide (final concentration 6.0 M). The reaction was monitored by observing the methylene peak in the ^{13}C NMR using methanol as an internal standard. After 30 minutes, the methylene peak has decreased, but the appearance of the epoxide peaks for either the cis or trans epoxide cannot be seen (Figure 3-21, left). After 18 hrs (Figure 3-21, right), it appears that the cis-alkene has been oxidized to any number of products, none of which have been identified at this time. From these data, a new water-soluble alkene was needed to examine the cis/trans isomerization of the Mn(II)/hydrogen peroxide/bicarbonate oxidation system in water.

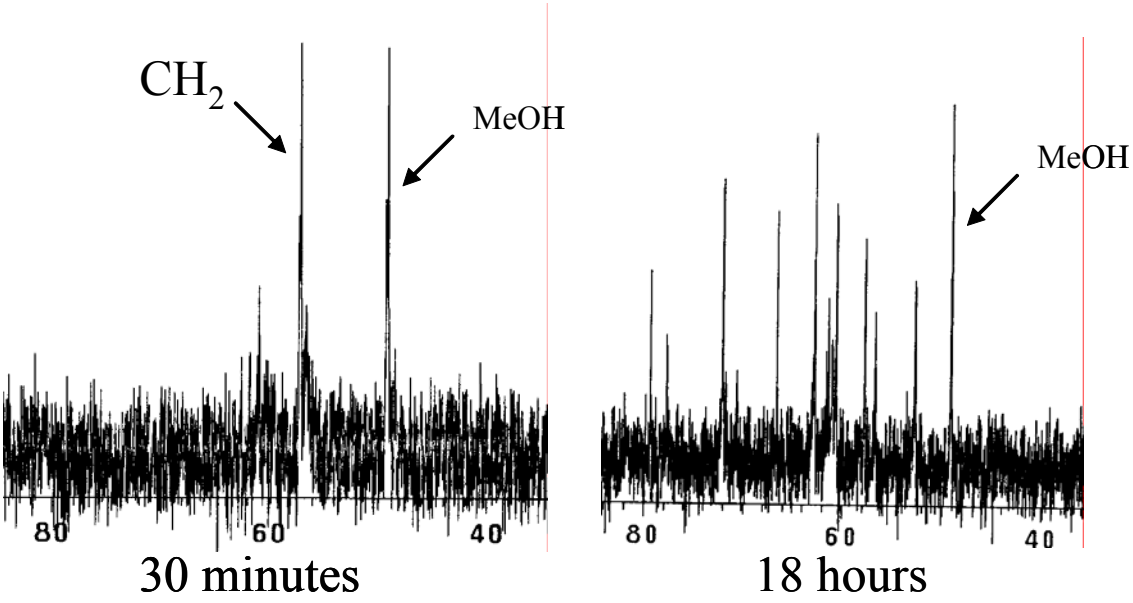

Figure 3-21. Epoxidation of cis-2-butene-1,4-diol (0.60 M) with 1.00 M HCO_3^-, Mn(II) (10 μM), and H_2O_2 (6.00 M) after 30 minutes (left) and 18 hrs (right).

Cis/Trans isomerization of maleic and fumaric acids

Two new alkenes were chosen to study the cis/trans isomerization in pure water. These alkenes are maleic and fumaric acid. The structures of these alkenes at the

operational pH of 8.4 are shown in Figure 3-22. While these may appear to be electrophilic alkenes, the dominant resonance structure at the operating pH allows these alkenes to react as nucleophilic alkenes. More on this topic will be presented in the following chapter. Once again, the determination of epoxide products are conveniently made using ^{1}H NMR, as seen in Figure 3-23.

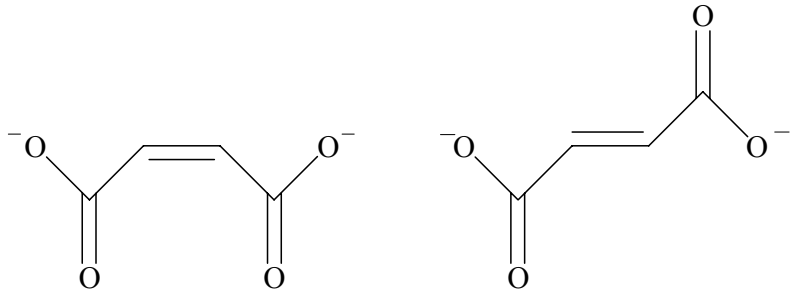

Figure 3-22. The structures of maleic and fumaric acids at the operating pH of 8.4.

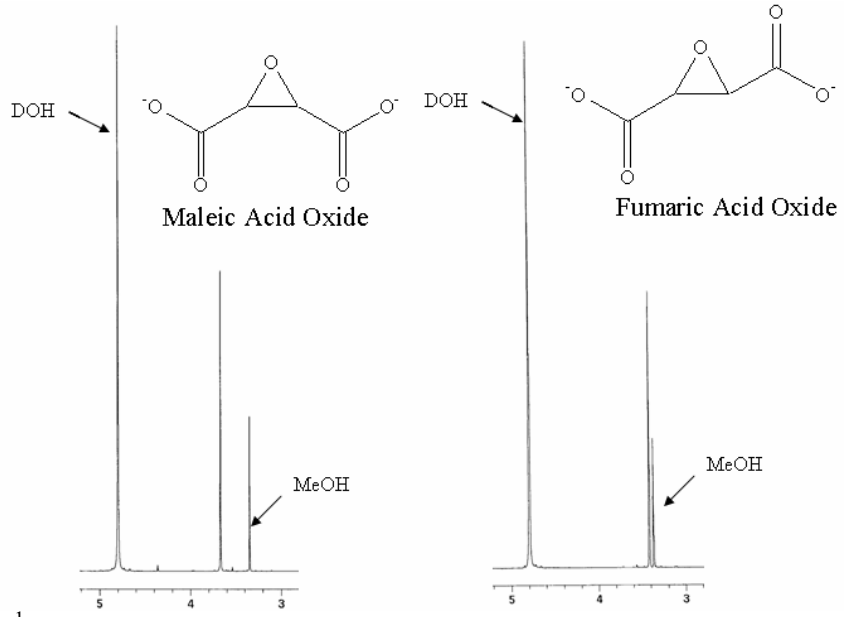

Figure 3-23. ^{1}H NMR of maleic and fumaric acid oxides in D_2O using methanol as an internal standard.

When 0.10 M maleic acid was allowed to react with 1.00 M peroxide in the presence of 0.80 M sodium bicarbonate and 10 μM Mn(II), a 34% conversion to epoxide was observed by NMR in 15 min, as seen in Figure 3-24.

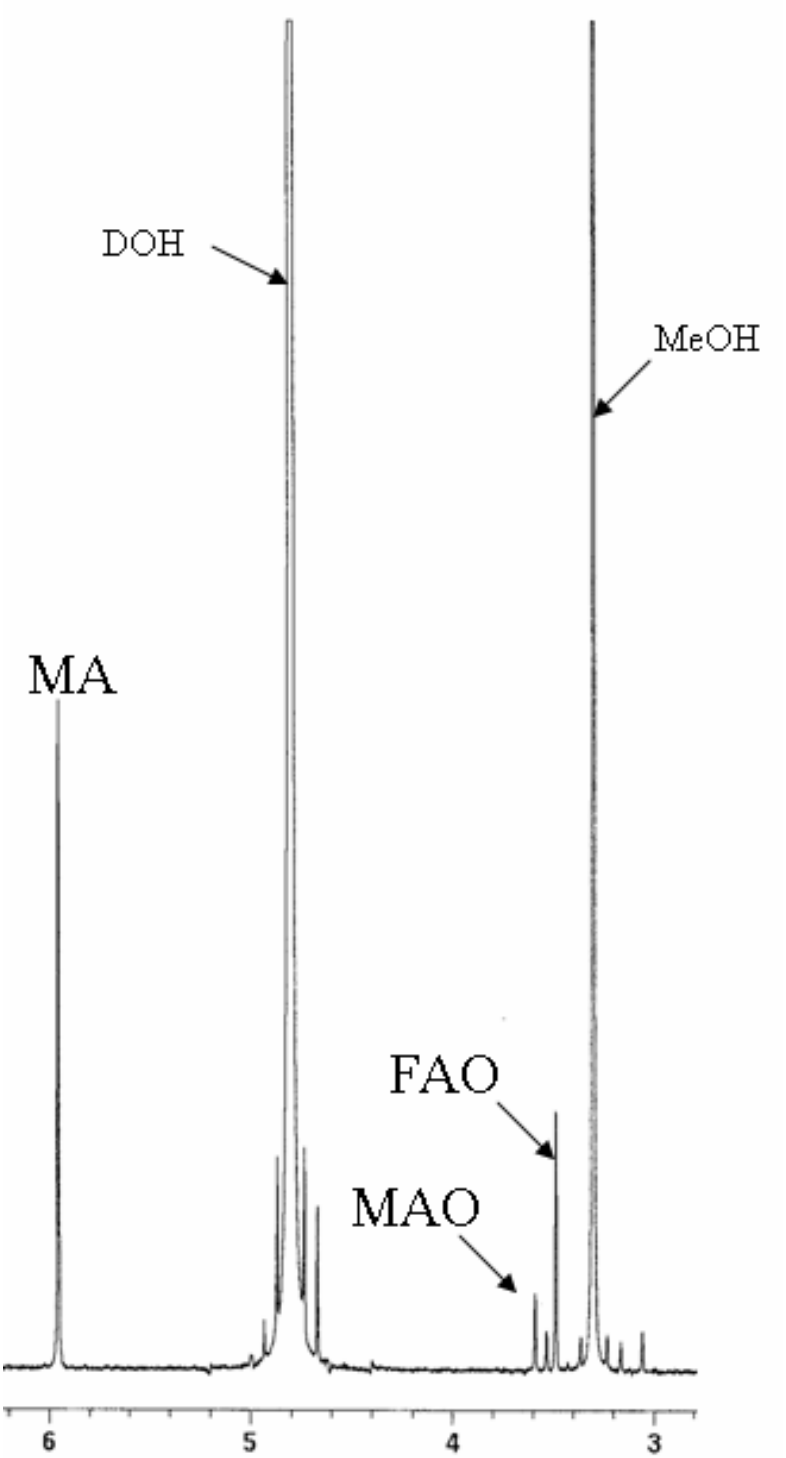

Figure 3-24. Epoxidation of maleic acid by hydrogen peroxide and manganese(II) in the presence of bicarbonate after 15 min. Reaction conditions: 0.10 M maleic acid, 1.00 M H_2O_2, 0.80 M $NaHCO_3$, and 10 μM Mn(II).

Of the 34% epoxide formed, 74% was the fumaric acid oxide and 26% was maleic acid oxide. This result indicates that even in pure water, the oxygen is not being added to the

alkene in a concerted mechanism, such as that seen in the oxidation by *m*-CPBA. This indicates that at some time during the epoxidation, the C-C sigma bond of the alkene has the opportunity to rotate into the more stable trans conformation before closure of the epoxide ring. This experiment does indicate that radical or carbocation formation is probable in the epoxidation of nucleophilic alkenes, a discussion of possible routes for the addition of the oxygen and rotation into the trans isomer will be discussed with the possible mechanisms of the reaction.

The observation that cis alkenes react with the active oxygen species to give the trans epoxide indicates that radical chemistry may play a role in the epoxidation of alkenes. This does not, however, indicate that free radicals are responsible for the epoxidation. Reaction mechanisms that are similar to those for Mn-salen epoxidation catalysts could also explain the rotation about the C-C bond during the epoxidation reaction. In addition, reactions involving electrophilic alkenes, which will be presented in the next chapter, led us to question Sychev's proposed hydroxyl radical mechanism. In the epoxidation of electrophilic alkenes, as was the case for the nucleophilic alkene epoxidations, the reactions cleanly yielded the epoxide products with no indication of any radical products.[66,67] In an attempt to exclude free radicals as a possible reaction pathway, an examination of the radical traps used by Sychev[47] was conducted.

Examination of Sychev's Radical Trap Experiments

As discussed in the introduction, the combination of hydrogen peroxide and iron(II), Fenton's reagent, is a useful method for the production of hydroxyl radicals. Fenton's reagent can then be used to oxidize organic molecules. For instance, benzene can be oxidized to form biphenyl and phenol in the presence of Fenton's reagent, as seen in Figure 3-25.[67]

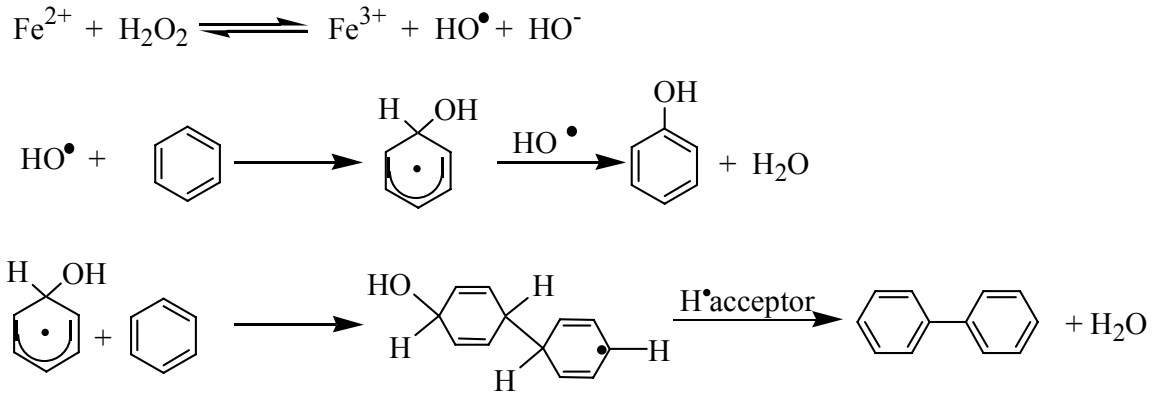

Figure 3-25. Fenton's reagent can be used to oxidize benzene to phenol and biphenyl.

In 1977, Sychev et al.[47] began investigating the role of manganese(II) in the disproportionation of peroxide in bicarbonate buffered solutions. His assumption was that manganese(II) reacted similarly to iron(II) ions in Fenton type chemistry. Following this assumption, a hydroxyl radical based mechanism was proposed, shown by Equations (3-4)-(3-14), the sum of which is the decomposition of hydrogen peroxide to molecular oxygen and water. As with Fenton type chemistry, free hydroxyl and peroxy radicals are formed in this mechanism, along with the carbonate radical anion.

$$[Mn(HCO_3)_2] + H_2O_2 \rightarrow [Mn(HCO_3)_2]^+ + OH^- + {}^{\bullet}OH \quad (3\text{-}4)$$

$$[Mn(HCO_3)_2]^+ + H_2O_2 \rightarrow [Mn(HCO_3)_2] + H^+ + HOO^{\bullet} \quad (3\text{-}5)$$

$$[Mn(HCO_3)_2] + {}^{\bullet}OH \rightarrow [Mn(HCO_3)_2]^+ + OH^- \quad (3\text{-}6)$$

$$[Mn(HCO_3)_2]^+ + HOO^- \rightarrow [Mn(HCO_3)_2] + O_2^{-\bullet} + H^+ \quad (3\text{-}7)$$

$$[Mn(HCO_3)_2] + HOO^{\bullet} \rightarrow [Mn(HCO_3)_2]^+ + HOO^- \quad (3\text{-}8)$$

$$[Mn(HCO3)_2]^+ + OH^- \rightarrow [Mn(HCO_3)_2] + {}^{\bullet}OH \quad (3\text{-}9)$$

$${}^{\bullet}OH + H_2O_2 \rightarrow O_2^{-\bullet} + H^+ + H_2O \quad (3\text{-}10)$$

$$2O_2^{-\bullet} + 2H_2O_2 \rightarrow 2O_2 + 2OH^- + 2\,{}^{\bullet}OH \quad (3\text{-}11)$$

$${}^{\bullet}OH + HOO^{\bullet} \rightarrow H_2O + O_2 \quad (3\text{-}12)$$

$${}^{\bullet}OH + HCO_3^- \rightarrow CO_3^{-\bullet} + H_2O \quad (3\text{-}13)$$

$CO_3^{-\bullet} + H_2O_2 \rightarrow O_2^{-\bullet} + H^+ + HCO_3^-$ (3-14)

$2H_2O_2 \rightarrow 2H_2O + O_2$

In order to support his claim of a free hydroxyl radical pathway, Sychev employed a set of experiments using *N*,*N*-dimethyl-4-nitrosoaniline (DMNA) as a free hydroxyl radical trap. In his experiments, he studied the production of O_2(g) as a function of time with increasing amounts of DMNA, Figure 3-26.

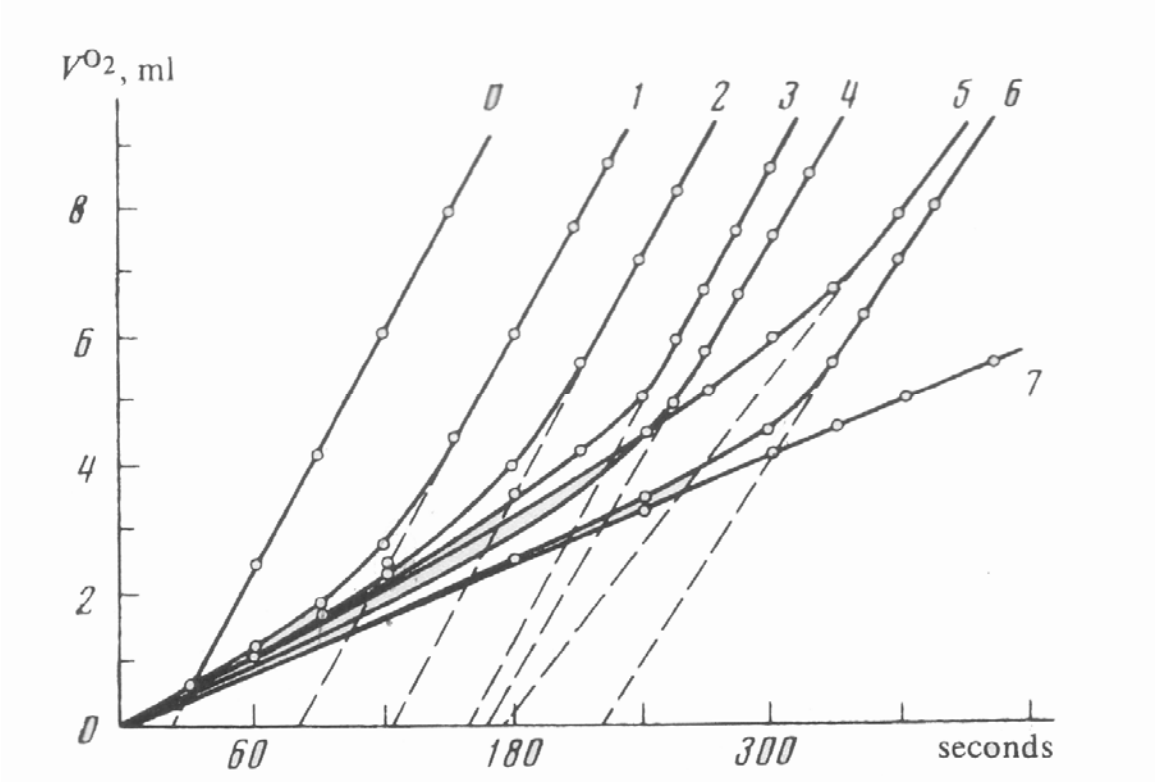

Figure 3-26. The influence of inhibitors on the catalase process in the Mn(II)/HCO_3/H_2O_2 system. [Mn(II)] = 4 x 10^{-6} M, [H_2O_2] = 0.10 M, pH 7.0, [HCO_3^-] = 0.4 M, and T = 25 ºC: 0) kinetic curve with no inhibitors; 1), 2), 3), and 6) in the presence of DMNA as the inhibitor(at concentrations of 1 x 10^{-5},1.5 x 10^{-5}, 2 x 10^{-5},and 4 x 10^{-5} M respectively; 4)in the presence of tetranitromethane(4 x 10^{-5} M); 5) in the presence of hydroquinone (1.5 x 10^{-5} M); 7) decomposition of H_2O_2 without Mn(II) ion (blank experiment). (Sychev, 1977)[47]

As expected for his free hydroxyl radical pathway, Sychev observed that when DMNA was present, the production of O_2(g) was suppressed to the background disproportionation of H_2O_2 without the addition of metal, Figure 3-26, line 7. As time

progressed, the O_2(g) production would begin to increase back to the purely catalytic production of O_2(g), as shown in Figure 3-26, line 0.

The conclusion reached by Sychev was that the DMNA was trapping the free hydroxyl radicals produced from the disproportionation, Equations 3-4, 3-9, and 3-11. Without the presence of free hydroxyl radicals to carry the reaction, O_2(g) production would be the same as the uncatalyzed O_2(g) production, Figure 3-26, line 7. Eventually, O_2(g) production would begin to follow that of the catalyzed reaction as the concentration of DMNA was reduced and an increase in free hydroxyl radicals occurred. This is seen in Figure 3-26 as all of the inhibited reactions eventually begin to produce O_2(g) at the same rate as the uninhibited reaction, Figure 3-26, line 0.

In all of Sychev's papers, the use of radical traps, such as DMNA, provide the entire basis for a free hydroxyl radical mechanism. In none of his papers, however, did Sychev identify the organic products of the reactions with DMNA. In the current study, it has been hypothesized that instead of a decomposition pathway that requires hydroxyl radicals, the mechanism of peroxide disproportionation may proceed through a high valent metal oxo species, or by carbonate radical anions, which are proposed in Sychev's model. The data presented for the interruption of hydrogen peroxide decomposition by Sychev could be the result of trapping of carbonate radical anions, instead of hydroxyl radicals. A discussion on the reactivity of carbonate radicals will be presented in the proposed mechanism for the oxidation of the radical traps.

The use of a high valent metal oxo species could also explain Sychev's loss in O_2(g) production seen with the use of DMNA. Instead of the O_2(g) production being inhibited by radical interruption, the oxygen normally being released as molecular

oxygen would instead be transferred to DMNA. In order to understand the effect DMNA is having on the hydrogen peroxide decomposition reaction, the organic products from the reaction need to be identified. Once the oxidized organic products are identified, a clearer understanding of the reaction mechanism may be possible.

A series of experiments were first conducted to determine what the oxidized products of DMNA could be. Initially, potassium peroxymonosulfate was employed as the oxidant. This experiment was done to determine what the product of a pure oxygen transfer would be, since peroxymonosulfate is an excellent electrophilic oxidant.[68,69] When peroxymonsulfate was allowed to react with DMNA in a 1:1 molar ratio, *N*,*N*-dimethyl-4-nitroaniline was produced nearly quantitatively after 30 minutes, as expected for an oxygen transfer to the nitroso moiety. A second control experiment was done using H_2O_2 and HCO_3^-, only. When one equivalent of H_2O_2 was added to 0.40 M chelexed HCO_3^-, *N*,*N*-dimethyl-4-nitroaniline was produced after 1 hr. In the presence of hydrogen peroxide alone, no reaction was detected even after 24 hrs. This result indicates that solutions of peroxycarbonate are able to convert the nitroso moiety to the nitro without the addition of any metals. Any products, other than the nitro compound, are then the result of the addition of the metal cations.

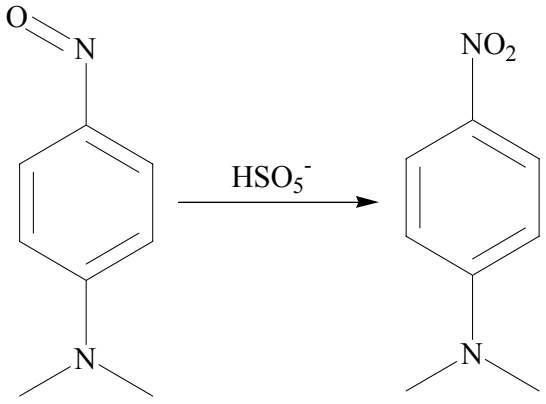

Figure 3-27. The reaction of *N*,*N*-dimethyl-4-nitrosoaniline with peroxymonosulfate to yield *N*,*N*-dimethyl-4-nitroaniline.

In a second set of reactions, DMNA was oxidized using H_2O_2 in bicarbonate with Mn(II). H_2O_2 was used as the terminal oxidant in 50x molar excess over the DMNA. The need to increase the H_2O_2 concentration to such a degree over the DMNA concentration is due to the fact that H_2O_2 disproportionation is much faster than the oxidation of DMNA. When reactions using only one equivalent of H_2O_2 were conducted, starting material was the only recovered organic compound. The final sodium bicarbonate and Mn(II) concentrations were set at 0.40 M and 4.0 μM, respectively.

DMNA oxidations were conducted by first dissolving the organic substrate in a mixture of CH_3CN:H_2O (30:70 (v: v)) with a solution of the manganese(II) sulfate. Equilibrated solutions of H_2O_2 and sodium bicarbonate were then slowly added dropwise over about 30 minutes. Reactions were considered to be complete when the production of O_2(g) from the H_2O_2 disproportionation ceased. This was usually 10-15 minutes after the final addition of the H_2O_2/HCO_3^- solution. Since the reaction is highly exothermic, ice was often employed to keep the temperature from exceeding 65ºC. Once the reaction reaches 65ºC, the H_2O_2 disproportionation becomes vigorous enough to cause the reaction mixture to boil out of the reaction flask. At the end of the reaction, the organic products were extracted into chloroform which was then dried over magnesium sulfate. The solvent was then removed under reduced pressure to give crude product, which was analyzed by ^{1}H NMR, Figure 3-28.

The ^{1}H NMR of the crude product shows multiple products, three of which have been identified at this time. Aromatic peaks still remained and retained the characteristic proton signal for a disubstituted aromatic compound. It was also noted that new peaks in

the 4 - 5.5 ppm region had appeared. The methyl peaks of the amine portion of the molecule seemed to have remained, but they were shifted upfield.

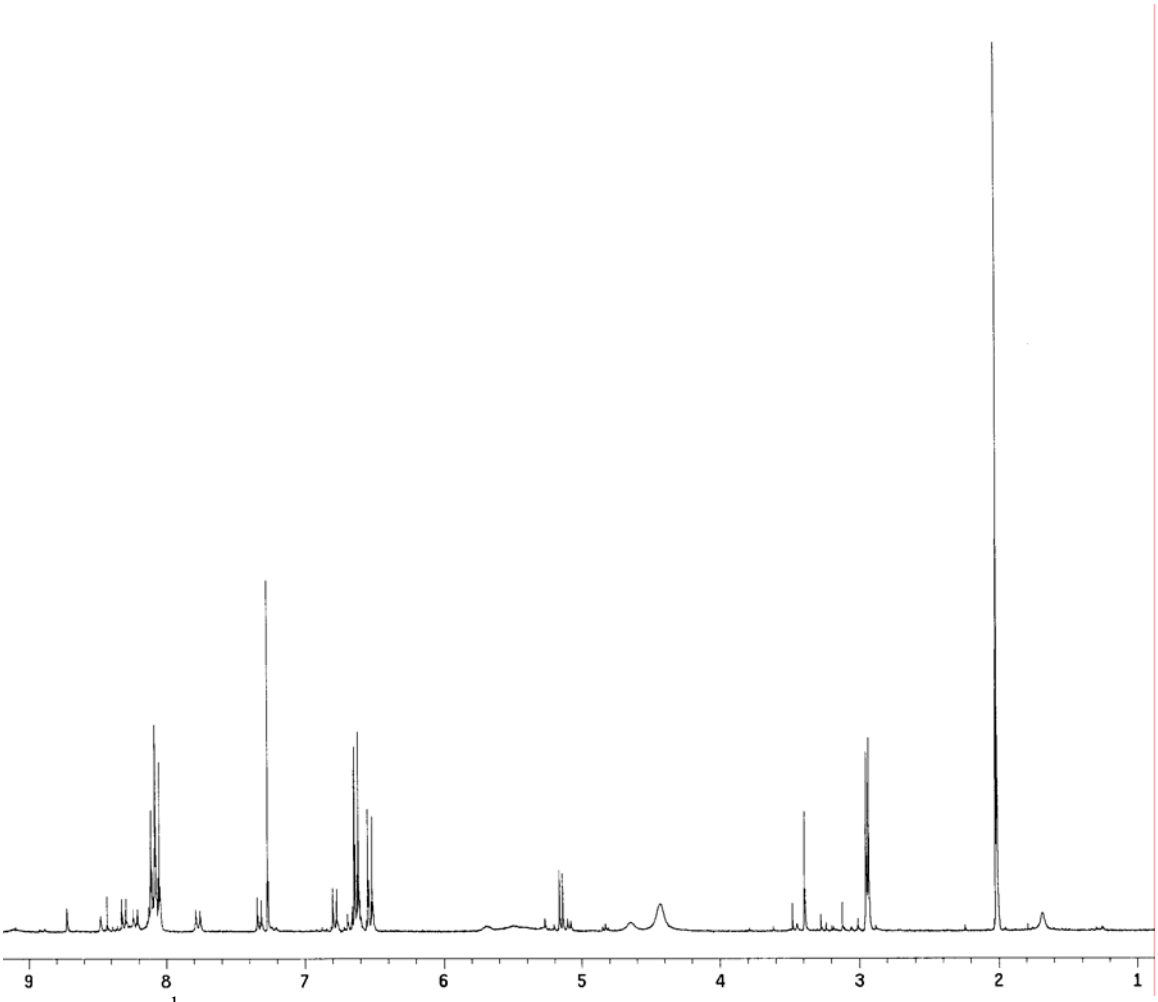

Figure 3-28. ^{1}H NMR of the crude reaction mixture after an oxidation of *N*,*N*-dimethyl-4-nitrosoaniline by hydrogen peroxide in the presence of bicarbonate and Mn(II). Reaction conditions: *N*,*N*-dimehtyl-4-nitrosoaniline (1 g, 6.66 mmol), 0.400 M sodium bicarbonate, 10 μM Mn(II), 6.64 M H_2O_2, 1 hr.

After analysis by ^{1}H NMR, gas chromatography was employed to help determine the number of products obtained from the reaction. GC analysis showed there were four volatile products formed. It can only be stated that these products are volatile, since GC will only separate compounds that can be volatized and have a low enough boiling point to remain in the gas phase. Both ^{1}H NMR and GC proved that none of the products obtained were that of *N*,*N*-dimethyl-4-nitrsoaniline, which should have been the case

since the nitroso moiety is easily oxidized by peroxycarbonate. Figure 3-29 is a GC trace using the same method employed for the crude reaction mixture, Figure 3-30, for which a peak is not observed at 14.6 min, indicating that all of the *N*,*N*-dimethyl-4-nitrsoaniline has been converted to other organic products.

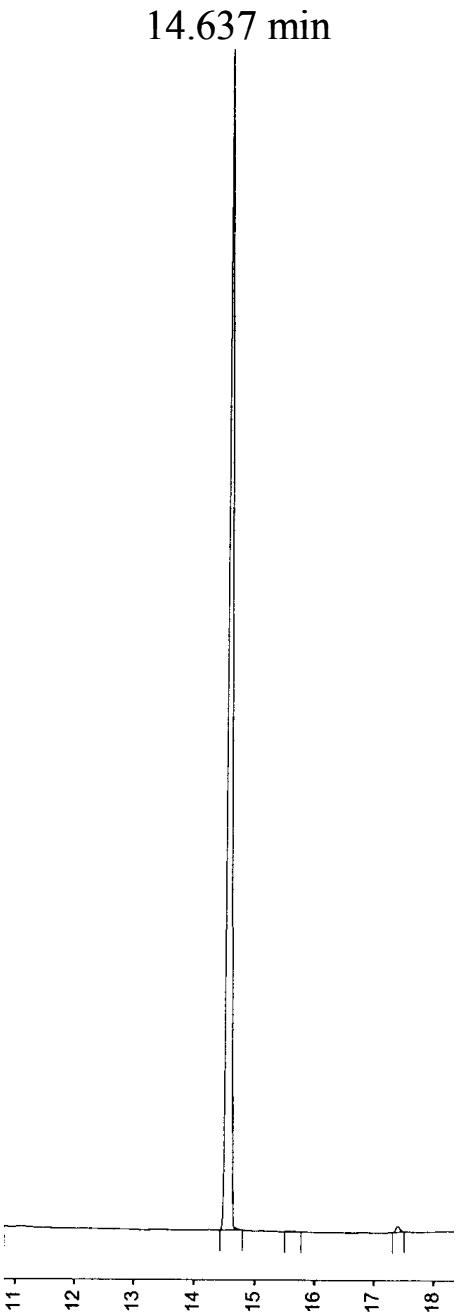

Figure 3-29. GC trace for a standard of *N*,*N*-dimethyl-4-nitrsoaniline. Non-linear gradient for 30 minutes, detection by FID.

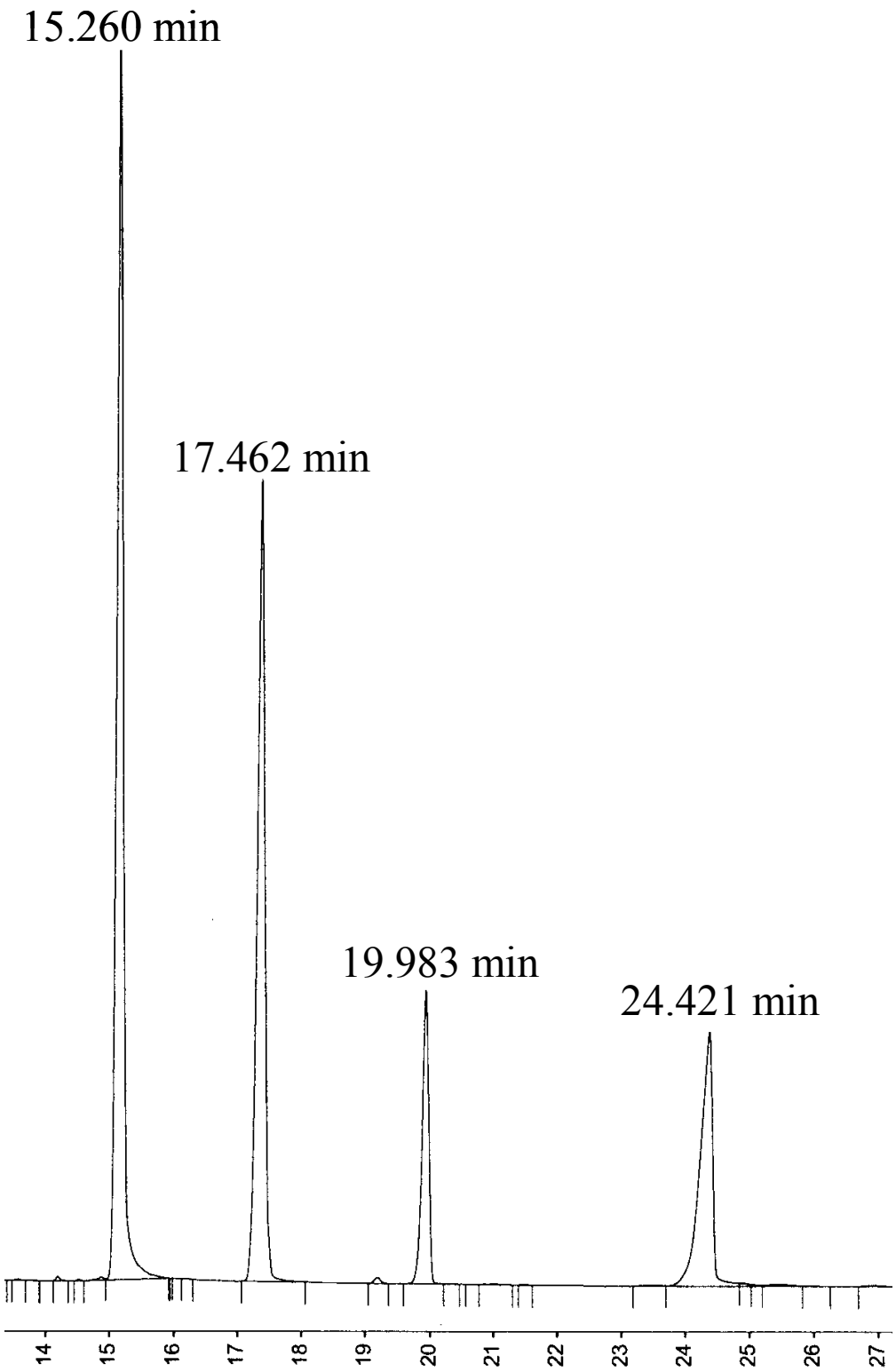

Figure 3-30. GC trace for the crude reaction material from the oxidation of *N*,*N*-dimethyl-4-nitrsoaniline from Figure 3-25. Lack of a peak near 14.637 min proves that no starting material remains. GC conditions: non-linear gradient for 30 minutes, Detection: FID.

After ^{1}H NMR and GC analysis, the reaction material was applied to a silica column employing chloroform as eluant. Fractions were collected and analyzed by GC. Fractions 4 and 9 were found to contain organic products and their GC traces and ^{1}H NMR are shown in Figure 3-31 and 3-32. The two compounds that were separated were found to be *N*,*N* -dimethyl-4-nitroaniline and 4-nitroaniline, by comparison with authentic samples. These two compounds account for about 80% of the crude reaction mixture, the last 20 % being the peaks at 19.983 and 24.421 min, Figure 3-27. The two remaining organic compounds remained at the top of the column.

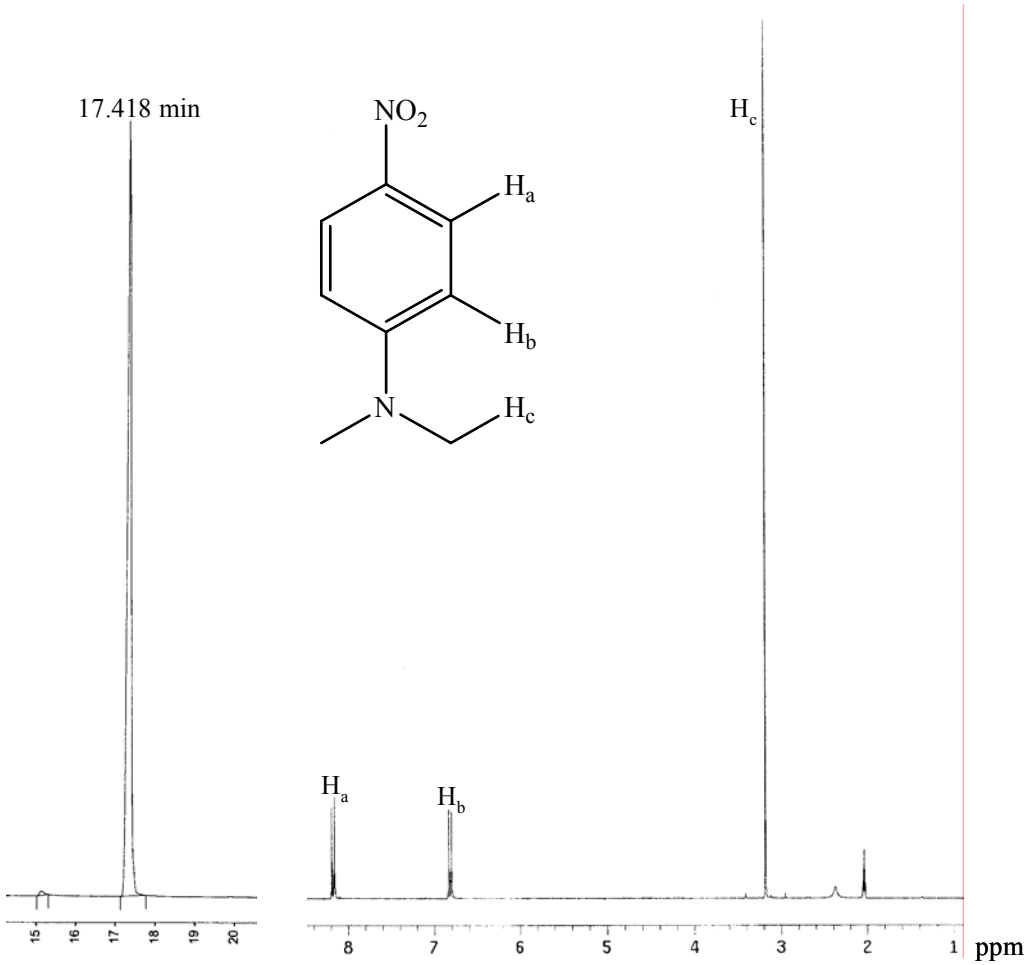

Figure 3-31. GC trace (left figure) and ^{1}H NMR (right figure) for Fraction 4 of the silica column. Identification of the product as *N*,*N*-dimethyl-4-nitroaniline was confirmed by comparison with a GC trace and ^{1}H NMR of an authentic sample.

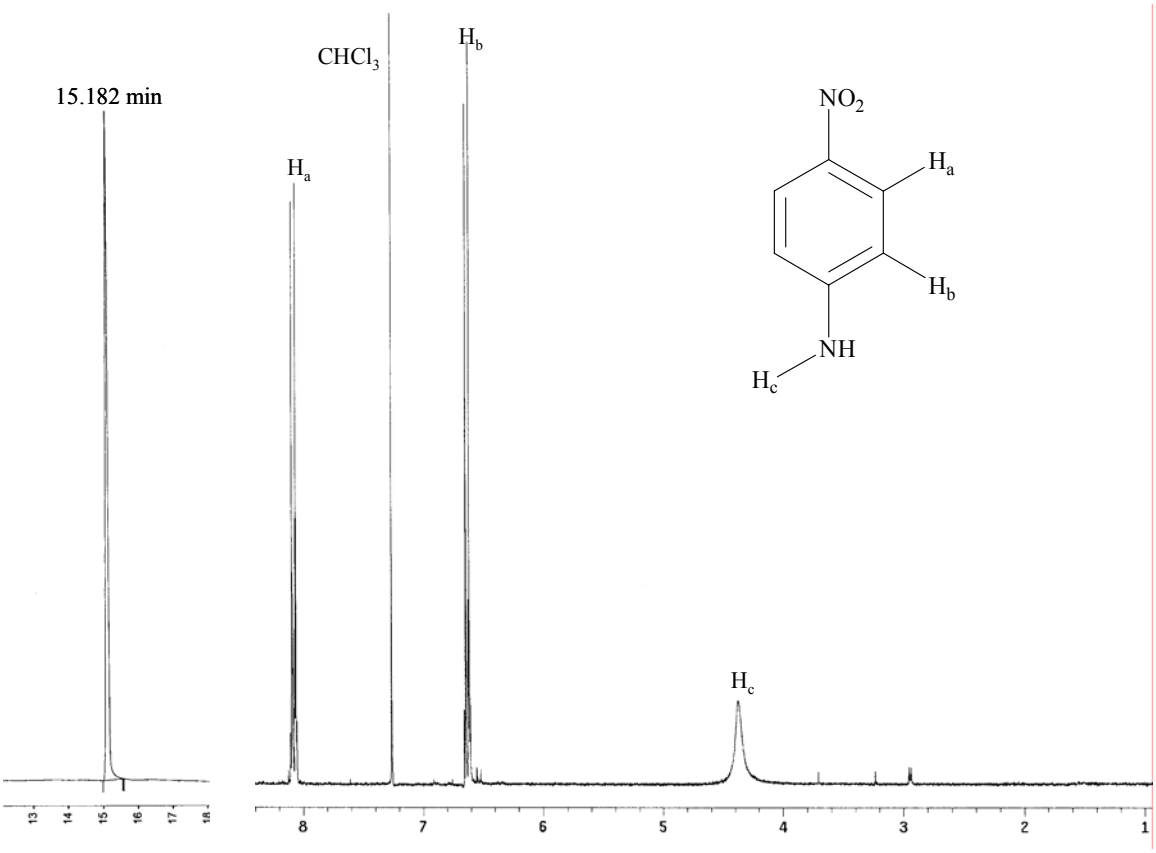

Figure 3-32. GC trace (left figure) and ^{1}H NMR (right figure) for Fraction 9 of the silica column. Identification of the product as 4-nitroaniline was confirmed by comparison with a GC trace and ^{1}H NMR of an authentic sample.

Once 4-nitroaniline was identified as a product, it was apparent that the amine was dealkylating. It was then likely that one of the other unidentified peaks was *N*-methyl-4-nitroaniline. A ^{1}H NMR was acquired of a sample of the pure material and compared with the crude reaction material, Figure 3-33. It was found that *N*-methyl-4-nitroaniline peaks were also present in the crude reaction mixture. The only peak not identified was the peak at 24.421 min, which accounts for less than 5 % of the crude reaction material.

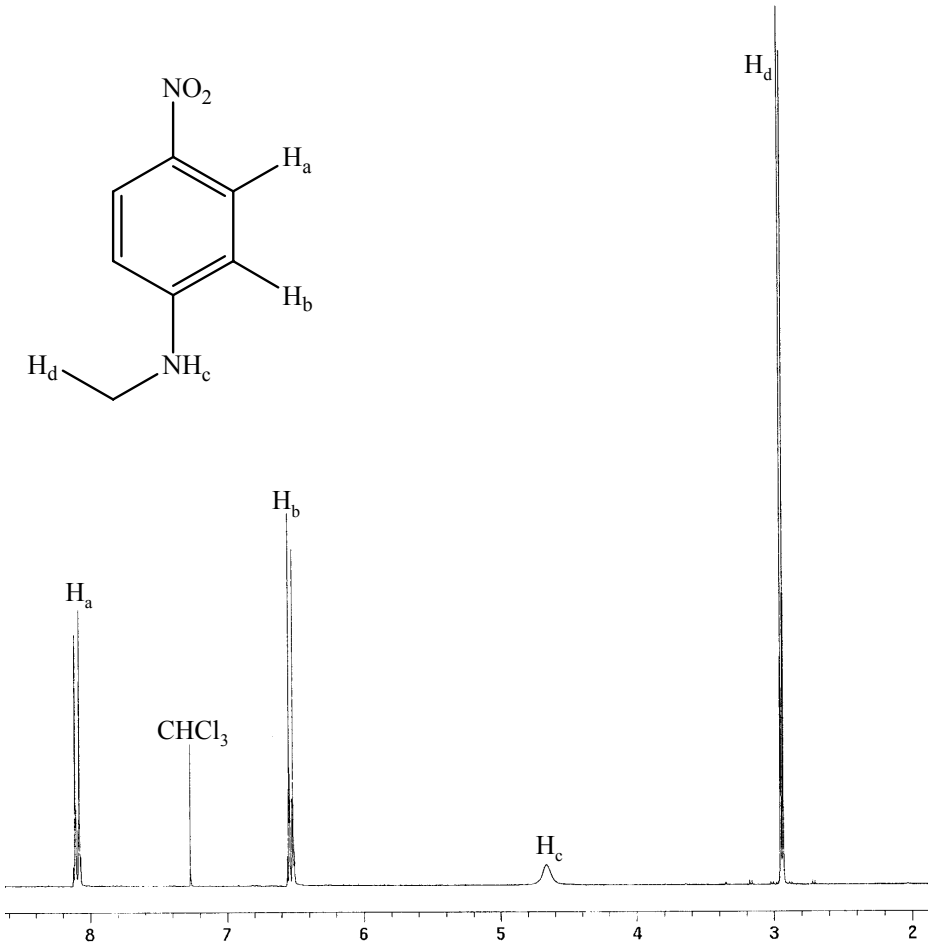

Figure 3-33. ^{1}H NMR of an authentic sample of *N*-methyl-4-nitroaniline. Comparison with the crude reaction mixture confirms its presence as a product.

For these products to be observed, *N*-dealkylation must be responsible for cleaving the C-N bond of the amines. In the case of DMNA, the cleaved carbon group is formaldehyde based on current literature that will be discussed shortly. In the ^{1}H NMR and GC analysis performed on the DMNA reactions, formaldehyde was never detected. This was probably due to the fact that the high temperature of the reaction volatilized formaldehyde. In order to observe the aldehyde produced from the reaction, *N*,*N*-diethyl-4-nitrosoaniline (DENA) was chosen as the next substrate.

Reactions were performed using a 50x molar excess of H_2O_2 over DENA and the final concentrations of bicarbonate and Mn(II) were 0.40 M and 4.0 μM, respectively. As

with the DMNA oxidations, the two major products formed were those from *N*-dealkylation, the *N*-ethyl-4-nitroaniline and 4-nitroaniline.

In order to trap the aldehyde produced, the reaction was performed in a multi-necked round bottom flask with a stream of nitrogen gas passing over the reaction. As the reaction progressed, the aldehyde would evaporate from the reaction solution and travel with the stream of nitrogen, which was passed through an ice cooled trap to condense the aldehyde. An initial Tollen's test of the condensed solution gave a positive result indicating the presence of an aldehyde. GC and ^{1}H NMR analysis of the condensed solution compared with an authentic sample proved that the product was acetaldehyde, Figure 3-34.

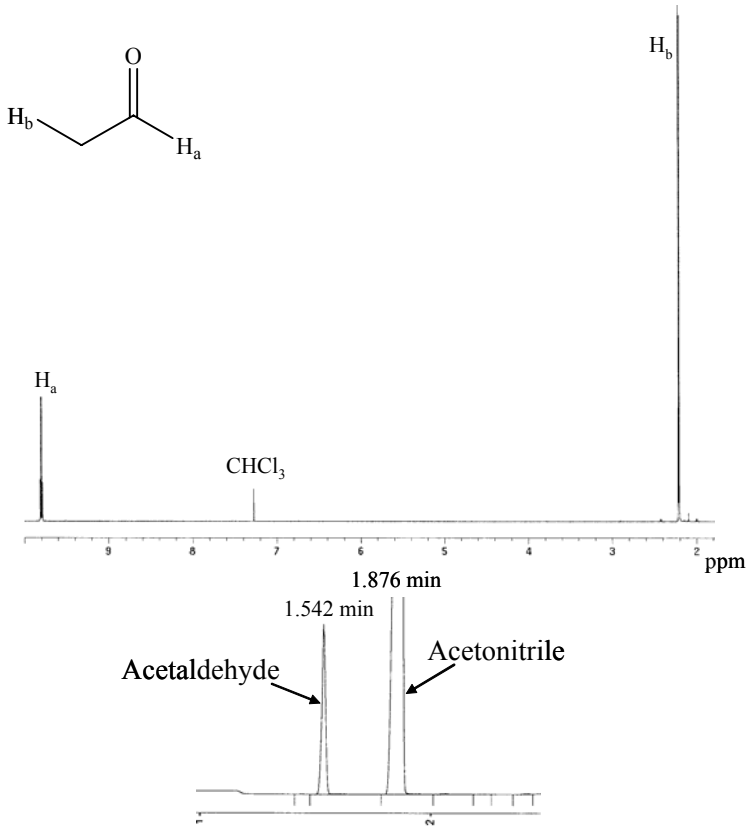

Figure 3-34. The solution collected from the reaction of *N*,*N*-diethyl-4-nitrosoaniline was analyzed by Gas Chromatography (lower figure), which was compared to an authentic sample of acetaldehyde. ^{1}H NMR (top figure) of the solution also confirmed that the product was acetaldehyde.

Proposed Mechanism of *N*-dealkylation

The *N*-methyl-4-nitroaniline, *N*-ethyl-4-nitroaniline, acetaldehyde, for DENA oxidation, and 4-nitroaniline observed from the oxidation of *N*,*N*-dimethyl-4-nitrosoaniline (DMNA) and *N*,*N*-diethyl-4-nitrosoaniline (DENA) by hydrogen peroxide catalyzed by manganese(II) in the presence of bicarbonate are due to oxidative *N*-dealkylation.

The mechanism of metal catalyzed oxidative *N*-dealkylation of amines currently reported in the literature is based on experiments conducted to determine the mechanism of cytochrome P-450 oxidative *N*-dealkylation. However, after more than 40 years of study, uncertainties still exist as to the mechanistic details in the oxidative *N*-dealkylation of amines by cytochrome P-450.[70-74] The current literature recognizes two dominant pathways for the production of the observed products in the presence of cytochrome P-450, hydrogen atom abstraction and single electron transfer.[71-81]

In addition, the products observed could be the result of oxidation by the carbonate radical anion, however, little is known about the reactivity of the carbonate radical anion with organic substrates, specifically, whether the products are phenols or biphenyls, such as are observed in reactions with the hydroxyl radical. Recently, the carbonate radical anion has been proposed to be the active oxidant in the peroxidase activity of the Cu,Zn-SOD in the presence of hydrogen peroxide and bicarbonate.[82-87] The carbonate radical has been implicated in these works to be the source of observed protein damage. Second-order rate constants of 4.2×10^8 $M^{-1}s^{-1}$ have been observed for the radical with several organic compounds including, indole, and its derivatives,[88] but no rate constants were found for reactions with amines.

The mode of attack of the carbonate radical anion could occur in one of three ways: 1) a single electron transfer from the substrate to the radical, 2) addition of the radical to the substrate, or 3) hydrogen abstraction by the radical. Unfortunately, the organic products for reactions with the carbonate radical anion have not been identified. Therefore, it is not know whether oxidative *N*-dealkylation may be a product of reactions with the carbonate radical anion.

The proposed pathways are presented in Figure 3-35, along with potential manganese complexes that are proposed in this study, carbonate radicals could also be replaced for any of the manganese species. Specific details about the identity of these manganese species and how they are generated in the hydrogen peroxide oxidation system with bicarbonate will follow in a later section. The figure only represents the products, a secondary amine and a molecule of ketone or aldehyde, depending on the substrate, of the first *N*-dealkylation of a tertiary amine. A tertiary amine can be oxidized a maximum of three times, as ammonia will be the final nitrogen containing compound of the last oxidative *N*-dealkylation. Also, amines can only be *N*-dealkylated when a hydrogen is present on the carbon α to the nitrogen.

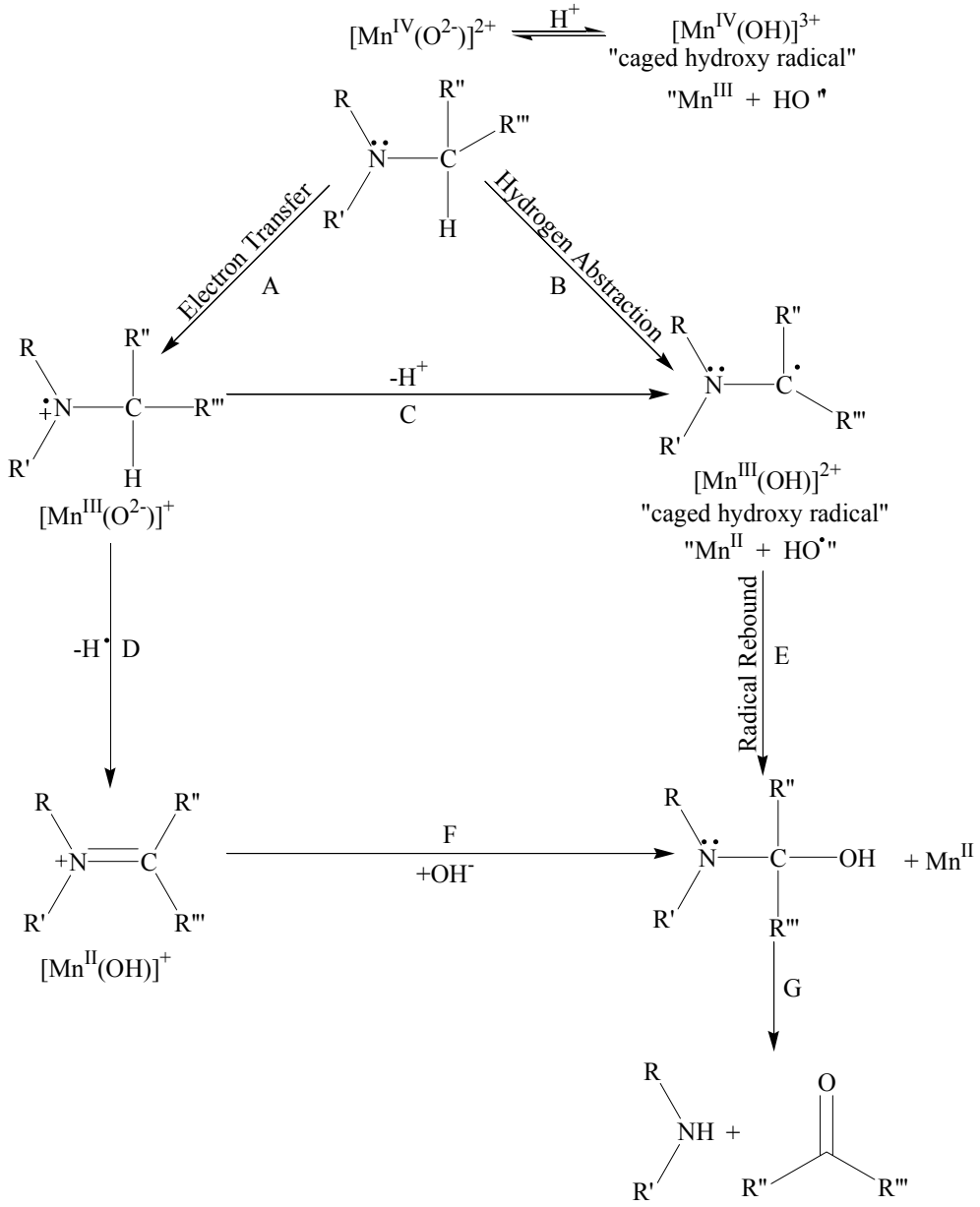

Figure 3-35. The proposed mechanism for the oxidative *N*-dealkylation of amines by hydrogen peroxide in the presence of bicarbonate as catalyzed by manganese(II). The secondary amine produced can cycle again as long as it contains a hydrogen on the carbon α to the nitrogen. A second molecule of aldehyde or ketone will also be produced.

For the hydrogen abstraction pathway, the oxidation of the amine begins with the abstraction of a hydrogen on the carbon α to the nitrogen on the substrate by the $[Mn^{IV}(O^{2-})]^{2+}$ complex, or a carbonate radical. This abstraction may be easier to recognize by using the protonated form of the $[Mn^{IV}(O^{2-})]^{2+}$ complex, $[Mn^{III}(OH)]^{3+}$.

This complex can be imagined to be the "caged" hydroxyl radical with a Mn^{III} ion. The abstraction of the hydrogen from the substrate is accomplished using the "caged" hydroxyl radical to yield the $[Mn^{III}(OH)]^{2+}$ complex and a carbon centered radical, Figure 3-35, pathway B. The $[Mn^{III}(OH)]^{2+}$ complex that is produced may also be imagined to be a "caged" hydroxyl radical with a Mn^{II} ion, $[Mn^{II}(OH)]^{2+}$. This "caged" hydroxyl radical can then rebound with the carbon centered radical, Figure 3-35, pathway E, to yield the carbinolamine and a Mn^{II} ion. The resulting carbinolamine intermediate then decomposes to yield the observed products, the *N*-dealkylated amine and a molecule of aldehyde or ketone, depending on the substrate. The carbinolamine intermediate has been isolated under certain conditions depending on the amine used.[89-92]

The second proposed pathway for the oxidative *N*-dealkylation of amines occurs via a single electron transfer. Initially, the $[Mn^{IV}(O^{2-})]^{2+}$ complex, or a carbonate radical, will oxidize the amine by removing a single electron from the lone pair on the nitrogen to form the $[Mn^{III}(O^{2-})]^{+}$ complex (a carbonate dianion in the case of the carbonate radical) and a nitrogen centered radical cation, Figure 3-35, pathway A. The nitrogen centered radical cation can be converted to the carbon centered radical by loss of a proton, at which time the above scheme can be followed to give the oxidative *N*-dealkylated products. On the other hand, the $[Mn^{III}(O^{2-})]^{+}$ complex is again a "caged" hydroxyl radical when protonated. This complex can then abstract a hydrogen from the nitrogen centered radical cation to yield the imine and $[Mn^{II}(OH)]^{+}$, Figure 3-35, pathway D. Once the imine is formed, attack of a hydroxide ion on the electrophilic carbon of the imine, Figure 3-35, pathway F, yields the identical carbinolamine as the hydrogen abstraction pathway, which then decomposes to yield the same final products.

Support for the Single Electron Transfer Pathway

Cytochrome P-450 is an important iron porphyrin enzyme responsible for a number of oxidative and reductive transformations.[72] Much of the current literature on the mechanism of oxidative *N*-dealkylation by cytochrome P-450 indicates that the single electron transfer (SET) mechanism is the more probable pathway over the hydrogen atom transfer (HAT).[72-74] Support for the SET mechanism has come from the work of Miwa et al.,[73,74] in which experiments were conducted using hydrogen and deuterium isotope labeled substrates and analyzing the resulting product distributions. A set of experiments using *N*,*N*-dimethyl-2-amino-2-methyl-3-phenylpropane, where the two methyl groups bonded to the nitrogen were deuterated, were conducted to determine the deuterium isotope effect. The measured isotope effects were observed in the range of 0.946-1.12 with a mean of 1.04 ± 0.06, a value close to unity.

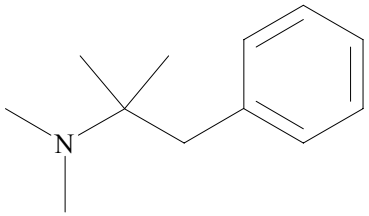

Figure 3-36. The structure of *N*,*N*-dimethyl-2-amino-2-methyl-3-phenylpropane, the substrate used by Miwa et al.[73,74] for use in experiments with cytochrome P450 on the oxidative *N*-dealkylation mechanism.

This small intermolecular deuterium isotope effect indicates that the breaking of the α-carbon-hydrogen bond is not the rate determining step as would be the case in the hydrogen abstraction pathway, Figure 3-35, pathway B. If the mechanism were to follow the hydrogen abstraction of Figure 3-35, pathway B, deuterium isotope values should be much greater than 1, since the observed rate for the substrate with all of the *N*-bound methyl groups having hydrogens would be larger than the observed rate where all of the *N*-bound methyl groups had been deuterated.

Solvent Isotope Effect

In addition to monitoring the kinetic effects of bicarbonate, hydrogen peroxide, and manganese, Bennett[46] also observed a large, inverse solvent isotope effect (0.49 ± 0.05 in 100% deuterium oxide) when the oxidation of nucleophilic alkenes was performed in increasing amounts of deuterium oxide. A proton inventory study was also carried out to determine the number of protons undergoing exchange during the reaction. From these data, it was determined that only one proton was undergoing exchange during the reaction. Unfortunately, no explanation was given as to why such a large, inverse isotope effect was found for the epoxidation of these alkenes using the manganese catalyzed system.

Solvent isotope effect experiments were conducted a second time to confirm their existence and that the value was indeed large and inverse. Sulfonated styrene (1.0 mM) was epoxidized in pure water and deuterium oxide with 1.00 M sodium bicarbonate, 0.5 μM Mn(II), and 0.3 and 1.0 M hydrogen peroxide. The observed first-order rate constants can be found in Table 3-3 and are similar to those found by Bennett.[46]

Table 3-3. Comparison of first-order rate constants for the epoxidation of sulfonated styrene in H_2O and D_2O. Reaction conditions: 0.001 M SS, 1.0 M Sodium Bicarbonate, 0.50 μM Mn(II).

$[H_2O_2]$, M	**k_{obs}, s^{-1} (H_2O)**	**k_{obs}, s^{-1} (D_2O)**	**Solvent Isotope Effect (k_H/k_D)**
0.30	3.67×10^{-3}	7.65×10^{-3}	.48
1.0	1.68×10^{-3}	3.57×10^{-3}	.47
1.0	2.01×10^{-3}	4.37×10^{-3}	.46

"Solvent isotope effect" is the effect of deuterium versus protium solvents often used in discussions of kinetic and equilibrium processes.[93] There are three main factors that affect the rates of reactions in these solvents: 1) The solvent may be a reactant 2) the reactant may rapidly exchange isotopically labeled hydrogens with the solvent or 3) the

nature of the weak solute-solvent interactions may change during the activation.[94] For any solvent isotope effect, a combination of all three factors most likely will contribute to the overall isotope effect.

Similar large, inverse isotope effects are rare, but have been reported in the literature.[95-97] Usually, inverse isotope effects are caused by the protonation of an electronegative atom, such as oxygen, in a rapid equilibrium prior to the rate determining step. For example, Pritchard and Long[95] have investigated the hydrolysis of simple epoxides in deuterium oxide-water mixtures. The proposed mechanism is shown in Figure 3-37.

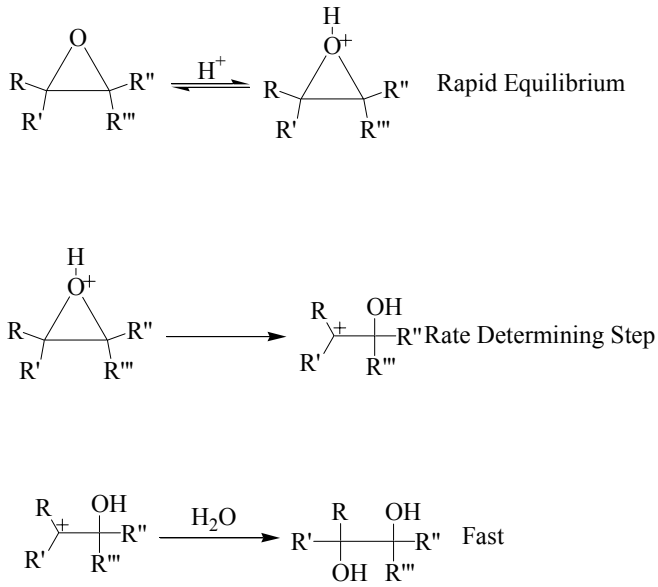

Figure 3-37. Mechanism of epoxide hydrolysis in acidic media.

Initially, there is a rapid equilibrium between the epoxide and a proton, followed by the rate controlling step, cleaving of one of the epoxide C-O bonds to give the carbocation alcohol intermediate. The last step of the reaction is the addition of water to the carbocation and is a fast step.

In the case of alkene epoxidation, two possible species could be protonated in solution, the high valent metal oxo species or carbonate radical anion. As is the case for

the epoxides, the protonated metal oxo species would be a strong acid and the reaction would need to be performed at lower pH for any appreciable concentration of the protonated species to be attainable for reaction. Since the pH of the performed reactions was 8.4, this is not a likely explanation for the observed solvent isotope effect. The protonation of the carbonate radical will be discussed shortly.

A proton transfer during the rate determining step could also lead to an inverse isotope effect. In the epoxidation of an alkene by a metal oxo complex, no proton exchange can be envisioned, as shown in Figure 3-38.

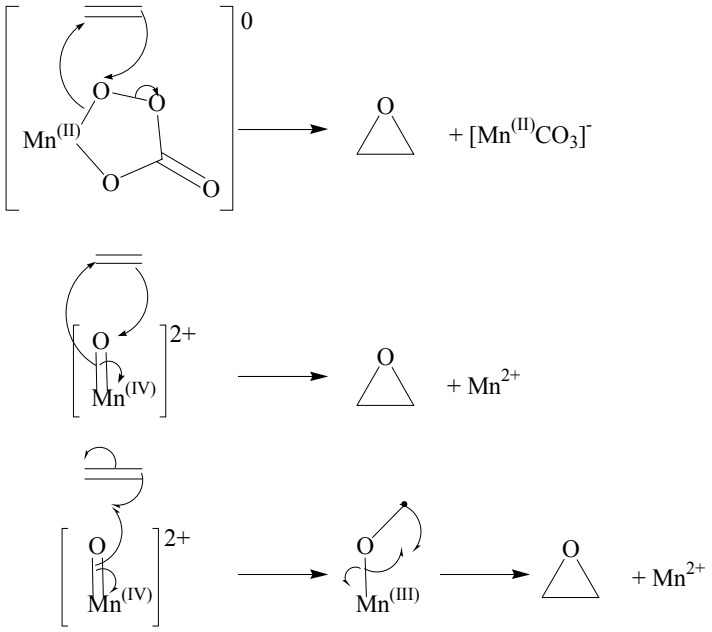

Figure 3-38. Possible epoxidation routes through a manganese(IV) oxo complex. None of the envisioned reactions has a proton transfer.

A proton transfer could be possible for the epoxidation of a nucleophilic alkene in which the manganese is only acting as a Lewis acid, Figure 3-39. This would be the simplest mechanism for the epoxidation of the alkene. In this scenario, the manganese(II) would facilitate the cleaving of the O-O bond and stabilize the formed carbonate leaving group. However, this mechanism does raise questions as to why other

metal cations with similar Lewis acidities do not have similar activities.[40] It does, however, satisfy the requirement noted in the epoxidation of styrene in micellar solution that the active species be uncharged. By simply binding a bicarbonate anion (or another peroxycarbonate) to the metal, the positive charge of the complex will be neutralized.

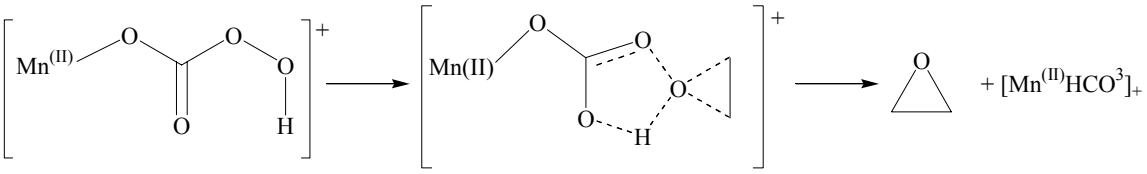

Figure 3-39. Mechanism of oxygen transfer by attack of the alkene on a manganese(II) bound peroxycarbonate. The proton transfer in the transition state may account for the inverse isotope effect observed.

It has also been proposed that the carbonate radical anion is formed in solutions of bicarbonate with hydrogen peroxide and manganese(II). The carbonate radical is a potent one electron oxidant (1.59 V vs SHE at pH 12),[98] that is believed to exist as an acid/base couple, although the pK_a has yet to be firmly established. There is literature to suggest that the pK_a lies in the range of about 7.9[99] to 9.5.[100] However, there has also been the suggestion that it is strong acid (pKa < 0).[101]

If the protonated carbonate radical were the active oxidizing agent for the epoxidation of nucleophilic alkenes, the epoxidations performed in cationic and anionic micellar solutions would suggest that the pK_a lies somewhere in the range of 7.9 – 9.5, since no difference in epoxidation rates were observed and the protonated radical is uncharged. The protonated carbonate radical would then be the primary oxidizing species. A proposed mechanism is suggested in Figure 3-40. The existence of the protonated radical would explain the inverse solvent isotope effect. As noted earlier, the protonated species will be in higher concentration in deuterium oxide than in water, therefore, increasing the concentration of the active oxidant. With an increase in the

active oxidant, an increase in the rate of the epoxidation would occur to give the observed inverse effect.

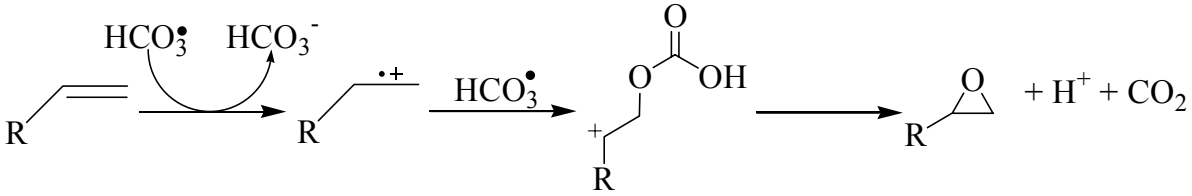

Figure 3-40. Oxidation of a nucleophilic alkene by two sequential reactions with the carbonate radical. The carbocation intermediate formed explains the loss of retention observed for cis-alkenes.

In addition to measuring the solvent isotope effect on the nucleophilic alkene epoxidation, the effect on the hydrogen peroxide decomposition was also studied. The results of reactions performed in deuterium oxide are presented in Table 3-4. From these experiments, it is observed that the hydrogen peroxide decomposition has a large, normal solvent isotope effect.

Table 3-4. Comparison of solvent isotope effect for hydrogen peroxide decomposition. Reaction Conditions: 0.40 M HCO_3^-, 0.10 M H_2O_2

[Mn(II)]	k_H/k_D
3 μM	1.47 ± 0.05
4 μM	1.49 ± 0.06

Proposed Mechanism

Based on the information gleaned from previous kinetic experiments, which were reported earlier, on hydrogen peroxide decomposition and nucleophilic alkene epoxidation, in both water and deuterium oxide, the following mechanism is proposed in this work (Figure 3-41). The free hydroxyl radical mechanism proposed by Sychev seems unlikely given the clean epoxidations of nucleophilic alkenes with a lack of any side products (polystyrene or 2-phenyl ethanol). This does not mean, however, that radical chemistry is not occurring. As discussed earlier, carbonate radicals are more than

likely being generated in this system. This was discussed earlier in relation to the products observed in the oxidation of *N*,*N*-dimethyl-4-nitrosoaniline and *N*,*N*-diethyl-4-nitrosoaniline. Chapter 4 will discuss the epoxidation of electrophilic alkenes by hydrogen peroxide in the presence of bicarbonate and manganese. As with the reactions of nucleophilic alkenes, no side products indicative of free hydroxyl radical chemistry are observed in the reactions that include manganese. Also, it will be shown that the oxidation of electrophilic alkenes occurs exclusively when hydroperoxide and hypochlorite are used.

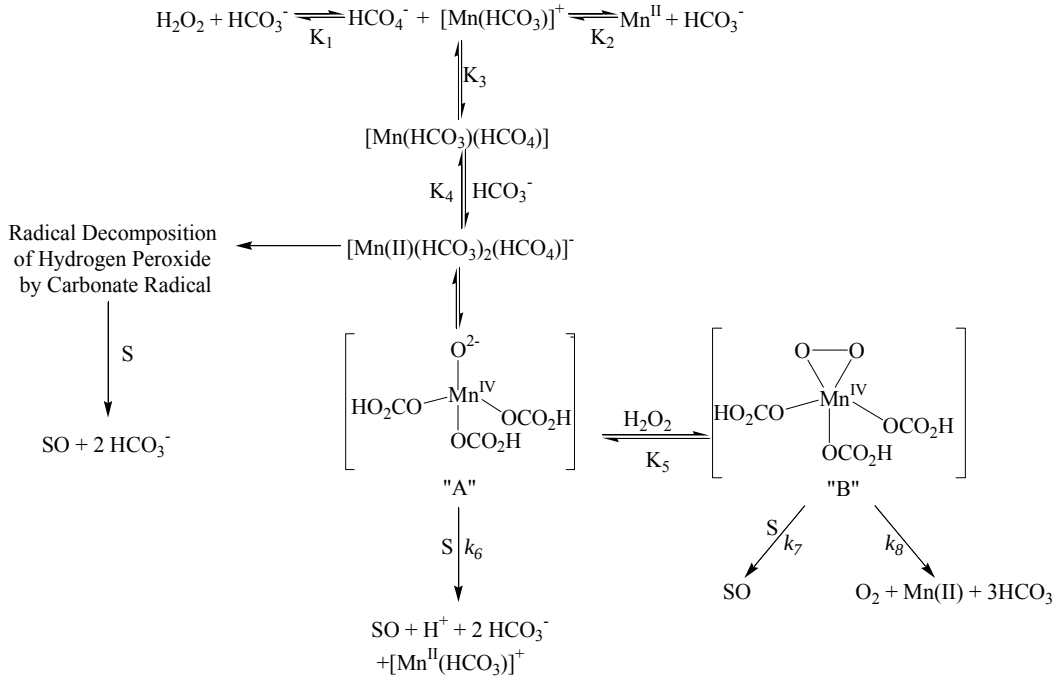

Figure 3-41. Proposed mechanism for hydrogen peroxide decomposition and nucleophilic alkene epoxidation in the presence of bicarbonate catalyzed by Mn(II).

The active epoxidation catalyst is proposed to be either the high oxidation state manganese oxo complex or the carbonate radical. High oxidation state metal oxo complexes have been proposed for the iron(III) tetrakis(pentafluorophenyl) porphyrin complex with hydrogen peroxide as observed by Traylor.[20] The generation of the manganese catalyst would occur via the two electron oxidation of manganese, as seen in

Figure 3-42. A high oxidation state Mn(IV) oxo complex is similar to the epoxidation route of the Mn-porphyrin[102-104] and Mn(salen)[105,106] complexes. A discussion of the nucleophilic alkene epoxidation pathway will be presented first, followed by the Fenton reactions of the catalytic species.

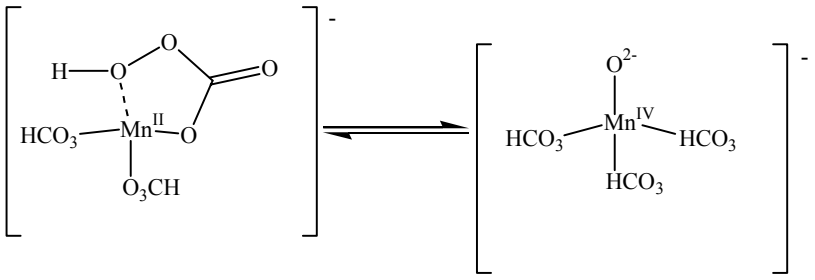

Figure 3-42. Proposed generation of the active manganese catalyst by from the $[Mn^{II}(HCO_3)_2(HCO_4)]^-$ complex by a 2 electron oxidation of manganese to form a high valent $[Mn\text{-}O^{2-}]^{2+}$ complex.

As was noted in Chapter 2, the reaction rate was not significantly different when alkene epoxidations were performed in cation or anion surfactants, indicating that the active epoxidation catalyst must be uncharged. These data also indicate that the carbonate radical anion may not be the active epoxidation catalyst, as a reduction in the rate of the reaction in the presence of anionic surfactant would be expected, unless the radical is protonated as mentioned earlier.

The reaction of the intermediate "A" with hydrogen peroxide could form the peroxo intermediate "B". This complex is similar to that seen for the addition of a molecule of hydrogen peroxide in the oxidation by MTO. The alkene can attack one of the electrophilic oxygens of the peroxo ligand to yield the epoxide. This is analogous to the observation by Espenson in the epoxidation of olefins by MTO/hydrogen peroxide. As with MTO, this intermediate reacts with olefins at a slower rate than the metal oxo complex. This could explain why a decrease in the rate of nucleophilic oxidation

catalyzed by manganese(II) is observed at higher hydrogen peroxide concentration. As the concentration of hydrogen peroxide increases, so will the concentration of "B". Since the oxidation of the alkene by "B" is slower, the reaction will slow down as hydrogen peroxide increases, as observed in the hydrogen peroxide dependence. If, however, the carbonate radical is responsible for the oxidation, the generation of carbonate radicals will decrease with an increasing hydrogen peroxide concentration. This will be demonstrated in the numerical simulations for the hydrogen peroxide decomposition.

In addition to the pathway involving the peroxycarbonate oxidation of the metal to generate the two electron metal oxo complex, $[Mn^{IV}(O^{2-})]^{2+}$, a one electron oxidation begins Fenton type chemistry. However, it is proposed that hydroxyl radicals are not generated under these conditions, since bicarbonate acts as a scavenger for the hydroxyl radicals to generate the carbonate radical anion. As discussed previously, there is little known in the current literature about the reactivity of the carbonate radical anion oxidation of organic substrates.

Numerical Simulation of the Proposed Mechanism

Unfortunately, an analytical solution to the rate expression for this reaction cannot be found. However, numerical simulation can be used as a tool to model the kinetics of a reaction for which an analytical solution cannot be derived. Therefore, numerical simulation provides a powerful tool to test kinetic models to determine whether they fit the observed data. While a particular simulation may fit the experimental data, it by no means indicates that this is the true or accurate mechanism of the reaction. Multiple simulations may, in fact, yield good fits to observed data. When a simulation fits the observed data, the simulation may provide a new angle on possible experiments with which to investigate the reaction. If the experiments are performed and the outcome is

contradictory to the simulated data, then that mechanism must be modified or replaced in an attempt to refine the model of the reaction. Kinetica 2003 was used for all the numerical simulations that will be presented.

Kinetica 2003 allows the user to input a series of single step reactions with their rate constants to calculate the concentrations of the species with time. It should be noted that only two reactants can combine in a single step, therefore, if three species must react, an intermediate species must be formed first and that intermediate then reacts with the third reactant. An example will be given shortly.

Initially, since many of the dependencies on the reactants were observed to be the same for the hydrogen peroxide decomposition and nucleophilic alkene epoxidation, it was thought that these reactions were proceeding through the same intermediates, both "A" and "B."

First, the common intermediate "A" must be generated. It is assumed that the generation of this intermediate is fast, since the order of addition in the hydrogen peroxide decomposition studies show that the order of addition of hydrogen peroxide, bicarbonate, or manganese(II), has no effect on the observed decomposition rate. The lack of a mixed order dependence on any of these species also indicates that the generation of the catalyst is rapid. We propose that hydrogen peroxide and bicarbonate equilibrate to form peroxycarbonate (K_1) and that peroxycarbonate combines with bicarbonate and manganese(II) to form the active catalyst. This would seem reasonable given the kinetic data suggests a rate = $k[\text{Mn(II)}][HCO_3^-]^2[H_2O_2]^x$, for the hydrogen peroxide decomposition.

It was thought that the generation of the active manganese compound, "A", could be generated by the simple equilibration of Mn(II), bicarbonate, and hydrogen peroxide, as seen by Equation (3-15)-(3-17).

$HCO_3^- + H_2O_2 \rightleftharpoons HCO_4^- + H_2O$ $K_1 = 0.32\ M^{-1}$ (3-15)

$Mn(II) + HCO_3^- \rightleftharpoons [Mn^{II}(HCO_3)]^+$ $K_2 = 19.05\ M^{-1}$ (3-16)

$[Mn^{II}(HCO_3)]^+ + HCO_4^- \rightleftharpoons A$ K_3 (3-17)

Only two of the equilibrium constants are known from literature data. The K_1 for the peroxycarbonate formation is 0.32 M^{-1},[32] and the K_2 for the generation of the $[Mn(HCO_3)]^+$ ion-pair is 19.05 M^{-1}.[107]

More than likely, manganese(II) is acting as a Lewis acid to rapidly establish the peroxycarbonate equilibrium. Experiments attempting to observe this phenomenon with manganese(II) proved unsuccessful. The paramagnetic nature of manganese(II) made acquiring ^{13}C NMR spectra difficult. Experiments by Yao[34] and Albert[108] show that the addition of zinc complexes, which act as carbonic anhydrase mimics, do rapidly equilibrate the peroxycarbonate. Therefore, the forward and reverse reactions for the production of peroxycarbonate have been accelerated while keeping the overall equilibrium constant the same.

The Kinetica 2003 equations used are shown below, as they appear in the program. The rate constant for a single step is listed after the equation. As noted earlier, only two reactants can be used in any given step, and equilibrium expressions must be written as two reactions, one for the forward reaction and one for the reverse. So, since there are three equilibria in the predicted generation of the active manganese species, six reactions are required in Kinetica to simulate the concentrations over time. Given that the order of

addition of hydrogen peroxide and manganese(II) made no significant impact of the reaction rate in the decomposition data, a rapid equilibrium step is used for the reaction of $[Mn(HCO_3)]^+ + HCO_4^-$, $k = 1 \times 10^7$, for both the forward and reverse steps. "A" in the following kinetic steps is the active manganese complex.

1; H2O2 + HCO3 → HCO4; 3.800E-02 (3-18)

2; HCO4 → HCO3 + H2O2; 1.200E-01 (3-19)

3; Mn(II) + HCO3 → Mn(II)HCO3; 1.900E07 (3-20)

4; Mn(II)HCO3 → Mn(II) + HCO3; 1.000E06 (3-21)

5; Mn(II)HCO3 + HCO4 → A; 1.000E07 (3-22)

6; A → Mn(II)HCO3 + HCO4; 1.000E07 (3-23)

When a simulation of the above mechanism for the formation of the active manganese catalyst was performed using 1.00 M hydrogen peroxide, 4 μM Mn(II), and varying bicarbonate, a second-order relationship was not found for the production of the active catalyst, Figure 3-43, which is the observed dependence for both the hydrogen peroxide decomposition and nucleophilic alkene epoxidation.

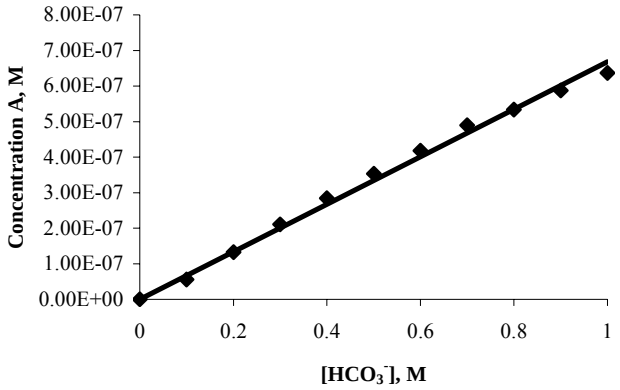

Figure 3-43. Simulation of the dependence on the concentration of the active catalyst with varying bicarbonate. Simulation conditions: 1.00 M hydrogen peroxide and 4 μM Mn(II). $y = ((6.55 \pm 0.37)x10^{-7})x$, error reported to the 95% confidence.

The predicted second-order dependence on bicarbonate is not observed from these simulations. The reason for the lack of second-order behavior is due to the equilibrium constant for the $[Mn(II)(HCO_3)]^+$ ion-pair. Since the equilibrium constant is large, the concentration of $[Mn(HCO_3)]^+$ quickly saturates, as seen in Figure 3-44.

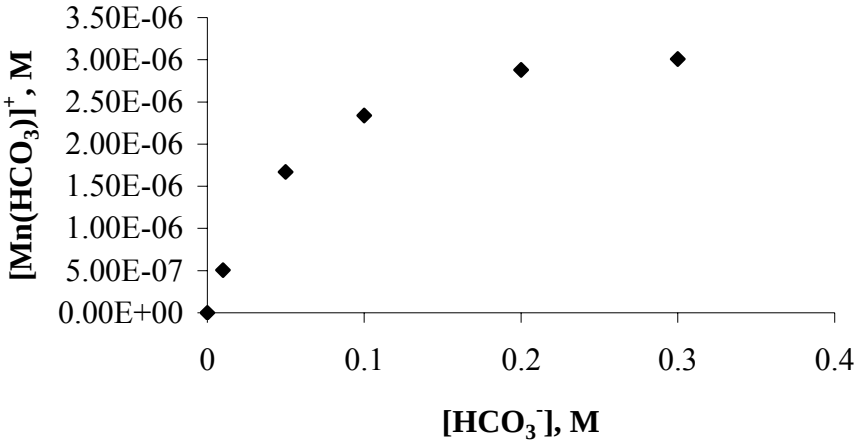

Figure 3-44. Plot of simulation results for $[Mn(HCO_3)]^+$ versus $[HCO_3^-]$. The $[Mn(HCO_3)]^+$ quickly saturates due to the large equilibrium constant of 19.05. Simulation conditions: 1.00 M H_2O_2, 4 μM Mn(II).

In order to counteract the saturation effect seen in the equilibrium of $[Mn(HCO_3)]^+$, a third bicarbonate anion is required in the generation of the active catalyst. The steps now required for the generation of the active catalyst are shown below.

1; H2O2 + HCO3 → HCO4; 3.800E-02; (3-24)

2; HCO4 → HCO3 + H2O2; 1.200E-01; (3-25)

3; Mn(II) + HCO3 → Mn(II)HCO3; 1.900E07; (3-26)

4; Mn(II)HCO3 → Mn(II) + HCO3; 1.000E06; (3-27)

5; Mn(II)HCO3 + HCO4 → [Mn(II)(HCO3)(HCO4); 1.000E07; (3-28)

6; [Mn(II)(HCO3)(HCO4) → Mn(II)HCO3 + HCO4; 1.000E07; (3-29)

7; [Mn(II)(HCO3)(HCO4) + HCO3 → A; 1.000E07; (3-30)

8; A→[Mn(II)(HCO3)(HCO4) + HCO3; 1.000E07; (3-31)

When a simulation is performed with varying bicarbonate concentration in the presence of 1.00 M hydrogen peroxide and 4 μM Mn(II), the graph presented in Figure 3-45 is obtained, for which a second-order dependence on bicarbonate is now observed.

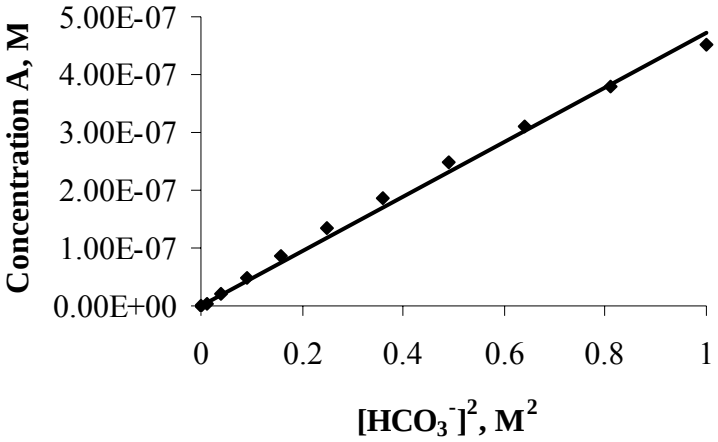

Figure 3-45. Simulation of the dependence on the concentration of the active catalyst with varying [HCO_3]. Simulation Conditions: 1.00 M hydrogen peroxide and 4 μM Mn(II). y = ((4.60 ± 0.22)x10^{-7})x, error reported to the 95% confidence.

Originally, before the discovery that carbonate radicals might be involved in the reaction, the nucleophilic alkene epoxidation studies and proposed rate equations (Equations 3-32 to 3-34) of Bennett[46] were used to determine the equilibrium constant for the generation of "B". The peroxide decomposition was ignored since it is slow compared to the epoxidation rate under the studied conditions.

$H_2O_2 + HCO_3 + Mn(II) \rightleftharpoons$ "A" K_1 (3-32)

"A" + $H_2O_2 \rightleftharpoons$ "B" K_2 (3-33)

"A" + HCO_3 + S $\rightleftharpoons$ SO + Mn(II) + $2HCO_3$ k_3 (3-34)

Equations (3-35)-(3-45) are the kinetic steps that have been found which describe the nucleophilic alkene epoxidation.

1; H2O2 + HCO3 → HCO4; 3.800E-01 (3-35)

2; HCO4 → HCO3 + H2O2; 1.200E00 (3-36)

3; Mn(II) + HCO3 → Mn(II)HCO3; 1.900E07 (3-37)

4; Mn(II)HCO3 → Mn(II) + HCO3; 1.000E06 (3-38)

5; Mn(II)HCO3 + HCO4 → Mn(II)(HCO3)(HCO4); 1.000E07 (3-39)

6; Mn(II)(HCO3)(HCO4) → Mn(II)HCO3 + HCO4; 1.000E07 (3-40)

7; Mn(II)(HCO3)(HCO4) + HCO3 → A; 1.000E07 (3-41)

8; A → Mn(II)(HCO3)(HCO4) + HCO3; 1.000E07 (3-42)

9; A + H2O2 → B; 1.100E07 (3-43)

10; B → A + H2O2; 1.000E05 (3-44)

11; S + A → *SO* + Mn(II)HCO3 + HCO3 + HCO3; 1.350E05 (3-45)

For these kinetic steps, the hydrogen peroxide dependence was used, initially, since the turnover in the hydrogen peroxide dependence is only observed in the nucleophilic alkene epoxidation. The fit of the numerical simulations to the hydrogen peroxide data is shown in Figure 3-46.

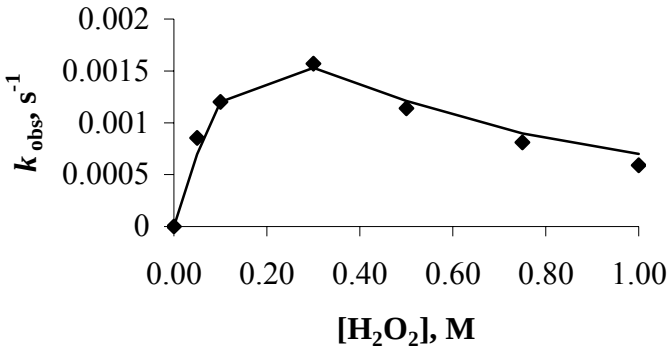

Figure 3-46. The generated curve for the hydrogen peroxide dependence on nucleophilic alkene oxidation. The points represent the observed k_{obs} experimentally determined by Bennett.[46] The line is the simulated k_{obs} at each H_2O_2 concentration. Reaction and simulation conditions: 0.5 μM Mn(II), 1.00 M bicarbonate, 0.001 M Sulfonated Styrene (SS).

Once the rate constants were determined to allow good fits to the observed data, the other dependencies needed to be check to assure that the kinetic steps and rate constants will predict the observed trends. Plots of simulations where the rate constants are varied from those above can be found in the Appendix. The bicarbonate and manganese dependencies are shown in Figures 3-47 and 3-48, respectively.

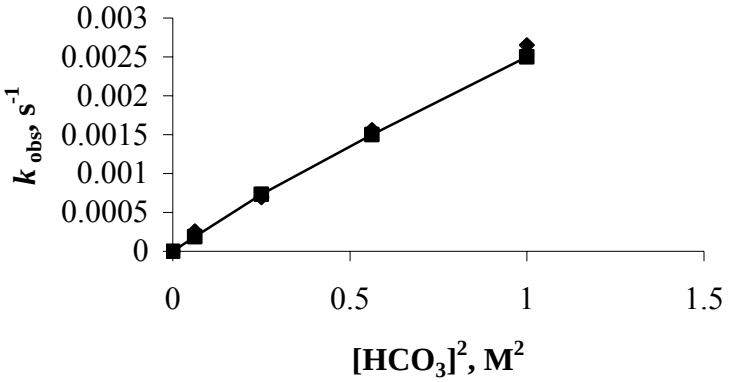

Figure 3-47. The generated curve for the bicarbonate dependence on nucleophilic alkene oxidation. The points represent the observed k_{obs} experimentally determined by Bennett.[46] The line is the simulated k_{obs} at each $[HCO_3]$ concentration. Reaction and Simulation Conditions: 0.5 μM Mn(II), 0.10 M hydrogen peroxide, 0.001 M Sulfonated Styrene (SS).

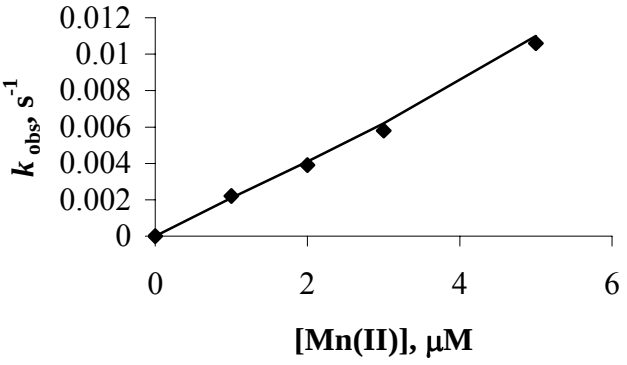

Figure 3-48. The generated curve for the manganese dependence on nucleophilic alkene oxidation. The points represent the observed k_{obs} experimentally determined by Bennett.[46] The line is the simulated k_{obs} at each [Mn(II)] concentration. Reaction and simulation conditions: 1.00 M bicarbonate, 0.55 M hydrogen peroxide, 0.001 M Sulfonated Styrene.

Once the nucleophilic alkene epoxidation kinetics in the absence of hydrogen peroxide decomposition were complete, simulations attempting to model the mechanism of the hydrogen peroxide decomposition were conducted. As stated earlier, our assumption was that the intermediates of the nucleophilic alkene epoxidation would be the same for the hydrogen peroxide decomposition. The simplest decomposition pathway for the decomposition of hydrogen peroxide would be for "B" to decompose to release oxygen and reduce Mn(IV) to Mn(II), as seen in Figure 3-41. The following set of kinetic steps (Equations 3-46 to 3-57) were then used to model this reaction. The alkene concentration (S in Equation 3-57) is set to 0, since there is no alkene epoxidation occurring in these reactions.

1; H2O2 + HCO3→HCO4; 3.800E-01 (3-46)

2; HCO4→HCO3 + H2O2; 1.200E00 (3-47)

3; Mn(II) + HCO3→Mn(II)HCO3; 1.900E07 (3-48)

4; Mn(II)HCO3→Mn(II) + HCO3; 1.000E06 (3-49)

5; Mn(II)HCO3 + HCO4→Mn(II)(HCO3)(HCO4); 1.000E07 (3-50)

6; Mn(II)(HCO3)(HCO4) →Mn(II)HCO3 + HCO4; 1.000E07 (3-51)

7; Mn(II)(HCO3)(HCO4) + HCO3→A; 1.000E07 (3-52)

8; A→Mn(II)(HCO3)(HCO4) + HCO3; 1.000E07 (3-53)

9; A + H2O2→B; 1.100E07 (3-54)

10; B→A + H2O2; 1.000E05 (3-55)

12; B→Mn(II)HCO3 + O2 + HCO3 + HCO3; 1.000E02 (3-56)

13; S + A→*SO* + Mn(II)HCO3 + HCO3 + HCO3; 1.350E05 (3-57)

Unfortunately, the hydrogen peroxide decay curves, for which an example is shown in Figure 3-49, never adequately predicted the observed hydrogen peroxide decay.

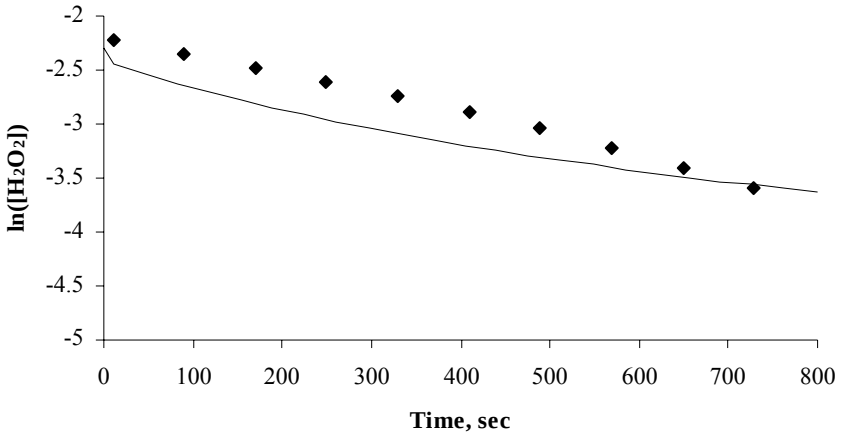

Figure 3-49. A typical numerical simulation plot attempting to model the hydrogen peroxide decay curves. Points represent observed ln[H_2O_2] versus time, while the line is the simulated ln([H_2O_2]) versus time. Reaction and simulation conditions: 0.10 M H_2O_2, 0.30 M HCO_3^-, 4.0 μM Mn(II).

Since the plots do not adequately predict the hydrogen peroxide decomposition, a new model was proposed based on Fenton type reactions of metal cations with hydrogen peroxide. This mechanism will be presented shortly.

The reaction of the carbonate radical alone does not explain the hydrogen peroxide dependence observed in the epoxidation kinetics. More than likely, an unreactive, or slightly reactive, hydrogen peroxide intermediate (intermediate "B") in the presence of a radical species is highly unlikely, therefore, the existence of the intermediate "B" has been excluded at this time. Since both the carbonate radical anion and the manganese oxo complex have been proposed to be the source of oxygen in the alkene epoxidation, the rate of alkene epoxidation will be the sum of the reactions of the alkene with both species. The alkene epoxidation was not attempted yet in the mechanism in which the carbonate radical is generated.

While Fenton chemistry of metal cations usually generates hydroxyl radicals, no hydroxyl radicals will be produced in this model. Since the concentration of bicarbonate is so much higher than the metal cation, all reactions that produce the hydroxyl and perhydroxyl radicals are replaced with the reaction of a bicarbonate ion to generate water, or hydrogen peroxide, and a carbonate radical anion. While this radical is known to react with redox active metals, little is know about its reactivity with organic substrates, specifically what the rate constants for reactions are. For all reactions shown, the rate constants used for the reaction of the carbonate radical were taken from the work Mazellier et al.[98] Rate constants for the reactions of Mn(II) and Mn(III) with superoxide were used from the work by Pick-Kaplan and Rabani.[109]

For now, current information available in the literature about the reactivity of the carbonate radical with organic substrates is limited. Future attempts to model the nucleophilic alkene epoxidation may become possible when new information concerning this radical species becomes available. In the mean time, kinetic data for the reactivity of the carbonate radical with hydrogen peroxide, and other active oxygen species, including the superoxide radical anion, the hydroxyl radical, and the perhydroxyl radical is currently available in the literature.[98,109]

Attempts to model the hydrogen peroxide decomposition based on Fenton chemistry have continued. Using Sychev's model of hydrogen peroxide decomposition, Equations 3-4 to 3-14, the hydroxyl radicals produced were replaced by carbonate radicals by reaction with bicarbonate. Equations 3-58 to 3-67 are the reactions generated to describe the decomposition of hydrogen peroxide.

$$H_2O_2 \rightleftharpoons H^+ + HOO^- \quad (3\text{-}58)$$

$$H_2CO_3 \rightleftharpoons H^+ + HCO_3^- \quad (3\text{-}59)$$

$$H_2CO_3 \rightleftharpoons H_2O + CO_2 \quad (3\text{-}60)$$

$$HCO_3^- \rightleftharpoons CO_3^{2-} + H^+ \quad (3\text{-}61)$$

$$HCO_3^- + H_2O_2 \rightleftharpoons HCO_4^- + H_2O \quad (3\text{-}62)$$

$$2Mn^{2+} + 2HCO_4^- \rightarrow 2Mn^{3+} + 2\ CO_3^{-\bullet} + 2OH^- \quad (3\text{-}63)$$

$$Mn^{2+} + CO_3^{-\bullet} \rightarrow Mn^{3+} + CO_3^{2-} \quad (3\text{-}64)$$

$$Mn^{3+} + HOO^- + HCO_3^- \rightarrow Mn^{2+} + H_2O_2 + CO3^{-\bullet} \quad (3\text{-}65)$$

$$2Mn^{3+} + 2CO_3^{-\bullet} \rightarrow 2Mn^{2+} + O_2 + 2CO_2 \quad (3\text{-}66)$$

$$CO2(aq) \rightarrow CO2(g) \quad (3\text{-}67)$$

Simulations using these reactions were performed in an attempt to simulate the hydrogen peroxide decomposition. Unlike the simulations using the intermediates "A" and "B", hydrogen peroxide decay curves, such as the one presented in Figure 3-50, can now be generated. Equation 3-67 must be added since the catalyst lifetime studies proved that bicarbonate is being lost. Equations 3-68 to 3-93 are the equations used in Kinetica with the rate constants that were used. Rate constants for each of the reactions involving protons have been adjusted for pH 8.3. Rate constants for the reactions are from the following sources: Fridovich,[110] estimates of Mn(II) and Mn(III) using Mn(II) and Mn(III)porphyrin complex with carbonate radical anion, Mazellier,[98] reactions of carbonate radicals with hydrogen peroxide, Palmer and van Eldik[111] and Roughton, [112] carbon dioxide hydration, dehydration, pK_a H_2CO_3, pK_a bicarbonate. All other rate

constants have been adjusted to fit the hydrogen peroxide decay curves observed by experiment.

1; $H_2O_2 \rightarrow HOO^-$; 2.000E-02 (3-68)

2; $HOO^- \rightarrow H_2O_2$; 5.000E01 (3-69)

3; $CO_2 \rightarrow H_2CO_3$; 3.000E-02 (3-70)

4; $H_2CO_3 \rightarrow CO_2$; 2.000E01 (3-71)

5; $H_2CO_3 \rightarrow HCO_3$; 4.000E07 (3-72)

6; $HCO_3 \rightarrow H_2CO_3$; 7.000E2 (3-73)

7; $CO_2 \rightarrow HCO_3$; 1.700E-02 (3-74)

8; $HCO_3 \rightarrow CO_2$; 2.000E-05 (3-75)

9; $HCO_3 \rightarrow CO_3^{2-}$; 3.160E-01 (3-76)

10; $CO_3^{2-} \rightarrow HCO_3$; 5.000E01 (3-77)

11; $H_2O_2 + HCO_3 \rightarrow HCO_4$; 3.800E-01 (3-78)

12; $HCO_4 \rightarrow H_2O_2 + HCO_3$; 1.200E00; (3-79)

13; $Mn(II) + HCO_3 \rightarrow Mn(II)HCO_3$; 1.900E07; (3-80)

14; $Mn(II)HCO_3 \rightarrow Mn(II) + HCO_3$; 1.000E06; (3-81)

15; $Mn(II)HCO_3 + HCO_3 \rightarrow Mn(II)(HCO_3)_2$; 1.000E07; (3-82)

16; $Mn(II)(HCO_3)_2 \rightarrow Mn(II)HCO_3 + HCO_3$; 1.000E07; (3-83)

17; $Mn(III) + HCO_3 \rightarrow Mn(III)HCO_3$; 1.900E07; (3-84)

18; $Mn(III)HCO_3 \rightarrow Mn(III) + HCO_3$; 1.000E07; (3-85)

19; $Mn(III)HCO_3 + HCO_3 \rightarrow Mn(III)(HCO_3)_2$; 1.000E07; (3-86)

20; $Mn(III)(HCO_3)_2 \rightarrow Mn(III)HCO_3 + HCO_3$; 1.000E07; (3-87)

21; $Mn(II)(HCO_3)_2 + CO_3RadAn \rightarrow Mn(III)(HCO_3)_2 + CO_3^{2-}$; 5.000E07; (3-88)

22; Mn(III)(HCO3)2 + CO3RadAn →Mn(IV)CO3(HCO3)2 ; 1.200E07; (3-89)

23; Mn(IV)CO3(HCO3)2+Mn(IV)CO3(HCO3)2→Mn(II)(HCO3)2+Mn(II)(HCO3)2 + O2 + CO2 + CO2; 1.000E07; (3-90)

24; Mn(II)(HCO3)2+HCO4→Mn(III)(HCO3)2 + CO3RadAn ; 4.500E06; (3-91)

25; Mn(III)(HCO3)2 + HOO-→Mn(II)HCO3 + CO3RadAn + H2O2; 4.500E06; (3-92)

26; CO2→CO2g ; 2.500E-03; (3-93)

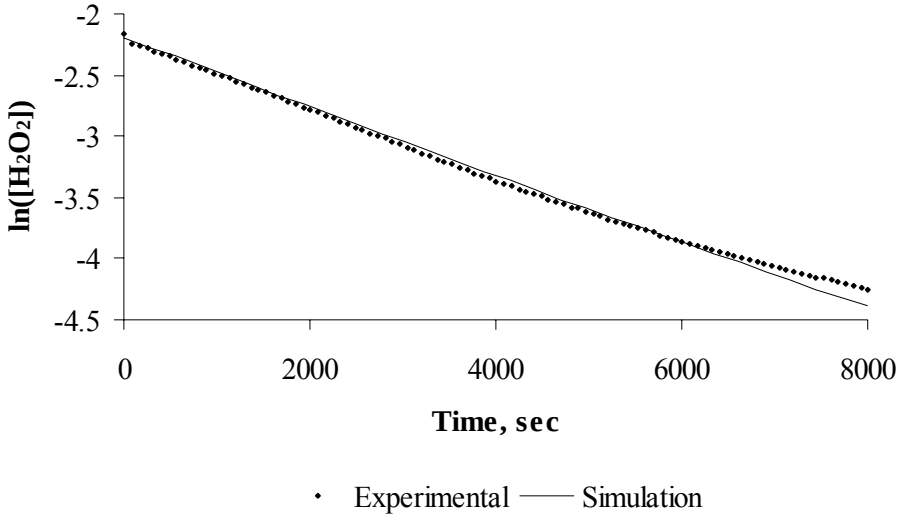

Figure 3-50. Simulation of hydrogen peroxide decay at lower bicarbonate concentration. Points represent data, while the line is the simulated decay. Reaction and simulation conditions: 0.10 M H_2O_2, 0.10 M HCO_3, 4 μM Mn(II).

From the data presented in Figure 3-46, it appears that the carbonate radical mechanism accurately predicts the hydrogen peroxide decomposition in the presence of bicarbonate and manganese(II). Figures 3-51, 3-52, and 3-53 represent the bicarbonate, manganese(II), and hydrogen peroxide dependencies for this mechanism.

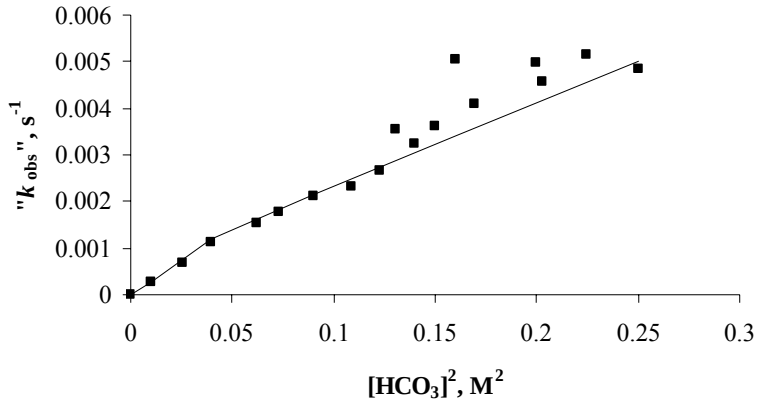

Figure 3-51. A plot of $[HCO_3]^2$ versus "k_{obs}" for the hydrogen peroxide decomposition. Reaction and simulation conditions: 0.10 M H_2O_2, 4 μM Mn(II).

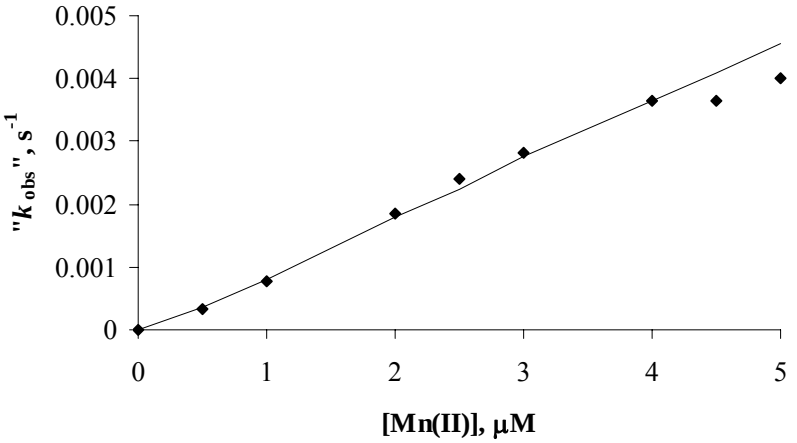

Figure 3-51. A plot of "k_{obs}" versus [Mn(II)] for the hydrogen peroxide decomposition. Reaction and simulation conditions: 0.10 M H_2O_2, 0.40 M HCO_3

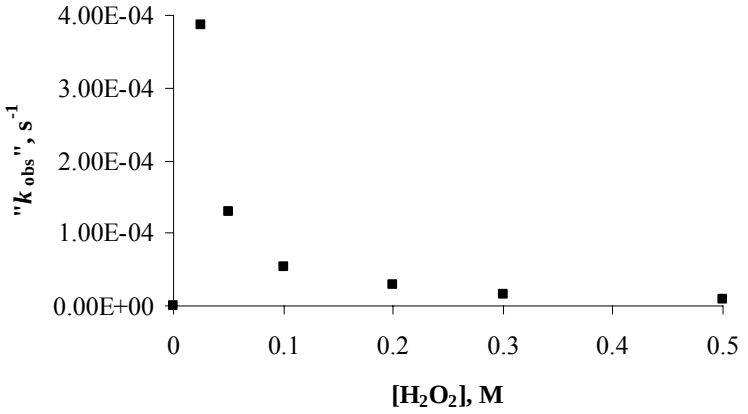

Figure 3-53. Simulated hydrogen peroxide dependence for the hydrogen peroxide decomposition reactions. Simulation conditions: 0.90 M HCO3, 0.5 μM Mn(II).

The hydrogen peroxide plot shown in Figure 3-53 is an interesting result from the simulation of this mechanism. Currently, the hydrogen peroxide dependence has never been adequately measured for the hydrogen peroxide decomposition. Another simulation was done to assure that this result occurs at different bicarbonate and manganese(II) concentrations. Figure 3-54 is a simulation using 0.4 M bicarbonate and 3.0 μM Mn(II). This result indicates that the dependence is not only simulated at low metal and high bicarbonate concentration.

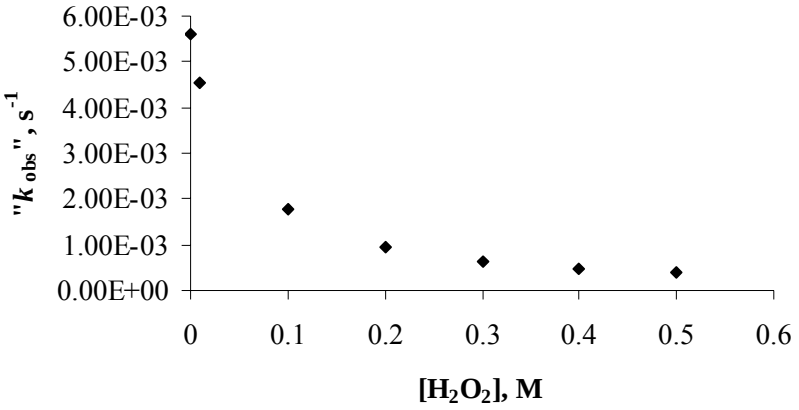

Figure 3-54. Simulated hydrogen peroxide dependence for the hydrogen peroxide decomposition reactions. Simulation conditions: 0.40 M HCO3, 3.0 μM Mn(II).

As stated earlier, ln plots for most of the hydrogen peroxide decomposition studies accelerated near the end of the reaction. The hydrogen peroxide dependence explains why this was true. As the decomposition occurred, the hydrogen peroxide concentration falls, and in doing so, the rate of the reaction will increase, as seen in Figure 3-55. For example, if a ln plot of one of the higher bicarbonate and hydrogen peroxide reactions is simulated, the acceleration can be easily seen.

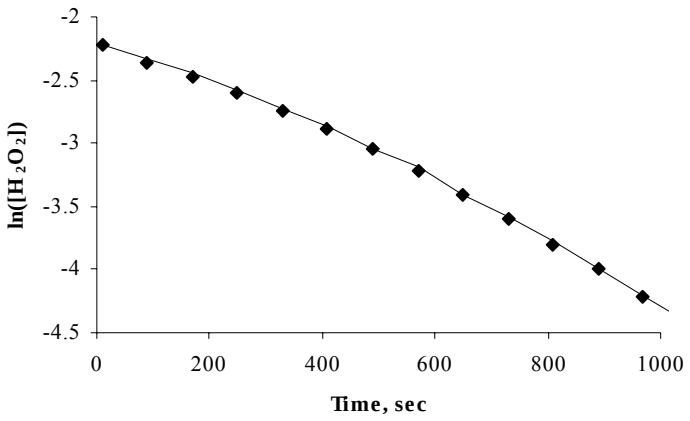

Figure 3-55. Plot of ln([H_2O_2]) versus time. The points represent observed data and the line is the simulation. Reaction and simulation conditions:0.10 M H_2O_2, 0.40 M HCO_3, 3.0 μM Mn(II). As the plot indicates the reaction accelerates as the decomposition occurs.

Conclusions

From the results presented, it can be concluded that the mechanism of hydrogen peroxide decomposition and nucleophilic alkene epoxidation must occur with similar intermediates. The kinetic experiments indicate that the dependence of manganese(II) on both reactions is first-order. This indicates that only one metal ion is present in the active catalyst. The bicarbonate dependence for both reactions is second-order. It would be reasonable to assume that one of the bicarbonate ions is in the form of peroxycarbonate, while the other is simply a bound bicarbonate or carbonate ion. The nucleophilic alkene epoxidation indicates that at higher hydrogen peroxide concentration, the reaction rate begins to fall. This could be explained by the hydrogen peroxide dependence that has been simulated, especially if the active oxidant of the alkene is the carbonate radical anion.

The lifetime of the active manganese catalyst has also been examined. From studies conducted where sequential additions of hydrogen peroxide are added to the same

solution, the observed rate of hydrogen peroxide decomposition decreases with each addition. This decrease in activity is due, in part, to the loss of bicarbonate from the solution. When a larger scale reaction was cycled 10 times, the final bicarbonate concentration was measured using the standard barium chloride method. It was found that the concentration of bicarbonate had fallen to about half of its original concentration. In addition, experiments using the malachite green assay for phosphate indicted that phosphate was present in the stock hydrogen peroxide. With each addition of hydrogen peroxide, phosphate was being added to the solution which causes the precipitation of the manganese catalyst. When a second study was conducted using distilled hydrogen peroxide and by adding small amounts of bicarbonate, to stabilize the bicarbonate concentration, the loss of activity was much less than when no bicarbonate was added and the hydrogen peroxide was not distilled. The loss in activity is attributed to the inability to adequately control the bicarbonate concentration and from normal dilution effects.

The source of manganese for the manganese dependent decomposition of hydrogen peroxide was also examined. A series of experiments were conducted using three manganese sources. First, manganese(II) sulfate was used. All of the kinetic experiments were conducted using this manganese source. Second, permanganate was used as the manganese for a series of experiments. Results from these experiments indicate that there is no significant change in the rate in using permanganate as the manganese source. Observed rate constants for the same concentration of manganese were nearly identical for reactions using manganese(II) sulfate and permanganate. The third manganese source was a Mn(IV) complex that has been reported to be an excellent

catalyst for the epoxidation of nucleophilic alkenes by hydrogen peroxide in the presence of bicarbonate. Experiments using this catalyst indicate that the catalyst is quickly destroyed upon addition to solutions of bicarbonate and hydrogen peroxide. The most likely decay mechanism is through the *N*-dealkylation of the triazacyclononane ligand. When equal concentrations of the Mn(IV) catalyst were used to decompose hydrogen peroxide, the observed rate constants were again within error for those found with manganese(II) sulfate.

The cis/trans isomerization in pure water has been studied. Reactions of maleic acid, a cis alkene, with hydrogen peroxide and manganese in the presence of bicarbonate yield the cis and trans epoxides. This result indicates that during the epoxidation reaction, the C-C sigma bond of the alkene is free to rotate to the more stable trans isomer before the epoxide ring is formed. Based on the proposed mechanism, the cis/trans isomerization is more than likely due to the generation of either a carbocation or carbon radical intermediate. If either intermediate has a long enough lifetime, rotation along the C-C sigma bond will allow for the generation of the trans epoxide.

A reexamination of the oxidation of DMNA has been investigated. Oxidation studies of DMNA and DENA by hydrogen peroxide and manganese in the presence of bicarbonate indicate that oxidative *N*-dealkylation is occurring, which was not accounted for in Sychev's proposed mechanism of hydrogen peroxide decomposition in the presence of bicarbonate and manganese. Sychev's mechanism, therefore, cannot be completely correct. The loss of O_2 (g) production by the addition of DMNA can be supported using a single electron transfer mechanism based on work exploring the

reactivity of cytochrome P-450, at least for the products that have currently been detected.

Solvent isotope effect studies have been conducted on the manganese catalyzed decomposition of hydrogen peroxide in the presence of bicarbonate. A normal isotope effect is observed for these reactions. This is not surprising since the cleavage of the O-H bond should be faster than that for O-D. The solvent isotope effect has also been examined for the nucleophilic alkene epoxidation. A large, inverse isotope effect is observed for these reactions. The explanation for the observed isotope effect has been rationalized using the carbonate radical anion as the oxidizing species.

A proposed mechanism for the decomposition of hydrogen peroxide and nucleophilic alkene epoxidation has been presented. The proposed catalytic species is the product of the reaction of bicarbonate, peroxycarbonate, and manganese. The proposed catalyst can react through a number of pathways to decompose peroxide, epoxidize nucleophilic alkenes, or *N*-dealkylate aromatic amines. Numerical simulation supports the carbonate radical as the active species involved in the hydrogen peroxide decomposition.

Future investigations of the hydrogen peroxide decomposition catalyzed by manganese(II) may prove difficult. The formed active metal species is in very low concentration and is formed *in situ*. If the Mn(IV)-TACN complex is any indication, other methods of trying to stabilize the metal center without the use of nitrogen containing ligands will be required due to the decomposition of the ligand.

Experimental

Materials and Instrumentation

Sodium bicarbonate, sodium acetate, styrene, *N*,*N*-dimethyl-4-nitrosoaniline, *N*,*N*-diethyl-4-nitrosoaniline, and manganese(II) sulfate were all analytical grades and obtained from Fisher (Atlanta, GA). Hydrogen peroxide (35 and 50%) was obtained from Fisher (Atlanta, GA) and standardized often by iodometric titration. Water was purified using a Barnstead E-Pure 3-Module Deionization System. Extraneous metal ions from salt solutions were removed by passing through a Chelex 100 resin obtained from Aldrich (St. Louis, MO). Sodium bicarbonate solutions were standardized using the method below before use to assure concentration.

Proton and ^{13}C NMR spectra were obtained on a Mercury 300 spectrophotometer. The residual solvent peaks were used as an internal standard except deuterated chloroform which used 0.05% TMS as internal standard. All deuterated solvents were obtained from Cambridge Isotope Laboratory, Inc (Andover, MA).

UV-Vis kinetic experiments were obtained using a Hewlett-Packer 8453 spectrophotometer using 1.0 cm quartz cells from Starna Cells, Inc. Temperature was maintained at 25 ± 0.1 ºC using a Fisher Isotemp 1600S water bath circulator.

Gas Chromatography experiments were performed using a Varian CP-3800 Gas Chromatograph equipped with a J. W. Scientific DB-35MS column. The method for DMNA oxidation analysis consisted of a linear gradient of 10ºC/min from 80ºC to 200ºC. The temperature was then maintained at 200ºC for 15 minutes providing for a total analysis time of 27 minutes. The method for acetaldehyde analysis consisted of an isothermal method of 40ºC for 5 minutes.

Styrene oxidation reactions were analyzed by High Performance Liquid Chromatography using a Rainin HPLX solvent delivery system on a C-18 reverse phase column. The method consisted of a non-linear gradient of H_2O:CH_3CN from 75:25 – 5:95 over a 15 minute period. Product was detected at 221nm.

Sulfonated styrene oxidations were analyzed by High Performance Liquid Chromatography using a Varian Prostar system. Analysis was performed using a C18 reverse phase column using tetrabutylammonium chloride as an ion-pairing reagent. The method was isocratic elution using 80% A: 80:20 CH_3CN:H_2O B: 0.1 mM in 80:20 CH_3CN:H_2O

Standardization of sodium bicarbonate solutions

Solutions of sodium bicarbonate were standardized before each kinetic experiment to assure the concentration eluting from the Chelex 100 column. All solutions were delivered using volumetric pipets. A 10mL aliquot of sodium bicarbonate solution exiting the Chelex 100 column was a placed in a clean, dry beaker. An excess amount of sodium hydroxide solution of a known concentration, by titration with potassium hydrogen phthalate, was added to the beaker. The solution was stirred to allow for complete deprotonation of the bicarbonate to form the carbonate dianion. An excess barium chloride solution is then added to precipitate all of the carbonate dianion as barium carbonate. Phenolphthalein is then added to the mixture to give a pink color due to the residual hydroxide ion. The mixture is titrated using a known concentration of hydrochloric acid until the solution just turns clear. The number of moles of hydrochloric acid added is equal to the excess moles of sodium hydroxide. The difference between the number of moles from the acid titration and the number of moles of hydroxide ion

initially added equals the number of moles of bicarbonate present in the initial 10mL aliquot (Equation 3-10).

$$\#\text{moles } OH_{init} - \#\text{moles } OH_{excess} = \#\text{moles bicarbonate} \quad (3\text{-}10)$$

The molarity of the solution can then be determined.

Hydrogen peroxide decomposition studies

The H_2O_2 decomposition studies were carried out in sodium acetate buffered solutions at a pH 8.4. All salt solutions had been passed through a Chelex 100 column to remove any extraneous metal ions. Hydrogen peroxide/bicarbonate/buffer solutions were allowed to equilibrate for at least 15 minutes to allow for formation of peroxycarbonate. Kinetic experiments were followed for at least 2.5 half-lives following the decreasing absorbance at 263 nm. Solutions of manganese(II) sulfate were always added last to initiate the decomposition of the hydrogen peroxide. Hydrogen peroxide was held at 0.1 M. The sodium bicarbonate concentration was in the range from 0.0 to 0.55 M. Manganese concentrations were in the range of 0-15 μM. Ionic strength was held constant at 1 M using sodium acetate, the buffering solution.

Synthesis of $[Mn^{IV}(Me_3TACN)(OMe)_3](PF_6)$

The synthesis is described in the literature by Kerschner.[63] To a solution of 1,4,7-trimethy-1,4,7-triazacyclononane (0.1 g, .578 mmol) in 8 mL of methanol is added $MnCl_2$ (0.074 g, .578 mmol) predissolved in 2 mL methanol. The solution will turn dark brown in color. The solution is stirred and cooled on ice to 0 ˚C, and Na_2O_2 (0.046 g, 0.578 mmol) was slowly added to the manganese/TACN solution. After 1 h of stirring at 0 ˚C, the solution was warmed to room temperature and stirred a further 1-2 h. Finally, $NaPF_6$ (0.100 g, 5.90 mmol) was added to the solution. The mixture was filtered through a porous glass frit and the solution was neutralized with dilute sulfuric acid. Then 5 mL

of water was added to the neutralized solution, and it was filtered again. The filtrate was concentrated to one-third the original volume under reduced pressure, and the resulting solution was chilled at 0 ˚C to precipitate the desired product. UV-Vis (CH_3CN): λ_{max} nm (ε, $M^{-1}cm^{-1}$) 326 (13200), 287 (12900), 228 (11500). Mp:160-164 ˚C.

Oxidation of *N*,*N*-dimethyl-4-nitrosoaniline (DMNA) by Oxone

To a stirred solution of DMNA (1.0 g, 6.7 mmol) in 30 mL 50:50 CH_3CN: H_2O (v:v) is slowly added a solution of Oxone (4.0 g, 6.5 mmol) in 20 mL H_2O over 30 minutes. During the course of the addition the starting green color is replaced by a yellow color and a yellow precipitate begins to float on top of the solution. Addition of a further 20 mL CH_3CN after the reaction is over allows for the yellow precipitate to dissolve. The entire mixture is placed in a separatory funnel and extracted 3 x 100 mL with $CHCl_3$. The yellow color was transferred to the organic layer. The combined organic washings were dried over anhydrous magnesium sulfate. After filtering, the organic solvent was removed under reduced pressure to afford pure *N*,*N*-dimethyl-4-nitroaniline. ^{1}H NMR (CD_3CN): δ 8.06 (d, J = 9.3Hz, 2H), 6.69 (d, J = 9.6Hz, 2H), 3.07 (s, 3H).

Oxidation of *N*,*N*-Dimethyl-4-nitrosoaniline (DMNA) by $H_2O_2/HCO_3^-/Mn^{2+}$

A typical reaction involves stirring a solution of DMNA (0.5 g, 3.3 mmol) with manganese(II) sulfate in a solution of 30:70 CH_3CN: H_2O (v:v). To this is added an equilibrated solution of H_2O_2 and sodium bicarbonate slowly over about 30 minutes. Multiple experiments were performed with H_2O_2 equal to 1x, 10x, and 50x molar excess over DMNA. Enough sodium bicarbonate and manganese(II) sulfate were added to make their final concentrations equal to 0.40 M and 4.0 μM, respectively. The results of these experiments were discussed earlier.

Oxidation of *N*,*N*-diethyl-4-nitrosoaniline (DENA) by $H_2O_2/HCO_3^-/Mn^{2+}$

To a solution of DENA (1.00 g, 5.61 mmol) in 70:30 H_2O:CH_3CN (v:v) is added a solution of manganese(II) sulfate. To this is slowly added, over 30 minutes, an equilibrated solution of H_2O_2 and bicarbonate, where the H_2O_2 concentration is 50x molar excess to DENA. The final bicarbonate and manganese(II) concentrations were 0.40 M and 4.0 μM, respectively. The acetaldehyde produced during the reaction was trapped by condensation of the gas in an ice cooled trap.

CHAPTER 4
ELECTROPHILIC ALKENE EPOXIDATION BY THE PEROXYCARBONATE DIANION

Introduction

The transfer of an oxygen atom is one of the most important biological transformations and is quite useful in synthetic organic chemistry.[113] Generally, oxidation reactions are catalyzed by metals,[114] as seen in Chapters 2 and 3 with the manganese(II) catalyzed epoxidation of nucleophilic alkenes, or main group catalysts.[115] Due to the important nature of this oxidative process many catalytically-active transition metals have been extensively studied, including high-valent d^0 metals, such as Mo(VI), Re(VII), Rh(VII), V(V) and Ti (IV), which catalyze the epoxidation of alkenes[116-118] by peroxides. For example, hydrogen peroxide reacts with methyltrioxorhenium[119,120] generating mono and bis-peroxides.[121,122] Both species are efficient oxygen donors, transferring oxygen to various nucleophiles[123] allowing significant rate enhancements compared to reactions involving hydrogen peroxide alone. Another example includes the oxygen transfer from the oxo-ligands of oxometalloporphyrin systems, such as $Mo^{VI}(TPP)(O)_2$ and $Fe^{IV}(TPP)(O)$, which are reported in the literature.[124,125] Some limitations of metal activators include: the toxic nature of the metals, separation of products from reaction mixtures, and the low solubility of metal catalysts.

Organic peracids, such as peracetic acid, have been widely used to oxidize alkenes. One of the most common oxidation reactions involving peracids is the Prileschajew epoxidation.[126] The peracid epoxidation of alkenes is influenced by several factors

including: the nature of the carbon-carbon double bond, peracid substituents, and solvent effects (such as intermolecular H-bonds).[127]

In 2000, it was reported that peroxycarbonate was an active oxidant of both nucleophilic and electrophilic alkenes.[33] Chapters 2 and 3 have focused on the use of manganese(II), which was discovered as a trace contaminant in the bicarbonate salts, as an activator of peroxycarbonate for use in the oxidation of nucleophilic alkenes and the disproportionation of hydrogen peroxide. These data do not explain how the manganese(II) system also has the ability to oxidize electrophilic alkenes. The lack of information currently available on the use of peroxycarbonate as an oxidant of electrophilic alkenes requires further investigation.

Results and Discussion

The oxidation of electrophilic alkenes to their corresponding epoxides was first reported by Weitz and Scheffer[128] in 1921 and can be easily achieved using a number of different nucleophilic oxidants including hypochlorite, $^{-}$OCl, and hydroperoxide, $^{-}$OOH. Numerous examples of nucleophilic oxidation of electrophilic alkenes can be found in the literature,[129-139] but only a couple of these focus on the kinetics of the epoxidation.[131,132]

Figure 4-1 shows the resonance structure of a common electrophilic alkene, an α-β unsaturated ketone, which provides a rationalization as to why electrophilic alkenes react with nucleophilic oxidants. As can be seen in the figure, the β-carbon of the resonance structure has a positive charge and will be the carbon attacked by a nucleophilic oxidant. Figure 4-2, illustrating a reaction of the hydroperoxide anion, shows the general mechanism by which nucleophilic oxidants can oxidize electrophilic substrates.

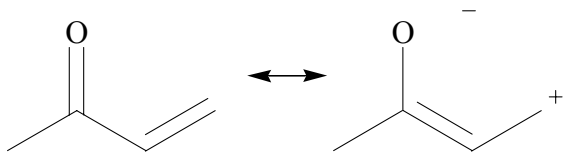

Figure 4-1. The resonance structure of an electrophilic alkene, an α,β-unsaturated ketone, explains the reactivity with nucleophilic oxidants. The β-carbon of the alkene, as seen in the resonance structure, is more electropositive and will be the site of attack by a nucleophilic oxidant.

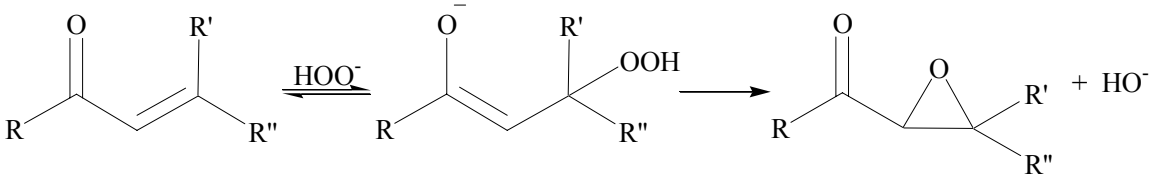

Figure 4-2. The mechanism of electrophilic alkene oxidation by the hydroperoxide anion is illustrated. The nucleophilic oxidant adds at the electrophilic carbon, the β-carbon. Reformation of the ketone moiety causes either the displacement of the hydroperoxide anion, regenerating the starting alkene and hydroperoxide, or ring closure to form the epoxide and the hydroxide anion.

Peroxycarbonate can exist as both the anion, HCO_4^-, and dianion, CO_4^{2-}, in aqueous solution. While the peroxycarbonate anion is an electrophilic oxidant as shown by sulfide oxidation,[41] the peroxycarbonate dianion will behave as a nucleophilic oxidant in a similar way as the hydroperoxide anion. Figure 4-3 illustrates how the peroxycarbonate dianion will react in a similar way in the oxidation of electrophilic alkenes. The only difference between the hydroperoxide dianion and the peroxycarbonate dianion is that the nucleofuge (leaving group) of the peroxycarbonate dianion is the carbonate dianion.

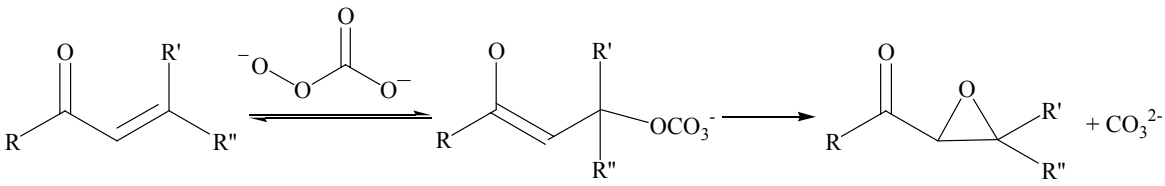

Figure 4-3. The mechanism of electrophilic alkene epoxidation by the peroxycarbonate dianion is illustrated. The mechanism is identical to that of hydroperoxide oxidation, except that the nucleofuge of the peroxycarbonate dianion is the carbonate dianion.

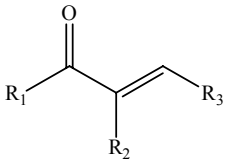

1 R_1=CH_3, R_2=H, R_3=H
2 R_1=OH, R_2=CH_3, R_3=H
3 R_1=OCH_2CH_3, R_2=H, R_3=H
4 R_1=C_6H_5, R_2=H, R_3=$C(O)C_6H_5$

Figure 4-4. Electrophilic alkenes used in this study.

Effect of Mn(II) on Electrophilic Alkene Epoxidation

While epoxidation of nucleophilic alkenes by peroxycarbonate are accelerated by the addition of manganese, the same is not true for electrophilic alkenes. For example, the NMR scale epoxidation of **1** (0.10 M) in D_2O were allowed to react with 1.00 M $NaHCO_3$ and 0.15 M H_2O_2 and has a $t_{½}$ of 60 min (pH 7.8), Figure 4-5.

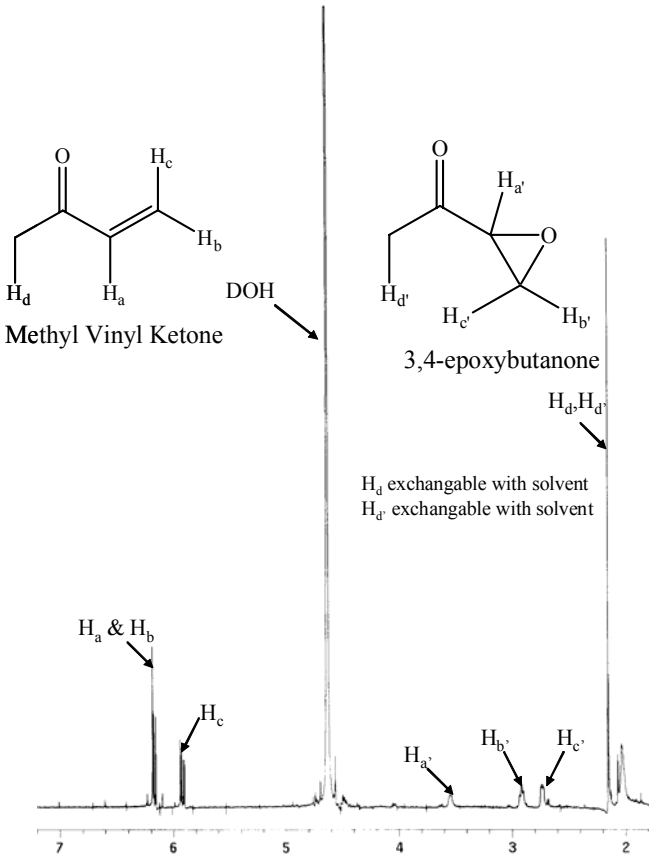

Figure 4-5. ^{1}H-NMR of **1** epoxidized by H_2O_2 at pH 7.8 at 60 min, in the presence of 1.00 M sodium bicarbonate (50% conversion).

When the same epoxidation reaction is performed in the presence of 4 μM Mn(II), only a 44% conversion to the epoxide is obtained in 60 min, as seen in Figure 4-6. The decrease in the rate of epoxidation is attributed to the metal assisted disproportionation of H_2O_2, which has a lower concentration as a result.

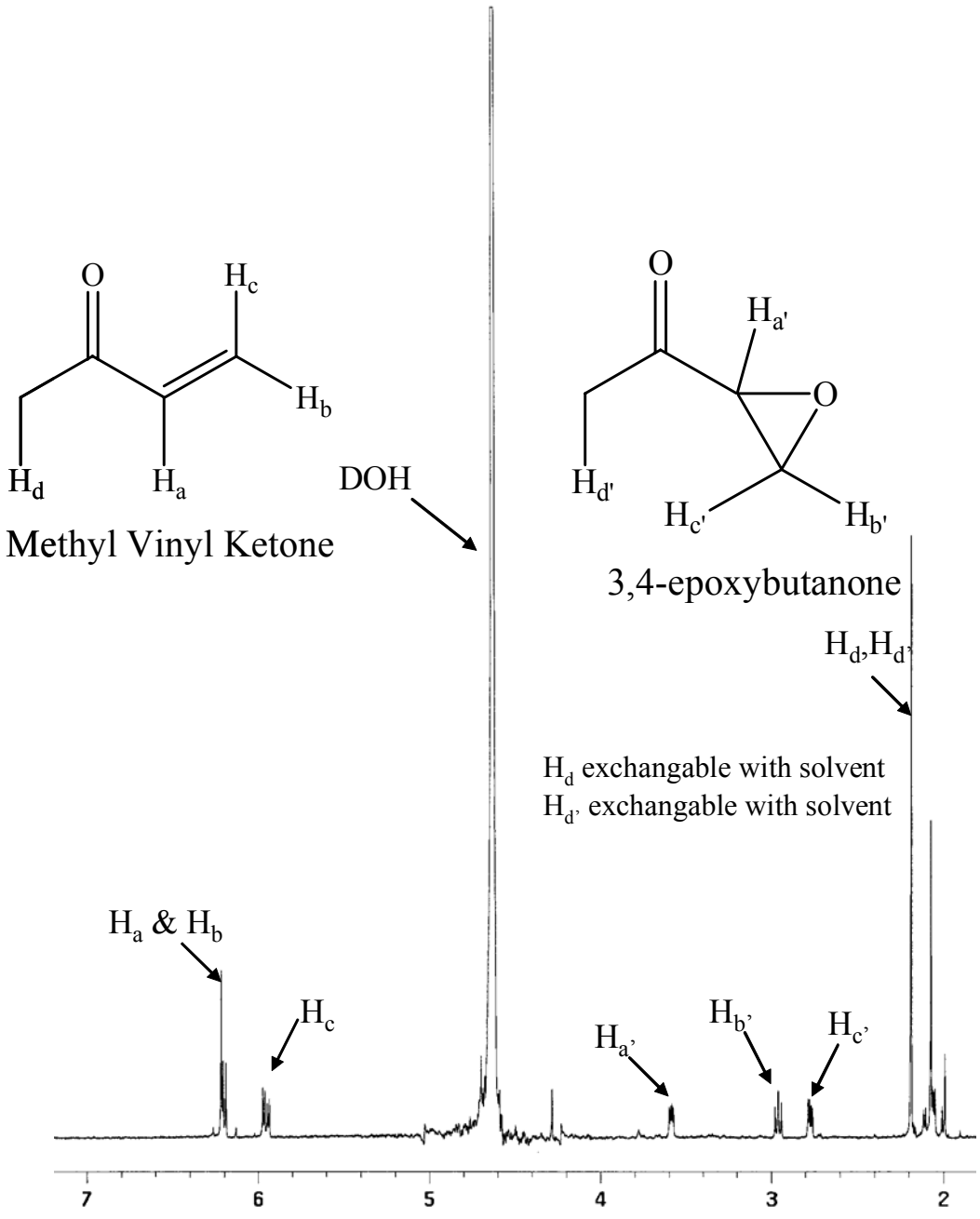

Figure 4-6. ^{1}H-NMR of **1** epoxidized by H_2O_2 at pH 7.8 with 4 μM Mn(II) in the presence of 1.00 M sodium bicarbonate at 60 min (44% conversion).

To further support the evidence that trace metal does not affect the reaction of electrophilic alkenes, **1** (0.10 M) in D_2O was allowed to react with 1.00 M $NaHCO_3$ and 0.15 M H_2O_2 with the addition of 5 mM diethylenetriaminepentaacetic acid (DTPA), a metal chelator. The reaction retains the same $t_{½}$ of 60 min as seen in the reaction without DTPA, Figure 4-7.

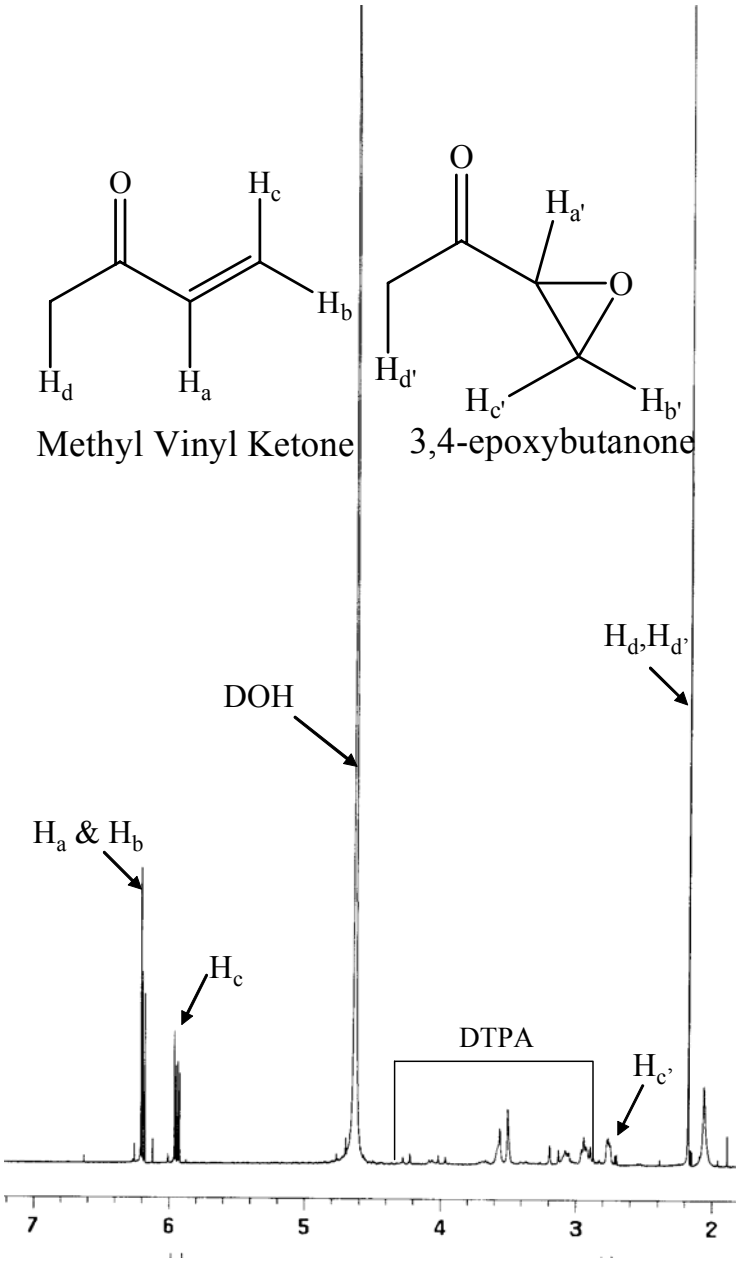

Figure 4-7. ^{1}H-NMR of **1** epoxidized by H_2O_2 at pH 7.8 with 5 mM DTPA in the presence of 1.00 M sodium bicarbonate at 60 min (50% conversion).

In contrast, when **1** (0.10 M) in D_2O is allowed to react with 1.00 M $NaHCO_3$, 0.15 M H_2O_2, and 10 μL saturated NaOH in D_2O (final pH 8.6) the $t_{½}$ is reduced to 15 min, Figure 4-8.

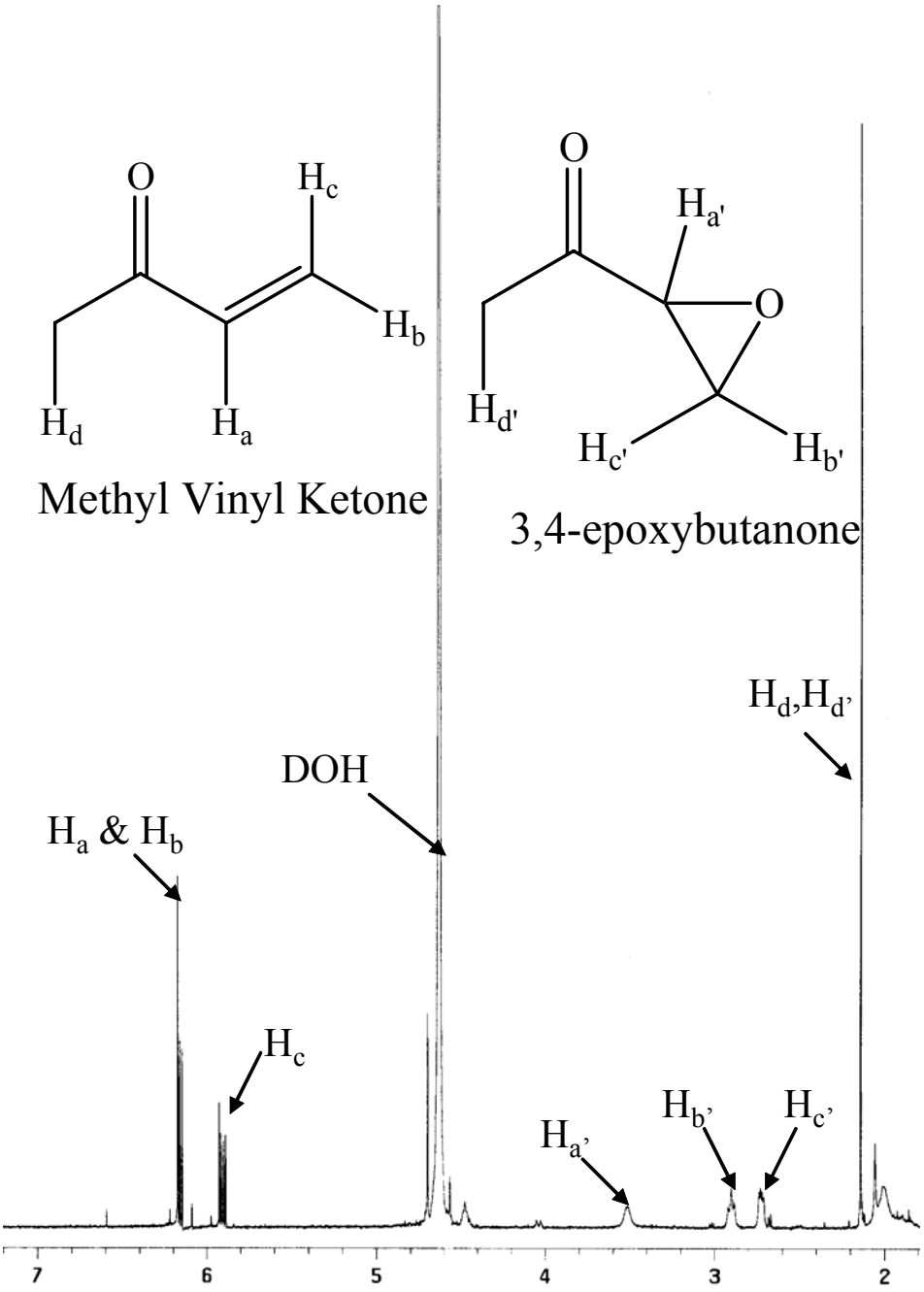

Figure 4-8. ^{1}H-NMR of **1** epoxidized by H_2O_2 in the presence of 1.00 M sodium bicarbonate at pH 8.6 after 15 min (50% conversion).

These results illustrate that the addition of manganese(II) only affects electrophilic alkene epoxidation by disproportionating the terminal oxidant, hydrogen peroxide, and thus, reducing the conversion of epoxide. Increasing the pH of the solution, however, affects the conversion of electrophilic alkenes to epoxide by increasing the equilibrium concentration of the nucleophilic oxidant, hydroperoxide.

Effect of pH on the Oxidation of Electrophilic Alkenes

To assure that the results are not substrate specific, **2** was chosen for study. When **2** (0.05 M) is allowed to react with 1.00 M $NaHCO_3$ and 0.30 M H_2O_2 (pH 7.8) for 24 hrs, there is a 75% conversion to the corresponding epoxide, Figure 4-9.

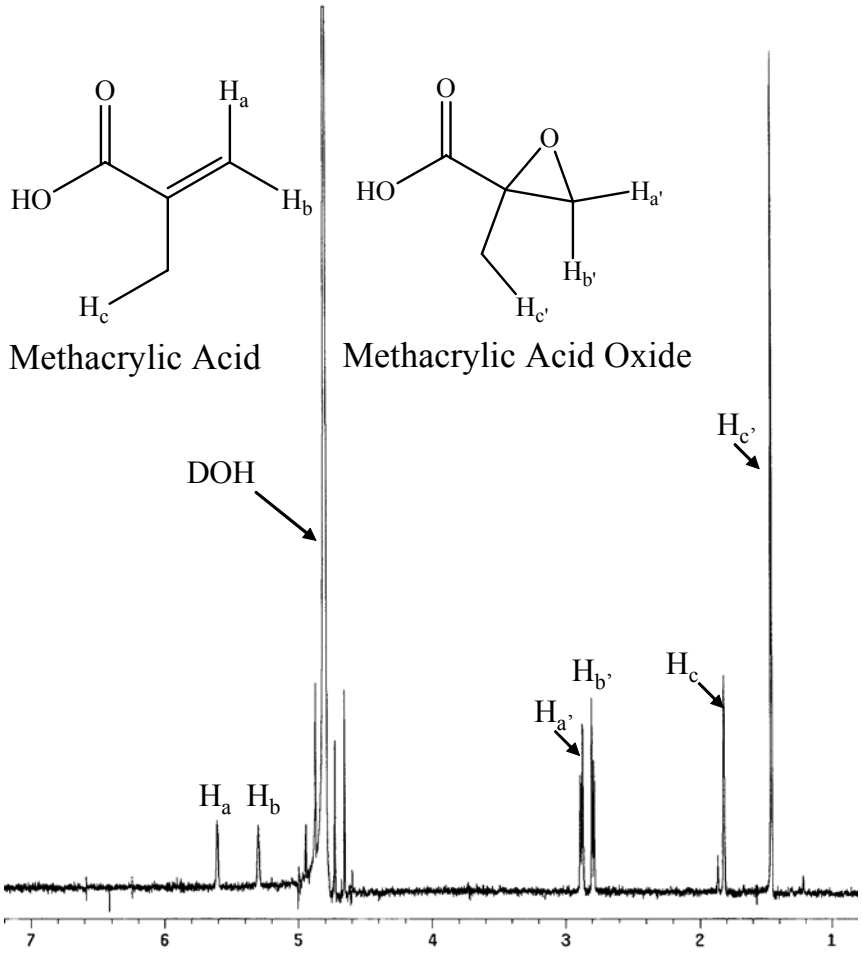

Figure 4-9. ^{1}H-NMR of **2** epoxidized by H_2O_2 in the presence of 1.00 M sodium bicarbonate at pH 7.8 in 24 hrs (75% conversion).

When the same reaction is repeated with the addition of 10 μL saturated NaOH in D_2O (final pH 8.6), only a 50% conversion is obtained after 24 hrs, Figure 4-10.

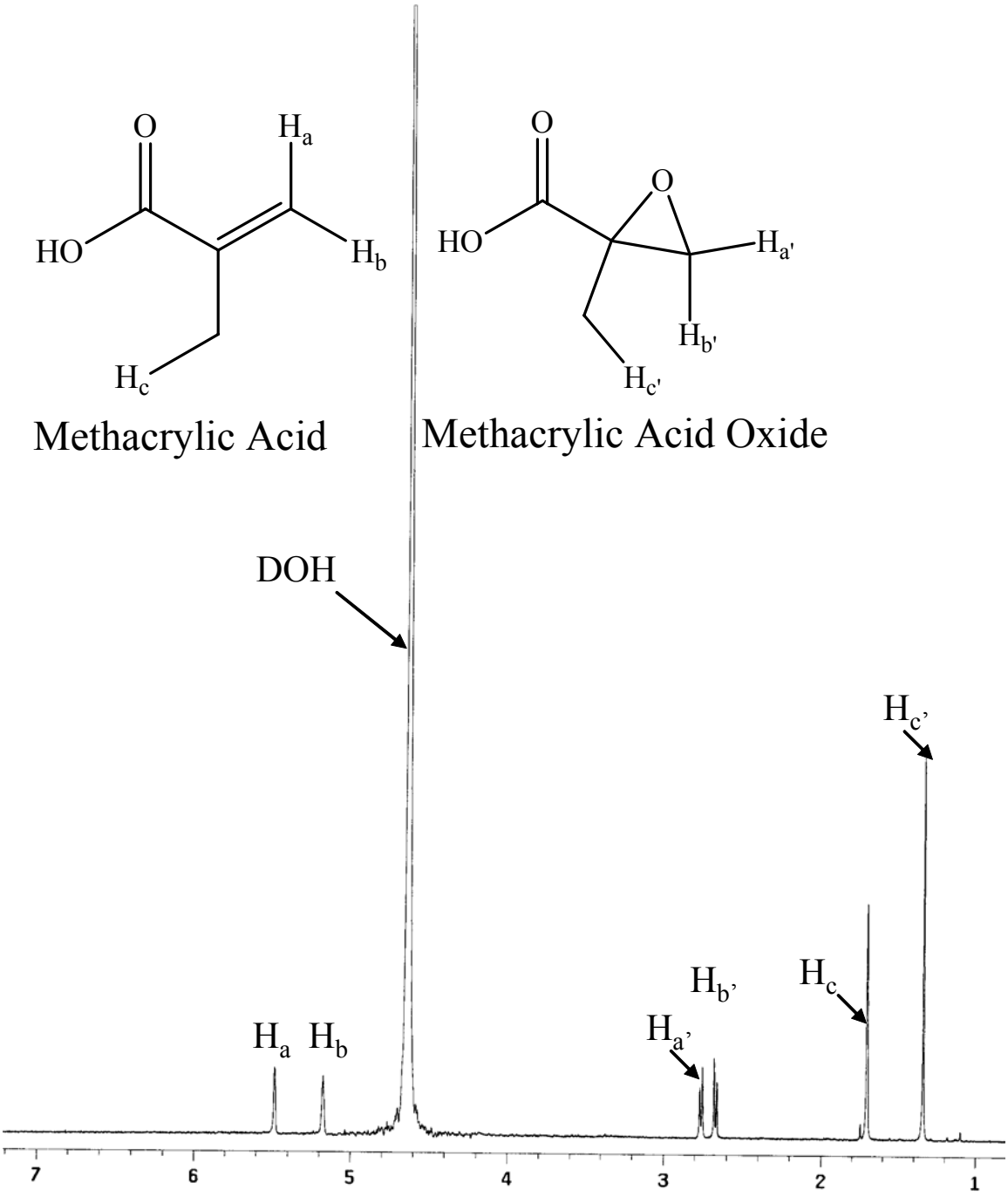

Figure 4-10. ^{1}H-NMR of **2** epoxidized by H_2O_2 in the presence of 1.00 M sodium bicarbonate at pH 8.6 at 24 hrs (50% conversion).

The decrease in reactivity of what is apparently an electrophilic alkene can be rationalized by the predominant resonance form at the operational pH, Figure 4-11. At pH 8.6, methacrylic acid will mainly be deprotonated and will not react with the hydroperoxide anion. Methacrylic acid at pH 7.80 should react more like a nucleophilic alkene, so the addition of Mn(II) should greatly enhance the reactivity, based on the evidence presented in Chapter 3. When **2** (0.05 M) is was allowed to react with 1.00 M $NaHCO_3$,0.30M H_2O_2, and 4 μM Mn(II) (pH 7.8), >90% conversion to the epoxide is observed in 15 minutes, Figure 4-12.

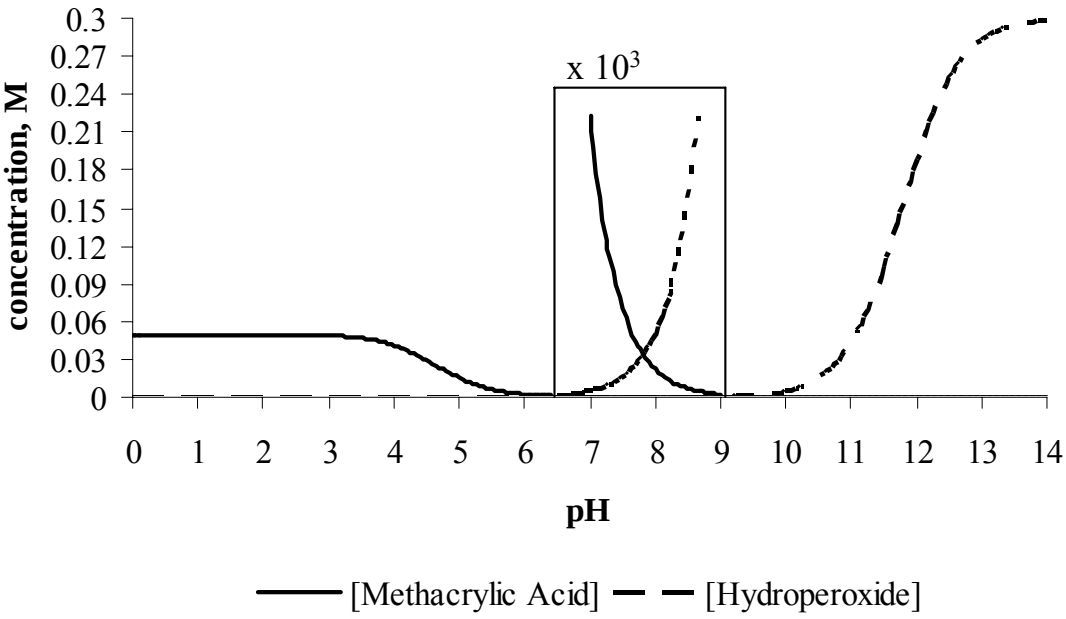

Figure 4-11. Speciation of methacrylic acid (MAA) at 0.05 M and hydrogen peroxide (0.30 M) as a function of pH. The maximum concentration of MAA and hydroperoxide happens to occur at pH 7.8, the buffering pH of sodium bicarbonate.

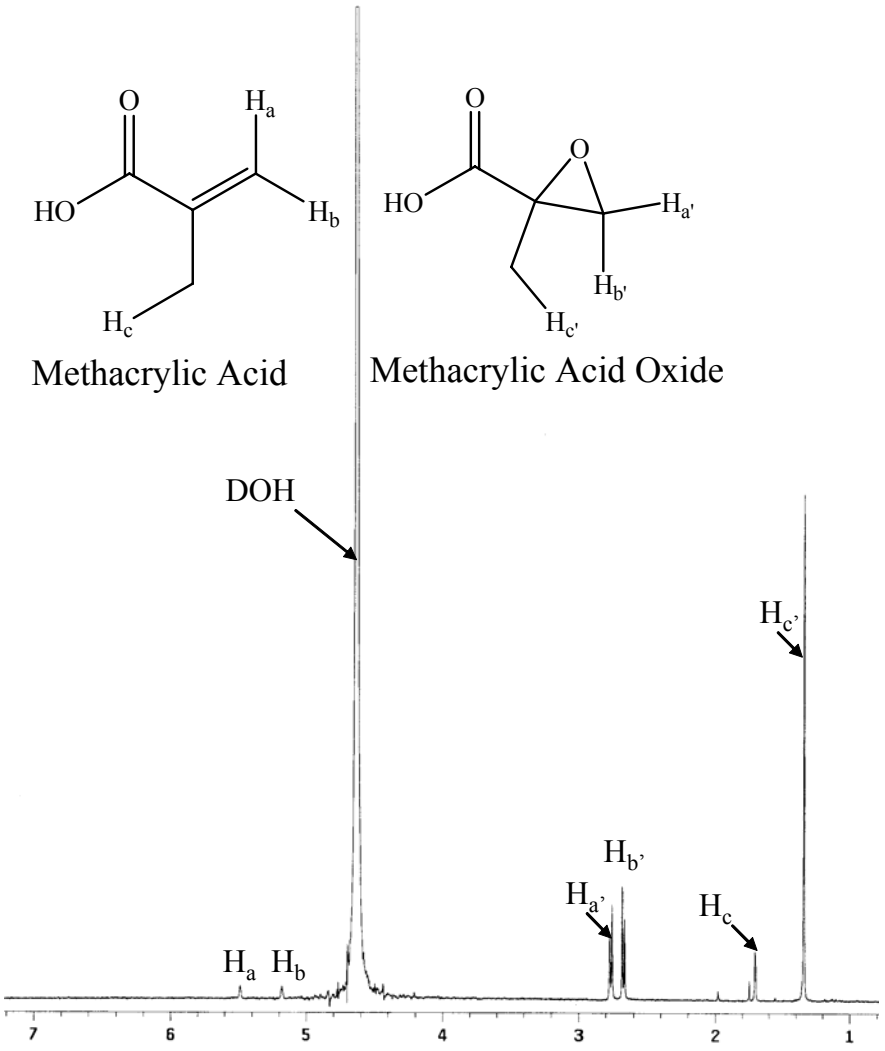

Figure 4-12. ^{1}H-NMR of **2** epoxidized by H_2O_2 in the presence of 1.00 M sodium bicarbonate at pH 7.8 with 4 μM Mn(II) in 15 min (>90% conversion).

Experiments were then conducted using **3**, since the ester moiety provides a similar chemical environment for the double bond as **2**, but without allowing for the disruption of the alkene delocalization caused by acid dissociation at the operational pH. When **3** (0.05 M) is allowed to react with 1.00 M $NaHCO_3$ and 0.30 M H_2O_2 (pH 7.8) for 24 hrs, a 44% conversion to the corresponding epoxide is observed by ^{1}H NMR, Figure 4-13.

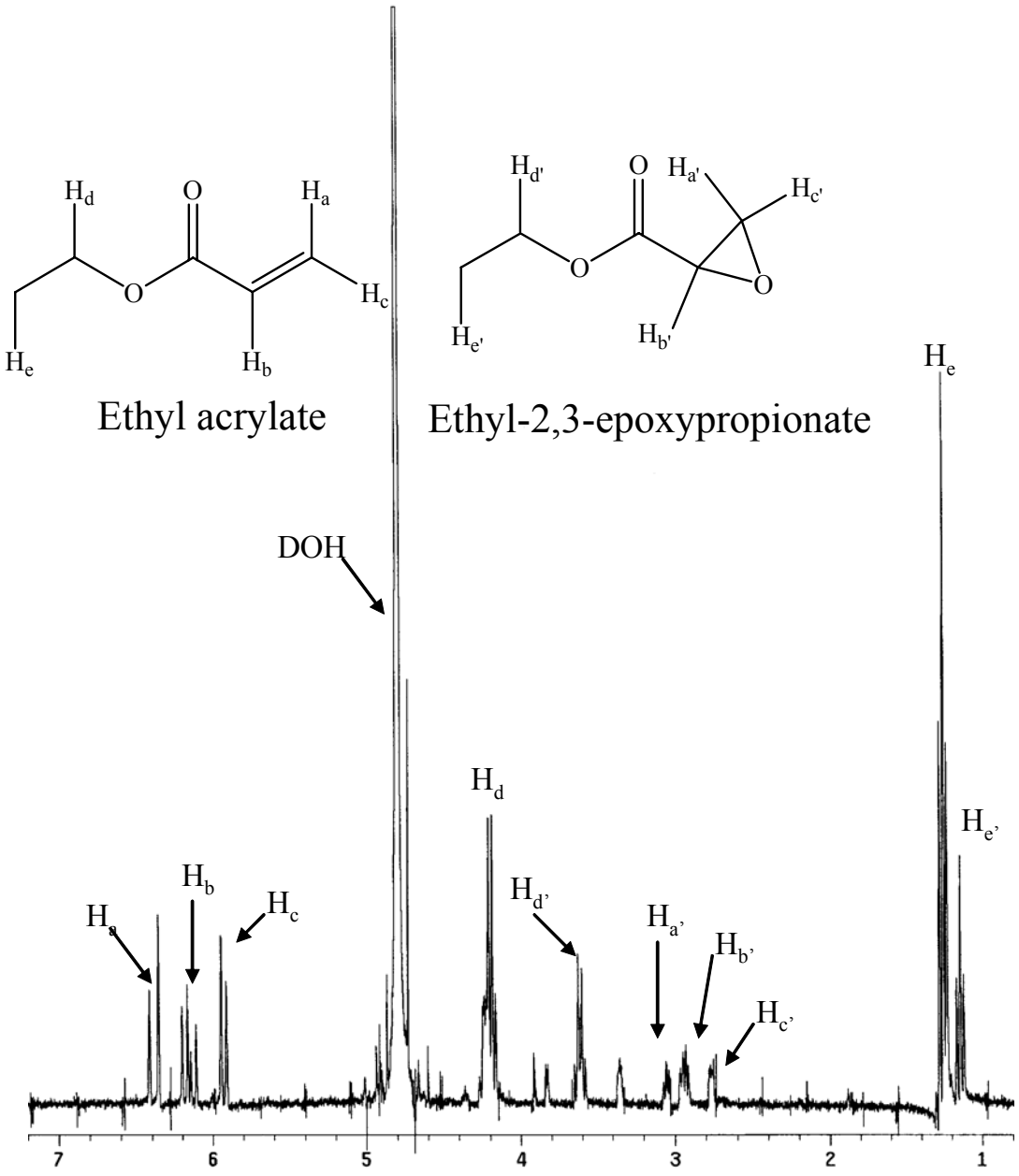

Figure 4-13. ^{1}H-NMR of **3** epoxidized by H_2O_2 in 1.00 M sodium bicarbonate at pH 7.8 in 24 hrs (44% conversion).

As predicted by the oxidation of **1**, when the same reaction is repeated using 10 μL of saturated NaOH in D_2O (final pH 8.6) for 24 hrs, a 66% conversion to the epoxide is observed, Figure 4-14. This experiment proves that if there is no change in the resonance structure of the electrophilic alkene, it will react with the nucleophilic oxidant as predicted.

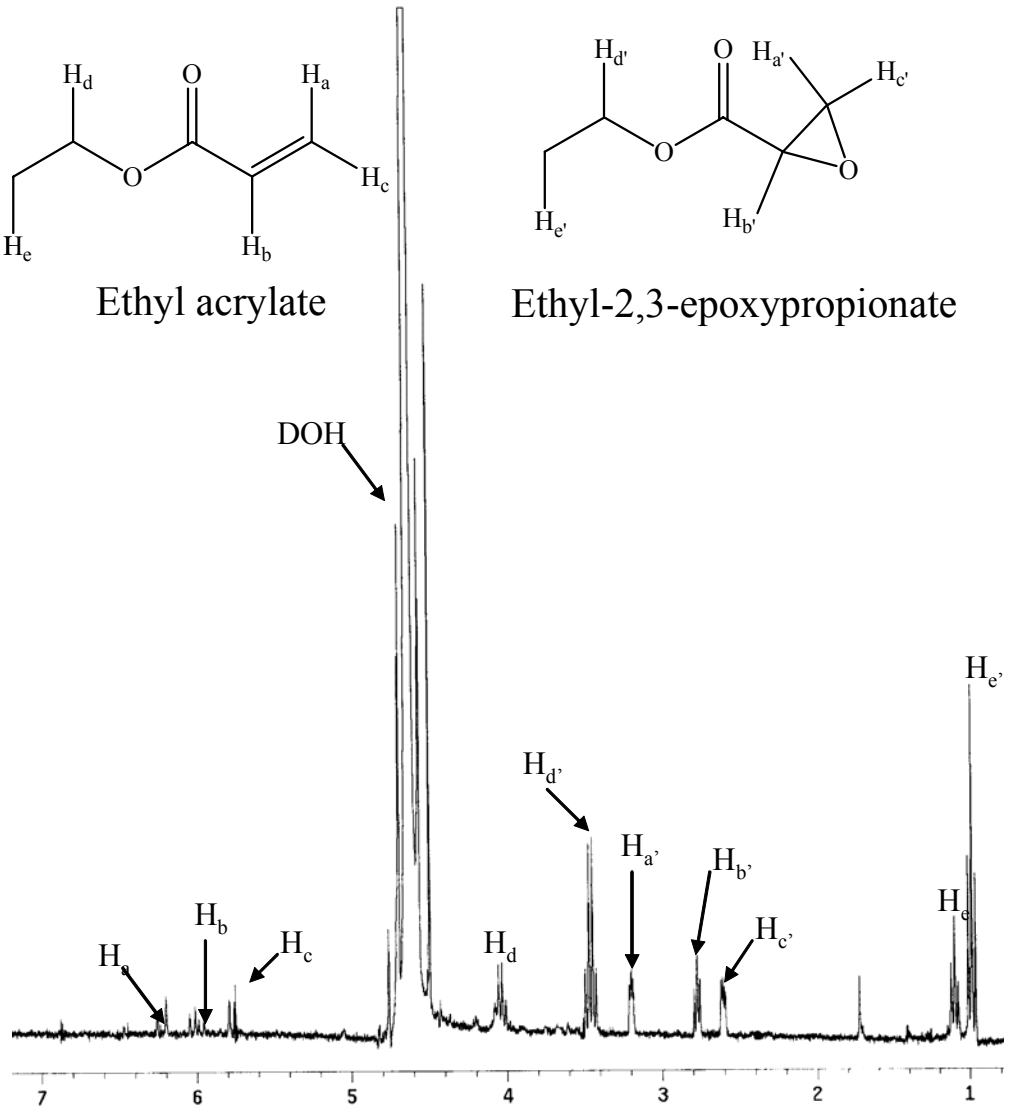

Figure 4-14. ^{1}H-NMR of **3** epoxidized by H_2O_2 in 1.00 M sodium bicarbonate at pH 8.6 in 24 hrs (66% conversion).

Effect of Buffer Choice on Electrophilic Alkene Epoxidation

In order to determine the role that the peroxycarbonate dianion has on the rate of electrophilic alkene oxidation, a study was conducted using $NaHCO_3$ and Na_2HPO_4 as buffering salts. When solutions of 0.10 M **1**, 1.00 M buffer, and 0.15 M H_2O_2 were allowed to react at varying pH, Table 4-1, it was observed that identical conversions to

the corresponding epoxide were found in the same amount of time and was not dependent upon buffer choice, but only on pH.

Table 4-1. The percent conversion of **1** in varying buffer at differing pH.

Buffer	pH 7.80, 150 min	pH 8.60, 90 min	pH 8.90, 60 min
$NaHCO_3$	74%	92%	>99%
Na_2HPO_4	74%	92%	>99%

Reaction conditions: 0.10 M **1**, 1.00 M Buffer and 0.15 M H_2O_2

This observation leads us to the conclusion that the peroxycarbonate dianion is at least as reactive as hydroperoxide in the epoxidation of electrophilic alkenes. This result is not surprising, since similar results have been seen in the use of the peroxycarbonate dianion in the cleavage of organophosphate esters.[140] Similar reactions of **2** and **3** in phosphate and bicarbonate buffer gave identical conversions to epoxide. The explanation for why similar yields of epoxide are obtained in the different buffers will be discussed shortly.

Electrophilic Alkene Oxidation Kinetics

Oxidations of **4** were conducted in aqueous, micellar solution under second-order conditions using hydrogen peroxide and sodium hypochlorite as terminal oxidants. The oxidation was followed by monitoring the loss in peak intensity at 320 nm spectrophotometrically. For the reactions with hydrogen peroxide, 4.00×10^{-4} M substrate and 8.00×10^{-4} M oxidant were used. Reactions were performed in aqueous solution consisting of 0.10 M phosphate buffer and 0.10 M cetyltrimethylammonium chloride (CTACl) as surfactant. The reactions were conducted over a pH range of 7.5 – 12. The data is presented as the $\log(k_{obs})$ vs. pH in Figure 4-15 to demonstrate that the k_{obs} at lower pH values are not zero. From this data, Equation 4-3 was derived using the steady-state approximation for HOO^-.

$$H_2O_2 \rightleftharpoons H^+ + HOO^- \qquad K_a \qquad (4\text{-}1)$$

$$S + HOO^- \longrightarrow SO + OH^- \qquad k_2 \qquad (4\text{-}2)$$

$$\frac{-\partial[S]}{\partial t} = \frac{k_2[H_2O_2]_0[S]}{(1+(\frac{[H^+]}{K_a}))} \qquad (4\text{-}3)$$

The rate law indicates that there are two parameters that can be fit to the data, the rate constant and the pK_a of the oxidant. Non-linear regression was used to provide values for the rate constant and pK_a of the hydrogen peroxide oxidation of **4**, presented as the solid line in Figure 4-15. From the fit, the value of $k_2 = 660 \pm 40$ $M^{-1}s^{-1}$ and the pK_a of hydrogen peroxide is 11.70.

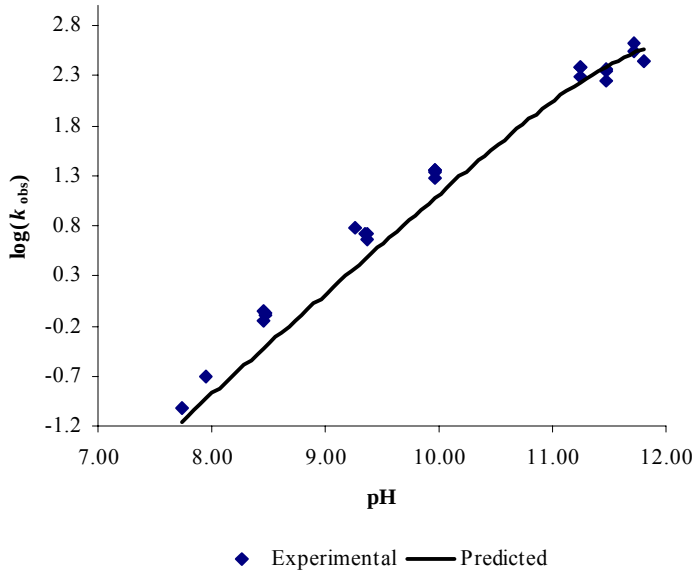

Figure 4-15. Plot of $\log(k_{obs})$ vs pH for the oxidation of **4** by H_2O_2.

Since hypochlorite is also a nucleophilic oxidant, similar results should be found for reactions with **4**. Reaction conditions were identical to that with hydrogen peroxide, except the hypochlorite concentration was 2.40×10^{-3} M and the pH range was from 5 – 10. A plot of the $\log(k_{obs})$ vs pH is shown in Figure 4-16. Non-linear regression analysis

using the derived rate law is shown in Figure 4-16 as the line. From the fit, the value of $k_2 = 118 \pm 2\ M^{-1}s^{-1}$ and the pK_a of hypochlorous acid is 8.26.

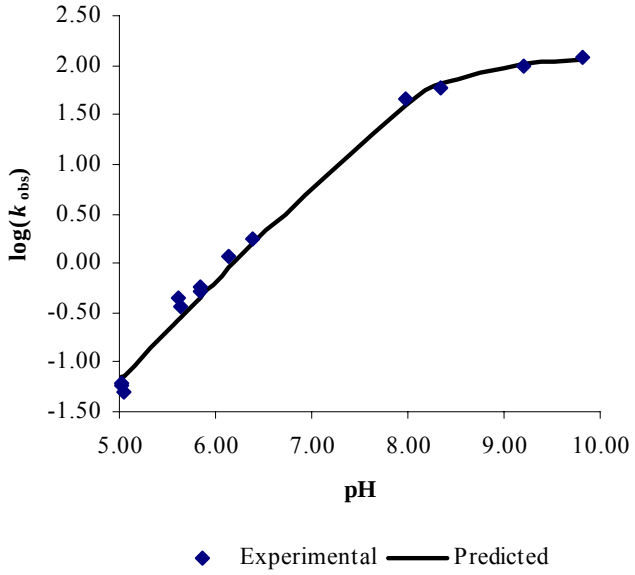

Figure 4-16. Plot of log(k_{obs}) vs pH for the oxidation of **4** by $^{-}$OCl.

Discussion of the Second-Order Rate Constants

As stated in the introduction, only two references in the literature have presented detailed kinetic data on the topic of electrophilic epoxidation by nucleophilic oxidants.[131,132] From the work of Rosenblatt and Broome,[131] the mechanism of the epoxidation has been attributed to the slow addition of the nucleophilic oxidant to the electrophilic alkene followed by a rapid internal cyclization to form the epoxide, as seen in Figure 4-17.

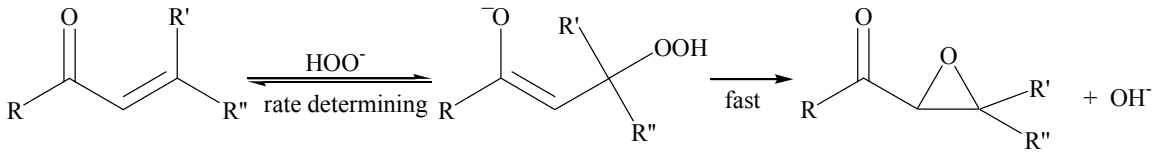

Figure 4-17. Reaction mechanism determined by Rosenblatt for the nucleophilic oxidation of electrophilic alkenes.[131]

Rosenblatt and Broome[131] studied the reaction of *o*-chlorobenzylidenemalononitrile, Figure 4-18, with hydroperoxide and hypochlorite at 25 ˚C in CH_3CN:H_2O (1:99 (v:v)) mixtures. The second-order rate constant for the reaction in the presence of hydroperoxide was 4.00 x10^5 $M^{-1}s^{-1}$, while the second-order rate constant for hypochlorite was 2.20 x10^4 $M^{-1}s^{-1}$. This indicates that the hydroperoxide anion is about 20 times more reactive than hypochlorite.

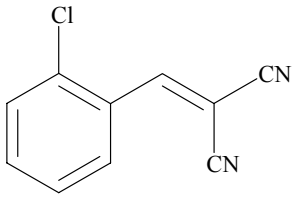

Figure 4-18. Structure of the substrate used by Rosenblatt and Broome,[131] *o*-chlorobenzylidenemalononitrile.

The explanation for the observed reactivity is due to the basicity of the corresponding nucleophiles. Since hydrogen peroxide is a weaker acid (pK_a =11.65)[141] than hypochlorous acid (pK_a = 7.40)[142], the hydroperoxide anion is a stronger base than hypochlorite. Since hydroperoxide is the stronger base, it will react with the electrophilic carbon of the alkene at a faster rate than hypochlorite. Since the rate determining step of the reaction is the nucleophilic addition to the electrophilic carbon, the reactivity of the nucleophilic anion will determine the rate of addition to a particular substrate.

The nucleophile basicity explains why there was no observed difference in the yields of the reactions of **1** in sodium bicarbonate and sodium phosphate presented in Table 4-1. Since hydroperoxide, pK_a 11.65,[141] and peroxycarbonate have similar pK_a values, their reactivity toward electrophilic alkenes would be nearly identical. Since they are both strong bases they will add at approximately the same rate to the same substrate giving rise to the identical conversions seen in the epoxidation data seen in Table 4-1.

The reactivity of peroxycarbonate and hydroperoxide also confirms the mechanism of Rosenblatt and Broome.[131] Since the fast step of the reaction has been proposed to be the internal cyclization to form the epoxide and the release of the leaving group, the stability of the leaving group is irrelevant. If the slow step of the epoxidation were the ring closure, the identity of the leaving group would become the dominant characteristic in the determination of reactivity, as seen in Figure 4-19. If the ring closure were the rate determining step, peroxycarbonate would react faster than hydroperoxide since carbonate is the more stable leaving group over hydroxide. Since there is no increase in reactivity of peroxycarbonate over hydroperoxide in the data presented in Table 4-1, the rate limiting step must be the addition of the nucleophilic oxidant to the electrophilic carbon, supporting the conclusion of Rosenblatt and Broome, Figure 4-20.

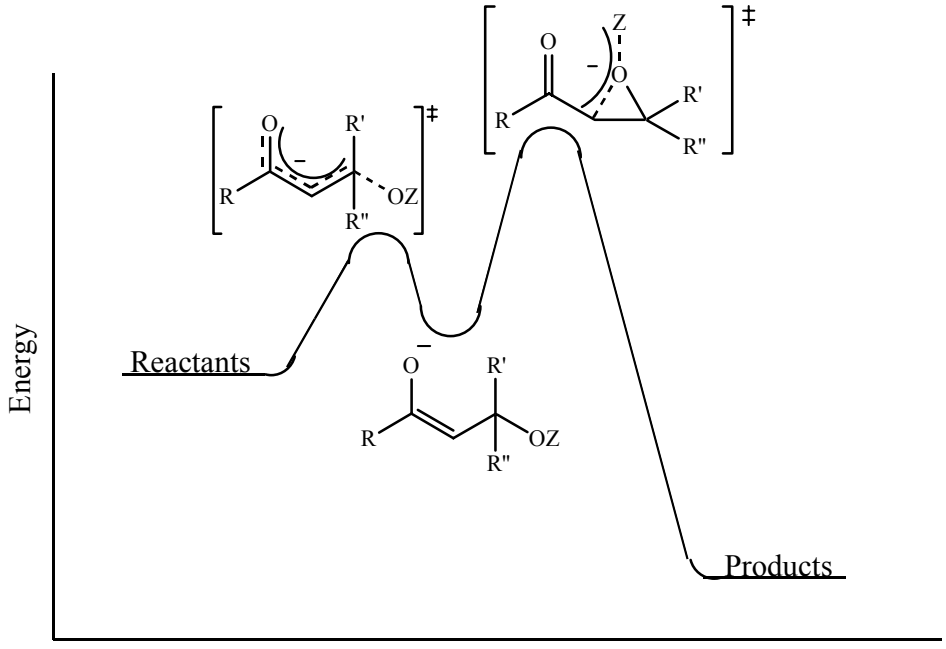

Figure 4-19. A reaction coordinate diagram for the addition of a nucleophilic oxidant to an electrophilic alkene. If the ring closure of the epoxide is the rate determining step, as seen in the diagram by a larger energy barrier for the formation of the epoxide, the identity of the nucleofuge (Z) will determine the reactivity of the oxidant. The more stable the nucleofuge, the more reactive the oxidant will be.

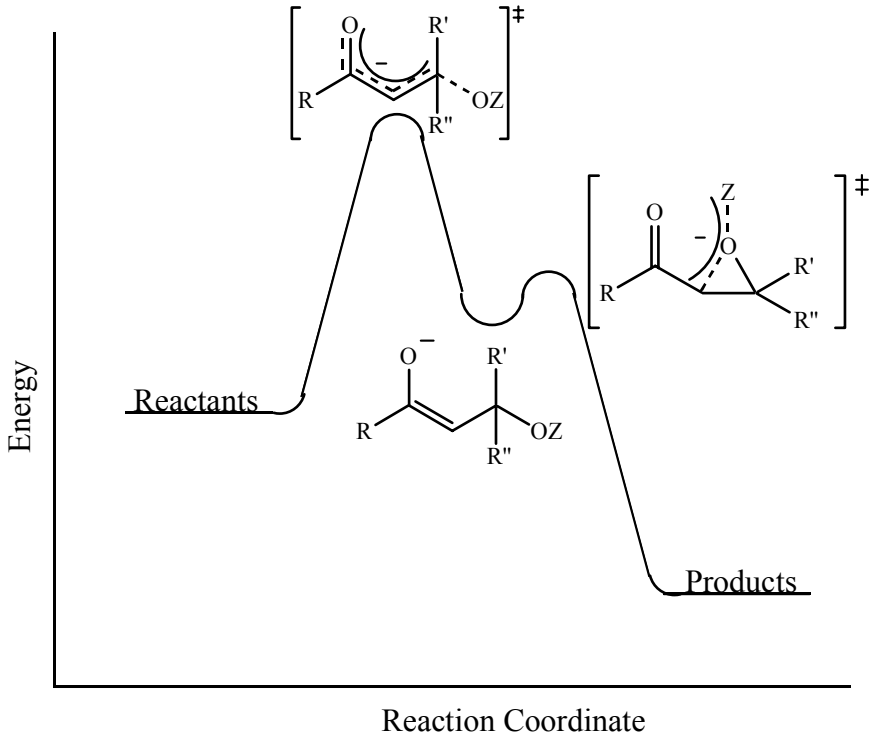

Figure 4-20. A reaction coordinate diagram for the addition of a nucleophilic oxidant to an electrophilic alkene. If the addition of the oxidant is the rate determining step, as seen in the diagram by a larger energy barrier to the formation of the intermediate, the identity of the nucleofuge (Z) will no longer determine the reactivity of the oxidant. The more basic oxidant will react faster.

Bunton and Minkoff[132] studied the epoxidation of mesityl oxide and ethylideneacetone by the hydroperoxide anion in aqueous solution. They observed second-order rate constants of 1.37×10^{-2} and 7.70×10^{-2} $M^{-1}s^{-1}$, respectively, for the oxidation at 0 ˚C. Using the general rule that reaction rates double for every 10 ˚C increase in temperature, the second-order rate constants would be 8.22×10^{-2} and 4.62×10^{-1} $M^{-1}s^{-1}$, respectively, at 25 ˚C. Given that hydroperoxide reacts faster than hypochlorite, the second-order rate constants observed by Bunton and Minkoff[132] are orders of magnitude smaller than that observed by Rosenblatt and Broome's,[131] 4.00×10^{5} $M^{-1}s^{-1}$.

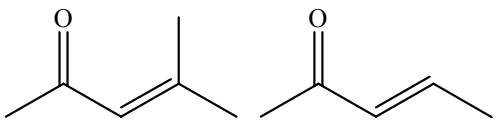

Mesityl oxide Ethylideneacetone

Figure 4-21. Substrates used by Bunton and Minkoff to study the oxidation of electrophilic alkenes by the hydroperoxide anion.

The apparent discrepancies in rate constant observed can only be rationalized by the particular substrate being epoxidized. In the case of Bunton and Minkoff, both substrates were α,β-unsaturated ketones, Figure 4-21, while in the case of the work by Rosenblatt and Minkoff, the substrate under investigation was a dicyano compound, Figure 4-18. The addition of two cyano groups on the α-carbon makes the β-carbon more electrophilic than the β-carbon for the substrates used by Bunton and Minkoff. The presence of a more electrophilic carbon then explains why such varying rate constants are observed for the reactions with hydroperoxide.

In the work presented in this report, the second-order rate constants observed for the epoxidation of **4** by hydroperoxide and hypochlorite were 660 ± 40 and 118 ± 2 $M^{-1}s^{-1}$, respectively. While the epoxidation by the hydroperoxide anion in this study is 5.6 times greater than that for hypochlorite, Rosenblatt and Broome[131] observed a 20 times greater reactivity for hydroperoxide over hypochlorite in the oxidation of *o*-chlorobenzylidenemalononitrile. The increased reactivity of hydroperoxide may depend on the substrate involved, as seen in the comparison with the second-order rate constants observed by Bunton and Minkoff[132] for the epoxidation of mesityl oxide and ethylideneacetone. Since the substrate used for this study has a second carbonyl group α to the alkene, this may account for the increased reactivity observed. The surfactant may also account for the difference in the second-order rate constants.

There are a couple of factors that might affect the reaction of electrophilic alkenes with nucleophilic oxidants in surfactant solutions. First, since a cationic surfactant was used for this study, the cationic head group could stabilize the enolate intermediate. By neutralizing the negative charge on the oxygen atom, the energy of the intermediate would be lowered. By lowering the energy of the intermediate, the rate of the reaction should be slower. In order to determine whether the surfactant is having the postulated effect, experiments would need to be conducted to observe the second-order rate constants in the absence of surfactant. Since the substrate is not soluble in aqueous solution, mixed solvent systems would need to be used, which may introduce new variables. Second, the introduction of the cationic surfactant may increase the observed second-order rate constants by concentrating the active oxidant at the micelle surface.

In addition to the differences in the second-order rate constants, the pK_a values for the two oxidants were also fit using Equation 4-3. It is known that micellar media affects the acid-base dissociation of organic dyes,[57,143-150] the substrates of choice for monitoring acid-base equilibria in micellar solution, since they can be easily monitored by their characteristic absorbance by Uv-vis. It has been suggested that effects on acid-base equilibria may be related to the repulsion of protons by cationic surfactants, and their attraction to anionic surfactants. Fernandez and Fromherz[143] have attempted to compute these attractive and repulsive forces using the micelle as a submicroscopic solvent, along with a term to account for the surface potential of the micelle.

To further complicate the prediction of acid-base equilibria in micellar media, attempts to understand the affect of added salts to the micellar media have been attempted by Romsted[149] and Quina.[150] In their work, equations have been developed to describe all

of the ionic exchanges between the bulk water and the micellar surface. For all of these studies, the acid-base equilibria of any given acidic substrate may increase or decrease upon incorporation in a micelle, depending on the particular substrate and the concentration of added salts.[151] Table 4-2 lists the pK_a values for a group of dyes in aqueous and micellar (CTACl) solution.

Table 4-2. pK_a values in water and CTACl for several different dyes.[151]

	water			**CTACl**		
dye	pK_{a1}	pK_{a2}	pK_{a3}	pK_{a1}	pK_{a2}	pK_{a3}
fluorescein	2.14	4.45	6.80	0.60	6.41	7.17
sulfonefluorescein	-	3.22	6.76	-	2.33	7.00
2,7-dichlorofluorescein	0.35	4.00	5.19	<-0.5	5.50	5.79
eosin	-2.0	2.81	3.75	-	1.83	5.76
ethyl eosin	-	1.91	-	-	1.11	-

Further kinetic studies on the epoxidation of electrophilic alkenes in both pure water and micellar media by nucleophilic oxidants need to be conducted to determine which of these two possibilities are more or less responsible for the observed second-order rate constants.

Conclusions

Unlike epoxidations of nucleophilic alkenes, electrophilic alkene oxidation is not catalyzed by manganese(II) with hydrogen peroxide as the terminal oxidant in the presence of bicarbonate. In fact, by adding manganese(II) to the reactions, the hydrogen peroxide is disproportionated, thus decreasing the concentration of the active oxidant, the hydroperoxide anion. Further evidence that manganese(II) does not affect the reaction is observed when 5 mM DTPA is added to a reaction of **1**. The half-life of this reaction is unaltered from that of a reaction with no metal added. This indicates that electrophilic alkenes do not react with either the proposed high valent manganese species, or the carbonate radical anion.

Reactions of methacrylic acid indicate that the dominant species of both the oxidant and substrate present in solution at the operating pH are important. This was demonstrated by plotting the concentrations of both methacrylic acid and hydroperoxide as a function of pH, Figure 4-11. From the plot, the greatest reactivity will occur where the methyacrylic acid and hydroperoxide concentrations are maximized. This occurs at a pH value of 7.8. For the reactions observed, the deprotonated alkene, methacrylate, does not react as an electrophilic alkene but has a reactivity that resembles a nucleophilic alkene. The addition of manganese(II) to these solutions, therefore, should increase the reactivity. In fact, when 4 μM manganese(II) was allowed to react with methacrylic acid at pH 7.8 in the presence of 1.00 M sodium bicarbonate, the reaction was observed to be more than 90% complete in 15 min.

Finally, in order to assure that the reactivity seen with methyl vinyl ketone was not substrate-specific, reactions of ethyl acrylate were conducted. Since ethyl acrylate does not contain the ester moiety, the problems encountered with methacrylic acid, namely the deprotonation of the acid, should not be present. When ethyl acrylate was allowed to react with hydrogen peroxide in the presence of bicarboante at pH 7.8, a 44% conversion to the epoxide was observed in 24 hrs. At pH 8.6, however, a 66% conversion to the epoxide was observed in 24 hrs, proving that the increase in pH is responsible for the increased reactivity.

Experiments with methyl vinyl ketone were also conducted to determine whether the peroxycarbonate dianion is an effective oxidant of electrophilic alkenes. Reactions were performed under identical conditions with sodium bicarbonate and sodium phosphate as the buffering salts. Conversions of methyl vinyl ketone at the same pH

values gave identical conversions in the different buffers. This result indicates that the choice of buffer does not make a difference, only the pH of the solution. Also, this result indicates that peroxycarbonate is nearly equal to hydroperoxide at oxidizing electrophilic alkenes. These data support the mechanism proposed by Rosenblatt and Broome[131] for the epoxidation of electrophilic alkenes by nucleophilic oxidants. The rate determining step is the attack of the nucleophilic oxidant at the β-carbon of the electrophilic alkene. Therefore, the hydroperoxide anion and peroxycarbonate dianion should have similar reactivities, which is supported by the data in Table 4-1.

Kinetic experiments were conducted for the reaction of dibenzoylethylene with hydroperoxide and hypochlorite. The second-order rate constant for the reaction with hydrogen peroxide is $660 \pm 40\ M^{-1}s^{-1}$ and the pK_a of hydrogen peroxide is 11.70. For the reaction of hypochlorous acid with dibenzoylethylene, the second-order rate constant is $118 \pm 2\ M^{-1}s^{-1}$ and the pK_a of hypochlorous acid was determined to be 8.26.

Limited kinetic data available in the literature for the reaction of electrophilic alkenes with nucleophilic oxidants make interpretation of the observed second-order rate constants difficult. From the data that has been reported, the identity of the substrate seems to make the greatest impact on the reactivity with nucleophilic oxidants. This can be examined by comparing the second-order rate constants observed by Rosenblatt[131] and Bunton.[132] The substrate used by Rosenblatt and Broome, *o*-chlorobenzylidenemalononitrile, has a second-order rate constant that is orders of magnitude greater than the substrates used by Bunton and Minkoff, mesityl oxide and ethylideneacetone. Since *o*- chlorobenzylidenemalononitrile has two cyano groups on the α- carbon of the alkene, the β-carbon is more electrophilic than the β-carbon of the

substrates of Bunton and Minkoff, which only have one electron withdrawing group bonded to the α- carbon of the alkene.

Limited data using surfactants for the nucleophilic oxidation of electrophilic alkenes has also made interpretation of the observed second-order rate constants difficult. For this work, the cationic surfactant used may contribute to the larger second-order rate constants observed by concentrating the active oxidant at the micellar surface, which would increase the observed second-order rate constants. The cationic surfactant may also affect the second-order rate constants by stabilizing the oxygen atom of the intermediate enolate. By stabilizing the intermediate, however, the rate constants would decrease, since the intermediate would be lower in energy.

Materials and Instrumentation

Hydrogen peroxide (35%) was purchased from Sigma-Aldrich and was standardized often by iodometric titration. Sodium hypochlorite was purchased from Fisher and its concentration was checked spectrophotometrically by observing the peak at 236 nm ($\varepsilon = 100\ M^{-1}cm^{-1}$). Methyl vinyl ketone (Aldrich), methacrylic acid (Aldrich), ethyl acrylate (Aldrich), and dibenzoylethylene (Acros) were purchased as their highest grade and used without further purification. Sodium bicarbonate, sodium phosphate dibasic, and sodium phosphate monobasic (Fisher) were purchased as analytical grade and used without further purification. Diethylenetriaminepentaacetic acid (Sigma-Aldrich), cetyltrimethylammonium chloride (Sigma-Aldrich), and manganous sulfate (Fisher) were purchased and used without further purification. Water was purified by a Barnstead E-Pure 3-Module Deionization System. ^{1}H-NMR spectra were obtained on a Mercury 300 or VXR 300 spectrophotometer in D_2O (Cambridge Isotope) and the residual proton peak (DOH) used as internal standard. UV-vis kinetic experiments were

obtained using a Hewlett-Packer 8453 spectrophotometer using 1.0 cm polystyrene cells from Fisher. The reaction temperatures were maintained at 25 ± 0.1 ºC using a Fisher Isotemp 1600S water bath circulator.

Experimental

Electrophilic Alkene Epoxidation

Electrophilic alkene reactions were performed in D_2O in both sodium phosphate (1.00 M) and sodium bicarbonate (1.00 M) solutions at pH 7.8. Reactions which were performed at pH 8.6 had 10 μL of added saturated NaOH dissolved in D_2O. Alkene concentration was 0.10 or 0.05 M, as indicated in the text. Hydrogen peroxide was 0.15 M for reactions with methyl vinyl ketone and 0.30 M for reactions with methacrylic acid and ethyl acrylate. Reactions were monitored by ^1H NMR by observing the disappearance of the alkene protons and the appearance of the epoxide protons. Percent conversions were determined using the integrations of the alkene and epoxide protons. NMR spectra were recorded on a VXR 300 MHz or Mercury 300 MHz instrument.

Dibenzoylethylene Kinetics

Reactions of dibenzoylethylene were performed in 0.10 M CTACl, 0.10 M phosphate buffer, and either 8.00 x 10-4 M hydrogen peroxide, or 2.40 x 10-3 M sodium hypochlorite at 25 ˚C. Dibenzoylethylene was dissolved in ethanol. L□Reactions were initiated by addition of 72 of dibenzoylethylene solution. Total organic solvent in the reactions was less than 2.5%. Reaction progress was monitored by loss of peak intesity at 320 nm using a Hewlett-Packer 8453 spectrophotometer with multi-cell capabilities.

CHAPTER 5
GENERAL CONCLUSIONS

Hydrogen peroxide decomposition and nucleophilic alkene epoxidation are easily achieved using bicarbonate and manganese(II) as catalysts. The formation of a high valent metal oxo species initiates the reaction for both the decomposition and nucleophilic alkene epoxidation. This oxidant can deliver an oxygen atom to other organic species as indicated by the products of amine oxidation.

In Chapter 2, large scale epoxidations in micellar media have been shown to be effective for producing large amounts of epoxide, although significant hydrolysis of the product epoxide has been detected when the reactions are performed in the absence of metal. The long reaction times can be overcome by performing the reaction in the presence of Mn(II). Surfactants have been used as a means of dissolving hydrophobic substrates into the aqueous solutions. From the observed kinetic data, the choice of surfactant, either cationic or anionic, does not have a significant impact of the reaction rate. Also, the source of manganese, either from a bulk stock of the ion or paired with the surfactant, has no significant impact on the reaction rate for the epoxidation. Purification of the resulting epoxide from the reaction solutions has been accomplished by using liquid-liquid extraction. This method provides a useful alternative to normal extraction techniques that in the presence of the surfactants produce emulsions. Interesting results of the kinetics of the reactions of nucleophilic alkenes in micellar solution led to the investigation of the background hydrogen peroxide decomposition.

Chapter 3 describes the investigations of the background metal-assisted decomposition of peroxide in bicarbonate solution. The kinetics of the reaction have been measured and the results are similar to work that has been previously reported. The dependence of the reaction on the metal cation has been observed to be first-order. This indicates that only one metal cation is present in the active metal complex. The bicarbonate dependence for the reaction has also been found. A second-order dependence was observed which is consistent with the results observed for the nucleophilic alkene epoxidation. This result indicates that two bicarbonate anions are present in the active metal species. The hydrogen peroxide dependence has also been observed for these reactions. For the hydrogen peroxide decomposition, the dependence is linear through a concentration of 0.5 M. This is in contrast to the inverse relationship observed for the oxidation of nucleophilic alkenes.

The lifetime of the active metal catalyst was also conducted. Results from these experiments indicate that the active species is easily regenerated from spent solutions by the reintroduction hydrogen peroxide. A loss in the catalytic rate is observed over time. Experiments were conducted to determine what factors were contributing to the loss of activity. Large scale cycling of a decomposition reaction was used to show that the concentration of bicarbonate is falling throughout the reaction. Since the reaction has a second-order dependence on bicarbonate the loss of bicarbonate has the most dramatic effect on the loss of activity. In addition to examining the bicarbonate concentration, the hydrogen peroxide was examined as a possible source of contaminants that would lead to the loss of activity on the catalyst lifetime. Results using the malachite green assay for phosphates indicate that the stock hydrogen peroxide solutions are stabilized with

phosphates. The introduction of these phosphates has a deleterious effect on the reaction by precipitating the metal cation. Reactions performed using distilled hydrogen peroxide and adding bicarbonate after each reaction was shown to help prevent the loss in the active catalyst. The inability to full control the bicarbonate is still a factor in the loss of activity.

In addition to examining the lifetime of the catalyst, the source of the manganese ion was also investigated. Manganese(II) sulfate, potassium permanganate, and a Mn(IV) TACN complex were each used to examine the decomposition of hydrogen peroxide. When reactions were performed using the same concentration of manganese(II) sulfate and potassium permanganate, identical observed rate constant, within error, are observed. This is not surprising since permanganate is known to react with hydrogen peroxide to generate Mn(II) cations.

A Mn(IV)-TACN complex that has been touted as an excellent epoxidation catalyst for nucleophilic alkenes using hydrogen peroxide as the terminal oxidant was also examined for its ability to catalyze the decomposition of hydrogen peroxide. Initially, the stability of the catalyst was examined spectrophotometrically in the presence of bicarbonate and hydrogen peroxide. When a solution of the catalyst is dissolved in a bicarbonate solution, the catalyst appears to be stable, as the absorbance of the complex does not change with time. Upon addition of 1 equivalent of hydrogen peroxide, the catalyst's absorbance rapidly drops to near zero. After time, however, a broad absorbance is detected and solutions turn bright yellow. When 2 equivalents of hydrogen peroxide were used, a different result was observed. Instead of a yellow color developing after the addition of the hydrogen peroxide, the absorbance remained close to zero for

several minutes. It is believed that the decomposition of the catalyst is being accomplished by oxidative *N*-dealkylation of the TACN ligand. In the presence of only 1 equivalent of hydrogen peroxide, the decomposition of the catalyst is incomplete and the generation of metal-amine coordination compounds explains the resulting yellow color. On the other hand, when two equivalents of peroxide were used, the catalyst is completely decomposed, and no metal-amine intermediates are produced to give rise to the yellow color observed. When the same concentration of the Mn(IV)-TACN complex was used for the decomposition of hydrogen peroxide in bicarbonate solution, similar observed rate constants to the manganese(II) sulfate reactions were found. This result indicates that the Mn(IV)-TACN complex quickly decomposes to release a manganese ion which decomposes the hydrogen peroxide at the same rate as if the metal ion had been introduced as a salt.

Cis/trans isomerization was also examined in this study in an attempt to understand how the active oxygen catalyst was delivering the oxygen atom. If the oxygen is being delivered via a concerted mechanism, rotation of the cis alkene upon oxidation should not be observed, as is the case for peracid epoxidation. However, if rotation to the more stable trans-epoxide is observed, the result would indicate that the C-C sigma bond has the ability to rotate in the transition state to the more stable trans conformation. A numbe of different substrates were attempted to be used for this study, but maleic and fumaric acid were eventually used in these experiments. When the cis acid, maleic acid, was epoxidized using the manganese system, both the cis and trans epoxides were observed by ^{1}H NMR. This result, as mentioned earlier, indicates that rotation to the more stable trans conformation in the transition state is occurring.

Examination of the oxidation of the radical traps used in other studies to confirm the presence of hydroxyl radicals was also conducted. Results from these experiments indicate that the oxidation system can react with amines to yield their oxidative *N*-dealkylation products. The proposed mechanism for the metal catalyzed oxidative *N*-dealkylation is based on current work investigating the reactivity of cytochrome P-450, an iron containing enzyme. Current literature proposes that the mechanism proceeds through a single electron transfer. Support for this mechanism has come from work involved with amines whose *N*-alkyl groups have been deuterated. Results of oxidation with these substrates yield deuterium isotope effects of near unity. These data suggest that the breaking of the alpha-carbon hydrogen bond is not rate limiting. If the reaction were progressing via a hydrogen abstraction, a normal isotope effect, $k_H/k_D > 1$, would be expected.

Solvent isotope effect studies have also been conducted for the nucleophilic alkene epoxidation and hydrogen peroxide decomposition. A large, inverse solvent isotope effect has been observed for the epoxidation reaction, while a normal isotope effect was measured for the decomposition reaction. The result of the inverse isotope effect for the alkene epoxidation reaction indicates that there is a proton transfer in the transition state of the reaction that proceeds faster in solutions of deuterium oxide than water. Possible reaction mechanisms have been proposed in an attempt to explain the observed effect. Two possibilities exist in this system. First, the metal may simply be acting as a Lewis acid to coordinate and activate the peroxycarbonate. The second proposed explanation is that the reaction is proceeding by reaction with the carbonate radical anion. Both of these

reactants can be uncharged and would rationalize the rates of epoxidation observed in cationic and anionic surfactants.

Finally, a mechanism is proposed for the activation of peroxycarbonate to form a high oxidation metal oxo complex which could be responsible for the observed reactions. In addition, a radical oxidation route is also proposed for the observed reactions of nucleophilic alkenes and hydrogen peroxide decomposition. Numerical simulation has been used in an attempt to either confirm or reject possible reaction mechanisms. This work indicates that the generation of carbonate radicals and a high oxidation state metal oxo complex are reasonable. In addition, simulations using the carbonate radical mechanism indicate that the hydrogen peroxide decomposition is inhibited with increasing concentrations of hydrogen peroxide. This interesting result might explain the downturn in the hydrogen peroxide dependence observed for nucleophilic alkene epoxidation.

Chapter 4 discussed the use of the peroxycarbonate dianion as a nucleophilic oxidant of electrophilic alkenes. Experiments conducted in the presence of metal indicate that the reaction has no dependence of metal, and in fact, the reaction is inhibited by the addition of metal by decomposing the active oxidant. Further support that the metal has no effect on the epoxidation of electrophilic alkenes has come from experiments using metal chelating agents. When DTPA is added to the reactions, no change in $t_{½}$ is observed. Therefore, the mechanism described in Chapter 3 is not responsible for the epoxidation.

The pH of the solutions was found to affect the rate of epoxidation of electrophilic alkenes. This would support the idea that a nucleophilic alkene is responsible for the

epoxidation. As the pH is raised, the concentration of the hydroperoxide anion would increase. Since this is proposed to be the active epoxidizing agent, a greater concentration of the oxidant will yield more epoxide.

The predominant resonance structure at the operating pH also plays an important role in the epoxidation of electrophilic alkenes. For example, the epoxidation of methacrylic acid is inhibited at higher pH. This is due to the fact that the acid will be deprotonated at the operating pH, and this alkene will react more similarly to a nucleophilic alkene. This was shown to be true when a reaction was conducted with the addition of manganese(II). An epoxidation that was only 50% complete in 24 hrs, was >90% complete with the addition of the metal. Experiments using the similar ethyl acrylate, where the ester moiety replaces the acid, resulted in trends that are consistent with the epoxidation of electrophilic alkenes by nucleophilic oxidants. The ester moiety provides a similar chemical environment to that of the methacrylic acid, but deprotonation is no longer an issue.

The kinetics of the epoxidation of dibenzoylethylene were conducted in cationic micellar solutions. The reaction was found to fit an expression that describes the nucleophilic attack of the oxidant on the substrate. Hydrogen peroxide and hypochlorite were the oxidants chosen for study. The second-order rate constant for the epoxidation by hydroperoxide was observed to be $660 \pm 40\ M^{-1}s^{-1}$, with a pK_a of hydrogen peroxide being 11.7. Hypochlorite reactions resulted in the observation of a second-order rate constant of $118 \pm 2\ M^{-1}s^{-1}$ and the pK_a of hypochlorous acid being 8.26.

In conclusion, it has been shown that the oxidation of organic substrates can be accomplished using peroxycarbonate. For substrates which are more nucleophilic, metal

activators are required to increase the rate of product formation. A mechanism based on a high oxidation state metal oxo complex and carbonate radicals are implicated in the reaction. On the other hand, electrophilic substrates can react with the peroxycarbonate dianion directly. The peroxycarbonate dianion has been shown to be the active species and has a reactivity similar to that of the hydroperoxide anion.

APPENDIX
VARIATIONS IN NUCLEOPHILIC ALKENE EPOXIDATION AND HYDROGEN PEROXIDE RATE CONSTANTS

The following figures were generated using the full mechanism of nucleophilic alkene epoxidation and hydrogen peroxide decomposition as presented in Chapter 3. Only the rate constant or equilibrium costant indicated has been changed from the constants listed in Chapter 3.

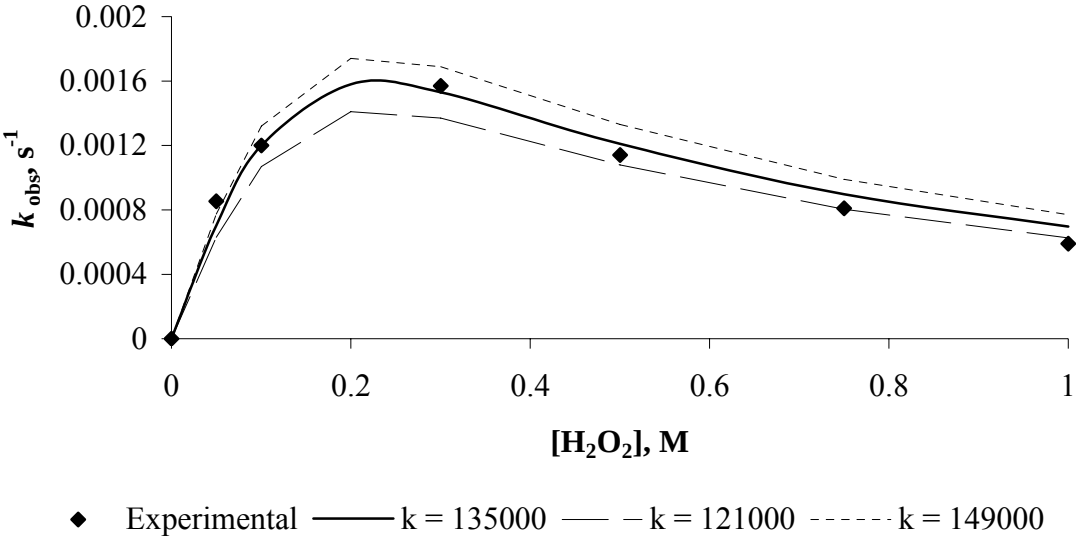

Figure A-1. Variation in the S + A → Products rate constant.

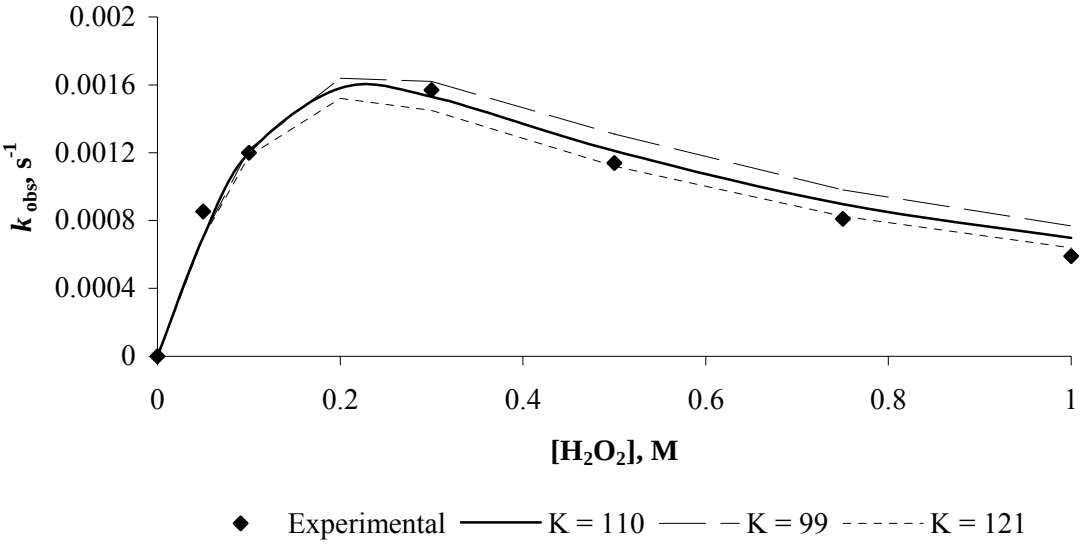

Figure A-2. Variation in the equilibrium constant for A + H_2O_2 ⇌ B.

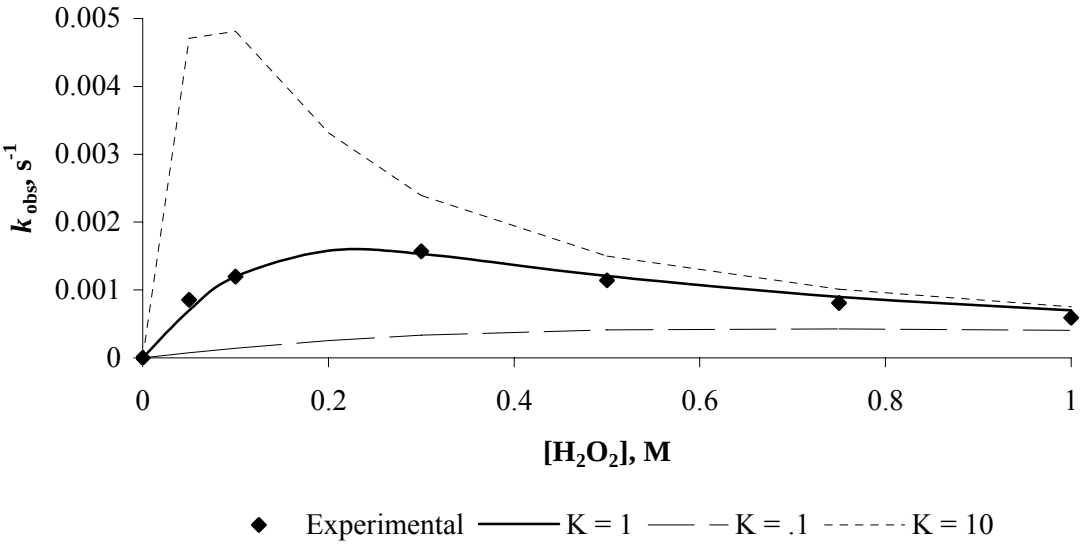

Figure A-3. Variation in the equilibrium constant for the formation of "A".

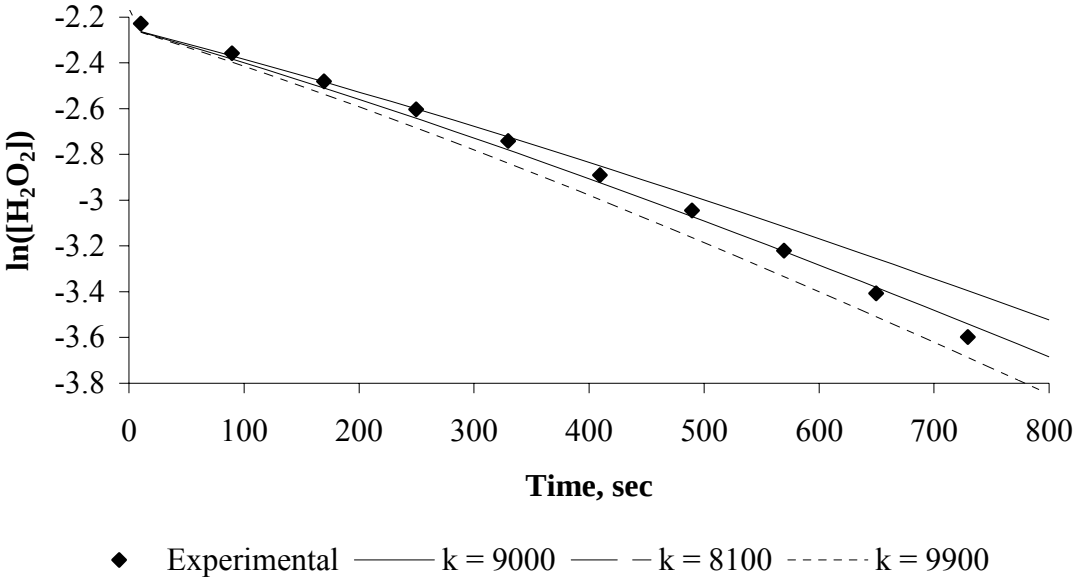

Figure A-4. Variation in the rate constant for A → radicals.

LIST OF REFERENCES

1. Ege, S. *Organic Chemistry: Structure and Reactivity*; D. C. Heath and Company: Lexington, Massachusetts, 1994; pp 470-472.

2. Calzaferri, G. *J.Chem.Ed.* **1999**, *76*, 362-363.

3. Gracy, R. W.; Talent, J. M.; Kong, Y.; Conrad, C. C. *Mutation Research* **1999**, *428*, 17-22.

4. Serrano, F.; Klann, E. *Ageing Research Reviews* **2004**, *3*, 431-443.

5. Paradies, G.; Petrosillo, G.; Pistolese, M.; Ruggiero, F. M. *Gene* **2002**, 135-141.

6. Lavrovsky, Y.; Chatterjee, B.; Clark, R. A.; Roy, A. K. *Experimental Gerontology* **2000**, *35*, 521-532.

7. Mlochowski, J.; Said, S. B. *Polish Journal of Chemistry* **1997**, *71*, 149-169.

8. Salem, I. A.; El-Maazawi, M.; Zaki, A. B. *Int.J.Chem.Kin.* **2000**, *32*, 643-666.

9. Monteagudo, J. M.; Rodrýguez, L.; Villasenor, J. *Journal of Chemical Technology and Biotechnology* **2004**, *79*, 117-125.

10. Goor, G. *Catalytic Oxidations With Hydrogen Peroxide As Oxidant*; Kluwer Academic Publishers: Dordrecht, The Netherlands, 2005; pp 45-96.

11. Patai, S.; Rappoport, Z. *The Chemistry of Alkenes*; John Wiley & Sons: New York, 1964; pp 469-584.

12. Sawaki, Y. In *Organic Peroxides*; Ando, W., ed. John Wiley and Sons, Inc.: New York, New York, 1992.

13. Bartlett, P. D. *Rec.Chem.Prog.* **1957**, *18*, 111.

14. Haber, F.; Weiss, J. *Proc.Roy.Soc.London* **1934**, *147*, 332-351.

15. Haber, F.; Weiss, J. *Naturwissenschaften* **1932**, *51*, 948-950.

16. Barb, W. G.; Baxendale, J. H.; George, P.; Hargrave, K. R. *Nature* **1949**, *163*, 692-694.

17. Barb, W. G.; Baxendale, J. H.; George, P.; Hargrave, K. R. *Transactions of the Faraday Society* **2003**, *51*, 935-946.

18. Barb, W. G.; Baxendale, J. H.; George, P.; Hargrave, K. R. *Transactions of the Faraday Society* **1951**, *47*, 591-616.

19. Barb, W. G.; Baxendale, J. H.; George, P.; Hargrave, K. R. *Transactions of the Faraday Society* **1951**, *47*, 462-500.

20. Traylor T.G.; Tsuchiya S.; Byun, Y.-S.; Kim, C. *J.Am.Chem.Soc.* **1993**, *115*, 2775-2781.

21. Beattie, I. R.; Jones, P. J. *Inorg.Chem.* **1978**, *18*, 2318-2319.

22. Herrmann, W. A.; Fischer, R. W.; Marz, D. W. *Angew.Chem.Int.Ed.* **1991**, *30*, 1638-1641.

23. Espenson, J. H.; Yamazaki, S.; Huston, P. *Inorg.Chem.* **1993**, *32*, 4683-4687.

24. Espenson, J. H.; Al-Ajlouni, A. M. *J.Am.Chem.Soc.* **1995**, *117*, 9243-9250.

25. Katsuki, T.; Sharpless, K. B. *J.Am.Chem.Soc.* **1980**, *102*, 5974.

26. Irie, R.; Hosoya, N.; Katsuki, T. *Synlett* **1994**, *4*, 255-256.

27. McGarrigle, E.; Gilheany, D. *Chem.Rev.* **2005**, *105*, 1563-1602.

28. Pietikäinen, P. *Tetrahedron* **1998**, *54*, 4319-4326.

29. Curci, R.; Fiorentino, M.; Serio, M. R. *Chem.Commun.* **1984**, 155-156.

30. Wang, Z.-X.; Tu, Y.; Frohn, M.; Zhang, J.-R.; Shi, Y. *J.Am.Chem.Soc.* **1997**, *119*, 11224-11235.

31. Shu, L.; Shen, Y.-M.; Burke, C.; Goeddel, D.; Shi, Y. *J.Org.Chem.* **2003**, *68*, 4963-4965.

32. Richardson, D. E.; Yao, H.; Frank, K. S.; Bennett, D. A. *J.Am.Chem.Soc.* **2000**, *122*, 1729-1739.

33. Yao, H.; Richardson, D. E. *J.Am.Chem.Soc.* **2000**, 3220-3221.

34. Richardson, D. E.; Regino, C. A. S.; Yao, H.; Johnson, J. *Free Rad.Biol.Med.* **2003**, *35*, 1538-1550.

35. Adam, A.; Mehta, M. *Angew.Chem.Int.Ed.* **1998**, *37*, 1387-1388.

36. Flanagan, J.; Jones, D. P.; Griffith, W. P.; Skapski, A. C.; West, A. P. *Journal of the Chemical Society, Chemical Communication* **1986**, 20-21.

37. Jones, D. P.; Griffith, W. P. *Journal of the Chemical Society, Dalton Transaction* **1980**, 2526-2532.

38. Uehara, A.; Nagatomo, S.; Fujinami, S.; Furutachi, H.; Ogo, S.; Suzuki, M. *Angew.Chem.Int.Ed.* **2002**, *41*, 1202-1205.

39. Lane, B. S.; Burgess, K. *J.Am.Chem.Soc.* **2001**, *123*, 2933-2934.

40. Lane, B. S.; Vogt, M.; DeRose, V. J.; Burgess, K. *J.Am.Chem.Soc.* **2002**, *124*, 11946-11954.

41. Bennett, D. A.; Yao, H.; Richardson, D. E. *Inorg.Chem.* **2001**, *40*, 2996-3001.

42. Aresta, M.; Tommasi, I.; Quaranta, E.; Fragale, C.; Mascetti, J.; Tranquille, M.; Galan, I.; Fouassier, M. *Inorg.Chem.* **1996**, *35*, 4254-4260.

43. Aresta, M.; Dibenedetto, A.; Tommasi, I. *Eur.J.Inorg.Chem.* **2001**, 1801-1806.

44. Hayward, P.; Blake D.; Wilkinson, G.; Nyman, C. *J.Am.Chem.Soc.* **1970**, *92*, 5873-5878.

45. Hayward, P.; Blake D.; Nyman, C.; Wilkinson, G. *Chem.Commun.* **1969**, *17*, 987-988.

46. Bennett, D. A. Dissertation, University of Florida, 2002.

47. Sychev, A. Ya.; Isak, V. G.; Lap, D. V. *Zhurnal Fizicheskoi Khimii* **1977**, *51*, 363-366.

48. Sychev, A. Ya.; Him, M. H.; Isak, V. G. *Zhurnal Fizicheskoi Khimii* **1984**, *58*, 906-909.

49. Sychev, A. Ya.; Isak, V. G.; Fyong, C. T. T. *Zhurnal Fizicheskoi Khimii* **1984**, *58*, 2331-2332.

50. Sychev, A. Ya.; Isak, V. G.; Lap, D. V. *Zhurnal Fizicheskoi Khimii* **1978**, *52*, 107-112.

51. Sychev, A. Ya.; Isak, V. G.; Pfannmeller, U. *Zhurnal Fizicheskoi Khimii* **1983**, *57*, 760-762.

52. Sychev, A. Ya.; Isak, V. G.; Pfannmeller, U. *Zhurnal Fizicheskoi Khimii* **1979**, *53*, 2790-2793.

53. Sychev, A. Ya.; Pfannmeller, U.; Isak, V. G. *57* **1983**, 1969-1973.

54. Sychev, A. Ya.; Pfannmeller, U.; Isak, V. G. *Zhurnal Fizicheskoi Khimii* **1983**, *57*, 1974-1978.

55. Sychev, A. Ya.; Pfannmeller, U.; Isak, V. G. *Zhurnal Fizicheskoi Khimii* **1983**, *57*, 2217-2221.

56. Sychev, A. Ya.; Pfannmeller, U.; Isak, V. G. *Zhurnal Fizicheskoi Khimii* **1983**, *57*, 1691-1694.

57. Clifford A.Bunton; Gianfranco Savelli *Advances in Physical Organic Chemistry* **1986**, *22*, 213-281.

58. Stadtman, E. R.; Berlett, B. S.; Chock, P. B. *Proc.Natl.Acad.Sci.* **1990**, *87*, 384-388.

59. Cleonice Rocha; Ana Maria da Costa Ferreira *Journal of the Brazilian Chemical Society* **1995**, *6*, 229-234.

60. Louloudi, M.; Kolokytha, C.; Hadjiliadis, N. *J.Mol.Cat.A: Chemical* **2002**, *180*, 19-24.

61. Boelrijk, A. E. M.; Khangulov, S. V.; Dismukes G.C. *Inorg.Chem.* **2000**, *39*, 3009-3019.

62. Romero, I.; Dubois, L.; Collomb, M.; Deronzier, A.; Latour J.; Pecault, J. *Inorg.Chem.* **2002**, *41*, 1795-1806.

63. Quee-Smith, V. C.; DelPizzo, L.; Jureller, S. H.; Kerschner, J. L.; Hage, R. *Inorg.Chem.* **1996**, *35*, 6461-6465.

64. van Es, T.; Backberg, O. G. *J.South African Chem.Inst.* **1964**, *17*, 95-100.

65. Schloss, J. V.; Hartman, F. C. *Bioorganic Chemistry* **1980**, *9*, 217-226.

66. Sheldon, R. A.; Kochi, J. K. *Metal-Catalyzed Oxidations of Organic Compounds*; Academic Press: New York, 1981.

67. Pryor, W. A. *Free Radicals*; McGraw-Hill Book Company: New York, 1966.

68. Kennedy, R. J.; Stock, A. M. *J.Org.Chem.* **1960**, *25*, 1901-1906.

69. Zhu, W.; Ford, W. T. *J.Org.Chem.* **1991**, *56*, 7022-7026.

70. Sayre, L. M.; Hanzlik, R. P. *Xenobiotica* **1995**, *25*, 635.

71. Hall, L. R.; Hanzlik, R. P. *J.Biol.Chem.* **1990**, *265*, 12349-12355.

72. Chen, H.; de Groot, M. J.; Vermeulen, N. P. E.; Hanzlik, R. P. *J.Org.Chem.* **1997**, *62*, 8227-8230.

73. Miwa, G. T.; Garland, W. A.; Hodshon, B. J.; Lu, A. *J.Biol.Chem.* **1980**, *255*, 6049-6054.

74. Miwa, G. T.; Walsh, J. S.; Kedderis, G. L.; Hollenberg, P. F. *J.Biol.Chem.* **1983**, *258*, 14445-14449.

75. Karki, S. B.; Dinnocenzo, J. P.; Jones, J. P.; Korzekwa, K. R. *J.Am.Chem.Soc.* **1995**, *117*, 3657-3664.

76. Wimalasena, K.; May, S. W. *J.Am.Chem.Soc.* **1987**, *109*, 4036-4046.

77. Taqui Kahn, M. M.; Chatterjee, D.; Sanal Kumar, S.; Merchant, R. R.; Bhatt, K. N. *J.Mol.Cat.A: Chemical* **1991**, *67*, 317-322.

78. Mahapatra, S.; Halfen, J. A.; Tolman, W. B. *J.Am.Chem.Soc.* **1996**, *118*, 11575-11586.

79. Sasaki, J. C.; Fellers, R. S.; Colvin, M. E. *Mutation Research* **2002**, *506-507*, 79-89.

80. Bietti, M.; Cuppoletti, A.; Dagostin, C.; Florea, C.; Galli, C.; Gentili, P.; Petride, H.; Caia, C. R. *Eur.J.Org Chem.* **1998**, 2425-2429.

81. Burka, L. T. *J.Am.Chem.Soc.* **1985**, *107*, 2549-2551.

82. Sankarapandi, S.; Zweier, J. L. *J.Biol.Chem.* **1999**, *274*, 1226-1232.

83. Sankarapandi, S.; Zweier, J. L. *J.Biol.Chem.* **1999**, *274*, 34576-34583.

84. Goss, S. P. A.; Singh, R. J.; Kalyanaraman, B. *J.Biol.Chem.* **1999**, *274*, 28233-28239.

85. Liochev, S. I.; Fridovich, I. *J.Biol.Chem.* **2002**, *277*, 34674-34678.

86. Elam, J. S.; Malek, K.; Rodriguez, J. A.; Doucette, P. A.; Taylor, A. B.; Hayward, L. J.; Cabelli, D. E.; Valentine, J. S.; Hart, P. J. *J.Biol.Chem.* **2003**, *278*, 21032-21039.

87. Ramirez, D. C.; Gomez Mejiba, S. E.; Mason, R. P. *Free Rad.Biol.Med.* **2005**, *38*, 201-214.

88. Hoffman, M. Z.; Chen, S. C. *J.Phys.Chem.* **1974**, *78*, 2099-2102.

89. Hall, L. R.; Hanzlik, R. P. *Xenobiotica* **1991**, *21*, 1127.

90. Hall, L. R.; Hanzlik, R. P. *J.Biol.Chem.* **1990**, *265*, 12349.

91. Iley, J.; Constantino, L. *Biochemical Pharmacology* **1994**, *33*, 275.

92. Kedderis, G. L.; Dwyer, L. A.; Rickert, D. E.; Hollenberg, P. F. *Mol.Pharmacol.* **1983**, *23*, 758.

93. Swain, C. G.; Bader, R. F. W. *Tetrahedron* **1960**, *10*, 182-199.

94. Schowen, K. B. *Transition States of Biochemical Processes*; Plenum, New York, 1978.

95. Pritchard J.G.; Long, F. A. *J.Am.Chem.Soc.* **1956**, *78*, 6008-6013.

96. Wiberg, K. B. *Chem.Rev.* **1955**, *55*, 713-743.

97. Dovletoglou, A.; Meyer, T. J. *J.Am.Chem.Soc.* **1994**, *116*, 215-223.

98. Mazellier, P.; Leroy, E.; De Latt, J.; Legube, B. *New J.Chem.* **2002**, *26*, 1784-1790.

99. Eriksen, T. E.; Lind, J.; Merenyi, G. *Radiat.Phys.Chem.* **1985**, *26*, 197-199.

100. Zuo, Z.; Cai, Y.; Katsumura, N.; Chitose, N.; Muroya, Y. *Radiat.Phys.Chem.* **1999**, *55*, 15-23.

101. Czapski, G.; Lymar, S. V.; Schwartz, A. *J.Phys.Chem.* **1999**, *103*, 3447-3450.

102. Meunier, B. *Chem.Rev.* **1992**, *92*, 1411-1456.

103. Groves, J. T.; Watanabe, Y.; McMurray, T. J. *J.Am.Chem.Soc.* **1983**, *105*, 4489-4490.

104. Groves, J. T.; Lee, J.; Marla, S. S. *J.Am.Chem.Soc.* **1997**, *119*, 6269-6273.

105. Finney, N. S.; Pospisil, P. J.; Chang, S.; Plucki, M.; konsler, R. G.; Hansen, K. B.; Jacobsen, E. N. *Angew.Chem.Int.Ed.* **1997**, *36*, 1720-1722.

106. Palucki, M.; Finney, N. S.; Pospisil, P. J.; Guler, M.; Isjida, T.; Jacobsen, E. N. *J.Am.Chem.Soc.* **1998**, *120*, 948-954.

107. Lesht, D.; Bauman, J. E. *Inorg.Chem.* **1978**, *17*, 3332-3334.

108. Albert, E. and Richardson, D. E. Work in Progress, 2005.

109. Pick-Kaplan, M.; Rabani, J. *J.Phys.Chem.* **1976**, *80*, 1840-1843.

110. Ferrer-Sueta, G.; Vitturi, D.; Batinic-Haberle, I.; Fridovich, I.; Goldstein, S.; Czapski, G.; Radi, R. *J.Biol.Chem.* **2003**, *278*, 27432-27438.

111. Palmer, D. A.; van Eldik, R. *Chem.Rev.* **1983**, *83*, 651-731.

112. Roughton, F. J. W. *J.Am.Chem.Soc.* **1941**, *63*, 2930-2934.

113. Finn, M. G.; Sharpless, K. B. *Assymmetric Synthesis* **1985**, *5*, 247.

114. Sharpless, K. B.; Townsend, J. M.; Williams, D. R. *J.Am.Chem.Soc.* **1972**, 295.

115. In *Organic Peroxides*; Swern, D., ed. Wiley-Interscience: New York, 1971; p 355.

116. Mimoun, H. *Angew.Chem.Int.Ed.* **1982**, 734.

117. Mimoun, H.; Saussine, L.; Daire, E.; Postel, M.; Fischer, J.; Weiss, R. *J.Am.Chem.Soc.* **1983**, 3103.

118. Mimoun, H.; Mignard, M.; Brechot, P.; Saussine, L. *J.Am.Chem.Soc.* **1986**, 3711.

119. Hermann, W. A.; Kuehn, F. E.; Fischer, R. W.; Thiel, W. R.; Romao, C. C. *Inorg.Chem.* **1992**, 4431.

120. Herrmann, W. A.; Kiprof, P.; Rydal, K.; Tremmel, J.; Blom, R.; Alberto, R.; Behm, J.; Albach, R. W.; Bock, H.; Solouki, B.; Mink, J.; Lichtenberger, D.; Gruhn, N. E. *J.Am.Chem.Soc.* **1991**, 6527-6537.

121. Ymazaki, S.; Espenson, J. H.; Huston, P. *Inorg.Chem.* **1993**, 4683.

122. Herrmann, W. A.; Fischer, R. W.; Scherer, W.; Rauch, M. U. *Angew.Chem.Int.Ed.* **1993**, *32*, 1157.

123. Al-Ajlouni, A. M.; Espenson, J. H. *J.Am.Chem.Soc.* **1995**, 9243-9250.

124. Ledon, H.; Bonnet, M. *J.Mol.Cat.* **1980**, 309-313.

125. Chin, D. H.; La Mar, G. N.; Balch, A. L. *J.Am.Chem.Soc.* **1980**, 5945.

126. Prileschajew, N. *Berichte der Deutschen Chemischen Gesellschaft* **1909**, 4811-4815.

127. Bartlett, P. D. *Rec.Chem.Prog.* **1957**, 111.

128. Weitz, E.; Scheffer, A. *Chem.Ber.* **1921**, *54*, 2327-2344.

129. Apeloig, Y.; Karni, M.; Rappoport, Z. *J.Am.Chem.Soc.* **1983**, *105*, 2784-2793.

130. Marmor, S. *J.Org.Chem.* **1963**, *28*, 250-251.

131. Rosenblatt, D. H.; Broome, G. H. *J.Org.Chem.* **1963**, *28*, 1290-1293.

132. Bunton, C. A.; Minkoff, G. J. *J.Chem.Soc.* **1949**, 665-670.

133. Yamaguchi, K.; Mori, K.; Mizugaki, T.; Ebitani, K.; Kaneda, K. *J.Org.Chem.* **2000**, *65*, 6897-6903.

134. Boyer, B.; Hambardzoumian, A.; Roque, J.-P. *Tetrahedron* **1999**, *55*, 6147-6152.

135. Rappoport, Z.; Avramovitch, B. *J.Org.Chem.* **1982**, *47*, 1397-1408.

136. Meth-Cohn, O.; Williams, D. J.; Chem, Y. *Chem.Commun.* **2000**, 495-496.

137. Garcia Ruano, J. L.; Fajardo, C.; Fraile, A.; Rosario Martin, M. *J.Org.Chem.* **2005**, *70*, 4300-4306.

138. Patai, S.; Rappoport, Z. Nucleophilic attacks on carbon-carbon double bonds; In *The Chemistry of Alkenes*; Patai, S., ed. John Wiley & Sons: New York, 1964; pp 469-584.

139. Berti, G. *Stereochemical Aspects of the Synthesis of 1,2-Epoxides*; Allinger, N. L., Eliel, E. L., eds. John Wiley & Sons: New York, 1973; pp 93-251.

140. Denevan, D. E. and Richardson, D. E. Work in Progress, 2005.

141. Schumb, W. C.; Satterfield, C. N.; Wentworth, R. L. *Hydrogen Peroxide*; Reinhold Publishing Company: New York, 1955.

142. Lordi, N. G.; Epsein, J. *J.Am.Chem.Soc.* **1958**, *80*, 509.

143. Fernandez, M. S.; Fromherz, P. *J.Phys.Chem.* **1977**, *81*, 1755-1761.

144. Mchedlov-Petrossyan, N. O.; Kleshcevnikova, V. N. *J.Chem.Soc.Faraday Trans.* **1994**, *90*, 629-640.

145. Mchedlov-Petrossyan, N. O.; Isaenko, Y. V.; Salamanova, N. V.; Alekseeva, V. I.; Savvina, L. P. *J.Anal.Chem.* **2003**, *58*, 1018-1030.

146. Saikia, P. M.; Bora, M.; Dutta, R. K. *Journal of Colloid and Interface Science* **2005**, *285*, 382-387.

147. Drummond, C. J.; Grieser, F.; Healy, T. W. *J.Chem.Soc.Faraday Trans.I* **1989**, *85*, 537-550.

148. Bunton, C. A.; Romsted, L. S.; Sepulveda, L. *J.Phys.Chem.* **1980**, *84*, 2611-2618.

149. Romsted, L. S. *J.Phys.Chem.* **1985**, *89*, 5113-5118.

150. Quina, F. H.; Politi, M. J.; Cuccovia, I. M.; Baumgarten, E.; Martins-Franchetti, S. M.; Chalmovich, H. *J.Phys.Chem.* **1980**, *84*, 361-365.

151. Mchedlov-Petrossyan, N. O.; Kleshchevnikova, V. N. *J.Chem.Soc.Faraday Trans.* **1994**, *90*, 629-640.

BIOGRAPHICAL SKETCH

Andrew P. Burke was born March 31st, 1977, in Fort Walton Beach, FL, as the youngest of three children to Andrew J. and Cynthia A. Burke. It was during his high school years at Choctawhatchee High School that Andrew developed his interest in chemistry.

After graduating from high school in 1995, Andrew went to Furman University in Greenville, SC. From the summer of 1998 until graduation, Andrew conducted undergraduate research under the direction of Dr. Laura Wright investigating Pt(0) diimine complexes. It was during this time that Andrew decided to pursue a doctoral degree in chemistry.

After graduating from Furman University in 2000 with Bachelor of Science degrees in chemistry and computer science, Andrew began pursuing a doctoral degree in inorganic chemistry at the University of Florida in Gainesville, FL, under the direction of Dr. David E. Richardson. In December 2002, Andrew married Erin Ringus, a member of the biochemistry division of the Chemistry Department. After graduating with his doctoral degree, Andrew will be moving to Charleston, SC, to join High-Purity Standards.